UNIVERSITY OF BIRMINGHAM

Laboratory investigation of nanoscale dispersed catalyst for inhibition coke formation and upgrading of heavy oil during THAI process

By

ABDULLAH ALMARSHED

A thesis submitted to

The University of Birmingham

for the degree of

DOCTOR OF PHILOSOPHY

School of Chemical Engineering

College of Engineering and Physical Science

University of Birmingham

September 2015

Abstract

It has previously been shown that in situ upgrading of heavy oil by Toe-to-Heel Air Injection (THAI) can be augmented by surrounding the horizontal production well with an annulus of pelleted catalyst. Despite the further upgrading achieved with this configuration, the accumulation of coke and metals deposits on the catalyst and pore sites, resulting from cracking of the heavy oil, have a detrimental effect on the catalyst activity, life span and process. An alternative contacting pattern between the oil and transition metal dispersed catalysts was investigated using a stirred batch reactor, to mitigate the above mentioned challenges. The effects of different hydrogen sources and tetralin hydrogen donor solvent were also investigated. The Taguchi method was applied to optimize the effect of reaction factors and select the optimum values that maximize level of heavy oil upgrading while suppressing coke yield. Detailed optimization of the reaction conditions with iron oxide dispersed NPs (≤ 50 nm) for in situ catalytic upgrading of heavy oil was carried out over the following ranges of operating variables; temperature 355 – 425 ^{o}C, reaction time 20 – 80 min, agitation 200 – 900 rpm, initial hydrogen pressure 10 – 50 bar, and iron metal loading 0.03 – 0.4 wt%. It was found that the optimum combinations of reaction factors are temperature 425 ^{o}C, initial hydrogen pressure 50 bar, reaction time 60 min, agitation 400 rpm and iron-metal loading 0.1 wt%. The properties of upgraded oil at the optimum condition are API gravity 21.1^{o}, viscosity 105.75 cP, sulfur reduced by 37.54 %, metals (Ni + V) reduced by 68.9 %, and naphtha plus middle distillate fractions (IBP – 343 ^{o}C) 68 wt% relative to the feed oil (12.8^{o}API, 1482 cP, sulfur content 3.09 wt%, metals (Ni+V) content 0.0132 wt%, and naphtha plus middle distillate fractions 28.86 wt%). Furthermore, it was found that the dispersed unsupported catalysts significantly suppressed coke formation 4.4 wt% (MoS_2), 5.7 wt% (NiO) and 6.8 wt% (Fe_2O_3) compared to 12 wt% obtained with thermal cracking alone. The results also showed that with dispersed unsupported catalysts in sulphide form the

middle distillate (177-343 ˚C) of the upgraded oil was improved particularly MoS_2 which gave 50 wt% relative to 43 wt% (thermal cracking) and 28 wt% (feed oil). The middle distillate yields for Fe_2O_3 and NiO are 47 wt% and 49 wt%, respectively. Moreover, it was noticed that in presence and absence of Fe_2O_3 as dispersed catalyst the coke formation was significantly reduced in the presence of tetralin solvent compared to H_2, CH_4 and H_2O. The coke yield reduced with addition of Fe_2O_3 as follows: 3.22 wt % (tetralin), 6.19 wt % (CH_4), 6.79 wt % (H_2), and 7.48 wt % (H_2O) relative to 3.54 wt (tetralin), 7.19 wt % (CH_4), 12 wt % (H_2) and 7.32 wt % (H_2O) without Fe_2O_3 NPs. The distillate fraction (177-343 °C) of the produced oil did not show further improvement which remained in the narrow range of 42-45 wt% for hydrogen source, tetralin and thermal cracking under N_2 relative to 28 wt% (feed oil). The produced oil physical properties under different hydrogen sources gave an average (20˚API and 140 cP) against an average of (23˚API and 64 cP) achieved with thermal cracking under N_2 and H_2 alone. The cost and availability of CH_4 and Fe metal compared to Mo counterpart and H_2 for heavy oil upgrading may justify their preference. Furthermore, the X-ray diffraction (XRD) and scanning electron microscopy (SEM) analysis showed that introducing dispersed catalysts, tetralin and different hydrogen sources helped to produce sponge-type coke which could be used as industrial fuel compared to shot-type obtained upon thermal cracking.

Dedication

To my Family

Acknowledgment

This job would not be at hand without the continuous encouragement, support, guidance and unlimited assistance of Prof. Joseph Wood (Supervisor) and Dr. Gary Leeke (Co-Supervisor). Also I would like to express my sincere thanks to Mr. David Boylin for his technical guidance.

Table of Contents

List of Figure

List of Table

Nomenclature

IEA	International Energy Agency
THAI	Toe-to-Heel Air Injection
CAPRI	CAtalytic upgrading PRocess In situ
OOIP	Original Oil In Place
CCCO	Combustion Cell Oil
CSS	Cyclic Steam Stimulation
EOR	Enhanced Oil Recovery
ES-SAGD	Expanding Solvent Steam Assisted Gravity Drainage
FCC	Fluid Catalytic Cracking
GC	Gas Chromatography
GOR	Gas to Oil Ratio
HTO	High Temperature Oxidation
HYD	Hydrogenation
ISC	In Situ Combustion
LDOD	Long Distance Oil Displacement
LTO	Low Temperature Oxidation
MOZ	Mobile Oil Zone
SAGD	Steam Assisted Gravity Drainage
VAPEX	Vapour Extraction

VIVP	Vertical Injection Vertical Producer
HDS	Hydrodesulphurization
HDT	Hydrotreating
HDA	Hydrodeasphaltization
HDS	Hydrodesulphurization
HDM	Hydrodemetalisation
SEM	Scanning Electron Microscopy
XRD	X-ray Diffraction
SG	Specific Gravity
TBP	True Boiling Point
TCD	Thermal Conductivity Detector

Chapter 1
Introduction

1.1 Technical background and motivations

Due to the rapid growth in energy demand worldwide, the world's energy resources are declining, although the search for new deposits continues apace (Hirsch et al., 2006). The latest international energy outlook released by the International Energy Agency (IEA, 2010) predicts that global energy consumption will increase by 56% between 2010 and 2040. Fossil fuels, nuclear power and renewable energy represent the major sources of world energy, with fossil fuels supplying around 80% of energy worldwide (Martínez-Palou et al., 2011). Fossil fuels are the general term for combustible materials extracted from the Earth's crust, such as conventional oil and unconventional oil. Conventional and unconventional oil are used to distinguish between different categories of oil. Conventional oil includes crude oil and natural gas, whereas unconventional oil includes heavy oil, extra heavy oil and bitumen (Hein, 2006). Since conventional resources have already been extensively exploited and are declining, unconventional oil resources could play an important role in securing the world's future energy needs in both the short and long term. However, production, transportation and upgrading processes of unconventional oil impose different challenges for the oil sector compared with conventional oil (Carrillo and Corredor, 2013).

Unconventional resources, represented by heavy oil, extra heavy oil and bitumen, can be considered as a major source of fuel for many reasons. First, heavy oil, extra heavy oil and natural bitumen deposits are abundant, well-known and widespread around the world (World Energy Council 2010). Surveys are conducted by different institutions and councils to update the regional quantities of heavy oil and natural bitumen around the world. In 2007,

the survey delivered by the US Geological Survey Library (USGS, 2007) stated that the Original Oil in Place (OOIP) for heavy oil is 3396 billion barrels; in addition, the same survey showed that the total resources of bitumen are 5505 billion barrels of OOIP. In total, unconventional resources reach up to 8.9 trillion barrels of OOIP, which far outweighs the reserves of conventional resources, estimated to be 1.7 trillion barrel OOIP. Figure 1.1 and Figure 1.2 shows the regional distributions of heavy oil and bitumen resources.

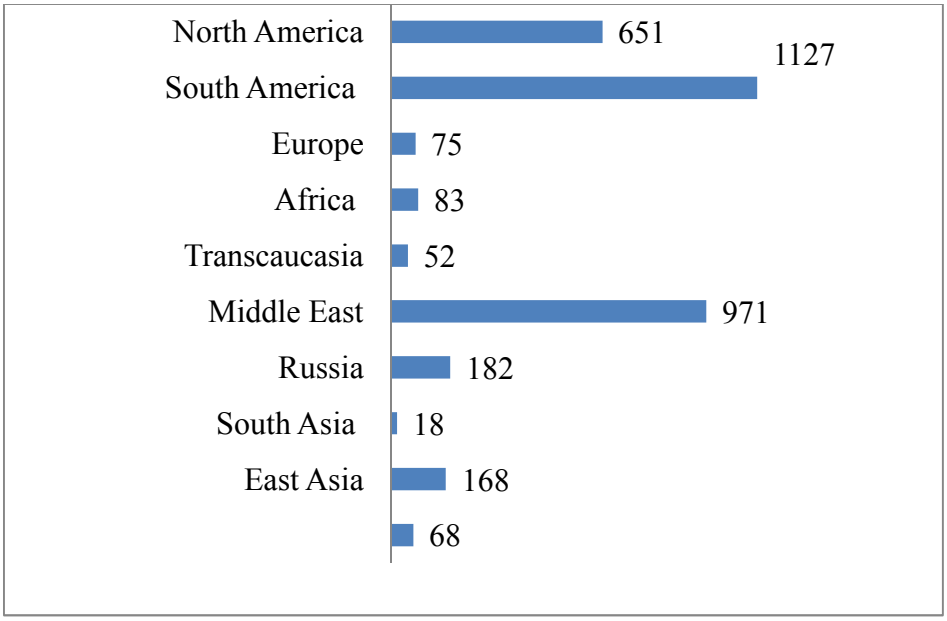

Figure 1.1. Regional distribution of heavy oil (billion barrels) (Meyer et al., 2007).

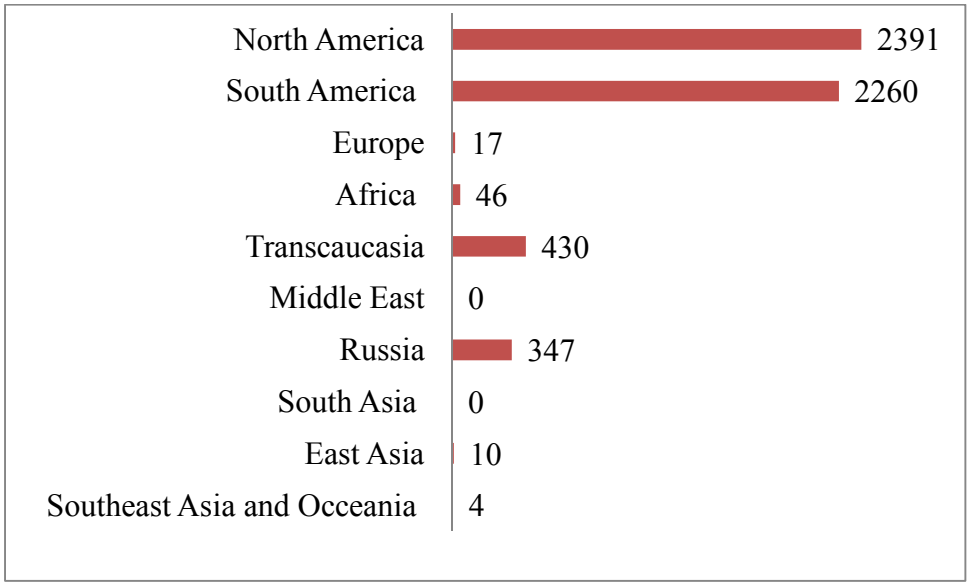

Figure 1.2. Regional distribution of bitumen (billion barrels) (Meyer et al., 2007).

Although the unconventional resources present quite a vast and promising source of energy for the long term, there have been only a few attempts from different nations to establish extraction and upgrading industries for unconventional resources. For example, both Canada and Venezuela, have between 50–65% (USGS, 2007) of the World's total reserves of unconventional oil, are actively working on unconventional resources, whereas Africa and the Middle East have still not made any real attempts at utilising unconventional resources (Blackwell, 2006; Hoshyargar and Ashrafizadeh, 2013). Unconventional oil can be characterised by low American Petroleum Institute gravity (API gravity), high viscosity, and it is deficient in hydrogen, rich in carbon and sulphur, and high concentrations of oxygen, nitrogen and heavy metals, such as nickel and vanadium (Hoshyargar and Ashrafizadeh, 2013). Due to the nature of unconventional oil, there are many hurdles that have slowed down its extraction and use, namely the energy required for extraction, greenhouse gas emissions during the production stage, transportation challenges, cost of upgrading processes and low market value (Rana et al., 2007). For example, compared with light oil, further surface processes are required to treat and upgrade heavy oil to meet the market quality requirements, and those treatments may introduce more costs, which could not be covered by the market price of unconventional oil. As a result, in order to develop the unconventional oil industries, extraction and upgrading technology should be studied. Techniques such as in-situ upgrading are attractive because they do not involve disturbance of the land and may achieve a high recovery of oil in place (Hart et al., 2014; Xia and Greaves, 2006; Xia and Greaves, 2002; Greaves et al., 2012). However the economics for enhanced oil recovery techniques are only favourable when the oil price is high.

Reservoir production involves three main stages in the extraction and production of crude oil for different applications. During the production process, multiple techniques are used to improve the production of reservoir fluids as well as to maintain the reserves. The

first phase of production is primary recovery, during which oil production is controlled by natural drive mechanisms, such as the force of gravity and associated gas evolution from reservoir fluids. In general, primary recovery efficiency is low, differing with the various natural drive mechanisms involved. Primary production efficiencies vary between 5 and 20% of the OOIP (Aurel, 1992). The secondary production stage begins when the energy from the natural driving mechanisms declines. The main goal of the secondary recovery phase is to raise or maintain the reservoir pressure. In order to achieve this, external energy, usually water injection (i.e., water flooding) is used. The net efficiency of both the primary and secondary methods combined is less than 40% of the OOIP (Sheng, 2015; Sheng and Chen, 2014; Holditch, 2013).

Enhanced oil recovery (EOR) is classified as the last stage in reservoir production. In this phase, external thermal energy, gas injection and chemical injection are used to stimulate production. EOR processes are selected based on the fluid's characteristics, such as oil viscosity and the geology of the reservoir, as well as the OOIP. The main goals for EOR technologies are to improve the displacement of heavy oil by reducing its viscosity, decreasing interfacial tension and increasing the contacted area of the reservoir during the extraction processes, which is known as the improvement of sweep efficiency. Thermal technology is highly recommended in order to improve the production of extra heavy oil and bitumen, while the injection of gas and chemical materials are more suitable for heavy oil (Donaldson et al., 1985). Details of the commercial technologies used to enhance heavy oil and bitumen recovery will be discussed later in the next chapter.

Enhanced oil recovery techniques and upgrading processes for unconventional oil are considered important issues in the oil industry. Improving unconventional oil production and the upgrading of it depends on the nature of the petroleum fluid, the geology of the reservoir and the physical properties of the reservoir fluid. It can be seen clearly from the literature

that extensive studies have been conducted to identify the most suitable technique to enhance the production of unconventional oil as well as upgrading it to cover the world's energy needs. In this respect, much attention has been directed toward thermal technology to extract and upgrade unconventional oil (Alpak et al., 2013; Shah et al., 2010). Thermal technology, in situ combustion, could be enhanced oil recovery as well as convert heavy oil to light oil with primary upgrading. Additionally, the application of thermal technology such as in situ combustion contributes to reducing the costs of surface upgrading heavy oil and bitumen (Komery et al., 1999). Steam-Assisted Gravity Drainage (SAGD) and Cyclic Steam Stimulation (CSS) are examples of implemented thermal technology for enhanced oil recovery which depend upon heat being introduced to a reservoir by injected steam to reduce the viscosity of heavy oil and bitumen to facilitate their mobilisation to the surface. In addition, the SAGD method provides a good recovery factor of 50% of OOIP, as well as the recovery factor for the CSS method varies from 10% to 40% (Zhao et al., 2014; Yee and Stroich, 2004). However, consumption of water and natural gas to generate steam are considered major drawbacks of those methods, where two to ten barrels of water are needed to produce one barrel of heavy oil. Furthermore, the produced oil needs addition of diluents to facilitate transportation, which will add more operational costs (Gates, 2007). Therefore, in situ combustion could offer some operational and economic advantages, where the heat generated from the combustion reaction may lead to primary upgrading of heavy oil and bitumen in situ.

Toe-to-Heel Air Injection (THAI) as well as the CAtalytic upgrading PRocess In situ (CAPRI) add on to the THAI method was studied extensively during the last fifteen years (Xia and Greaves, 2002; Hart et al., 2014; Greaves et al., 2012; Xia and Greaves, 2006; Xia et al., 2003). The THAI method is classified as an advanced thermal technology to enhance the recovery of heavy oil where compressed air is injected to initiate the combustion. (THAI)

processes design is to be considered an integration of vertical wells and horizontal producer wells, the latter arranged in a directed drive line. Figure 1.3 illustrates THAI process design

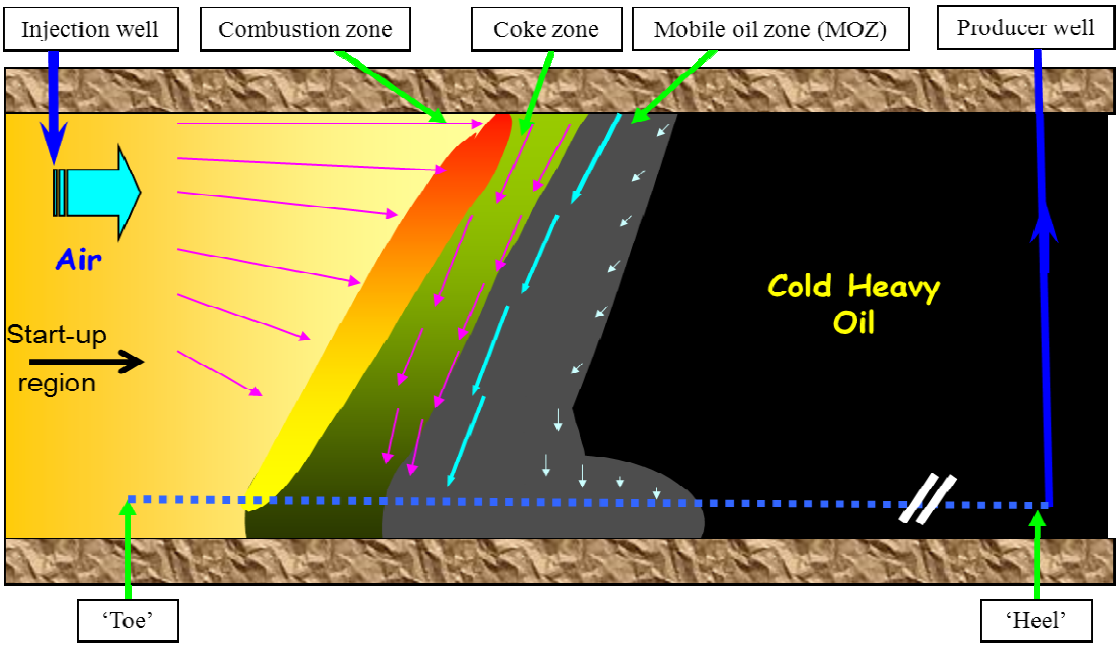

Figure 1.3. Toe-to-Heel Air Injection process (Xia and Greaves, 2006).

The THAI process generates high temperatures (between 400 °C and 600 °C) at reservoir pressure (30 to 50 bar) where the thermal cracking reaction takes place (Xia and Greaves, 2006). In addition, the high temperature partially upgrades the bitumen and heavy oil in place through the carbon rejection reaction. In general, through the THAI process, the heavy oil and bitumen API gravity value increases by several orders, light ends are produced from heavy hydrocarbons, the viscosity of heavy oil decreases and the recovery factor reaches 80% of the OOIP (Xia et al., 2003). THAI-CAPRI process is a modified version of THAI process equipped with a catalytic bed fitted in the perforation of the horizontal well. The high temperature generated from the combustion reaction creates suitable conditions for catalytic upgrading, which leads to upgrading bitumen and heavy oil in place through the hydro conversion reaction that takes place at the CAPRI section.

Earlier studies were conducted to test the ability of the THAI-CAPRI process and the optimum conditions were identified. It was observed that the upgrading of heavy oil in terms of API gravity further increased by 3° to 7° points compared with the THAI process alone. In addition, there is a significant reduction of heavy metals (Ni, V) and sulphur contents, and the viscosity magnitude. On the other hand, according to those studies, the deactivation of the catalysts and horizontal well packing with commercial catalysts were considered as major drawbacks (Xia et al., 2003).

During this study, a laboratory-scale investigation was conducted to examine the effectiveness and activity of different types of dispersed unsupported transition metal catalysts for in situ heavy oil upgrading instead of pellets of catalyst packed in an annulus around the horizontal well. Also, this study is devoted to investigate the effects of different hydrogen sources (methane, steam) instead of hydrogen in the presence and absence of unsupported dispersed catalyst ($Fe_2O_3 \leq 50$ nm) for in situ heavy oil upgrading instead of pellets of catalyst packed in an annulus around. Additionally, effect of tetralin with and without dispersed catalysts was studied and compared with upgrading reaction achieved under different reaction conditions.

Ultradispersed in situ catalytic upgrading has been reported to outperform the augmented catalytic upgrading achieved by incorporating pelleted refinery catalyst to the horizontal production well of the THAI process (Hart et al., 2015). Using ultrafine particles and pelleted Co-Mo/Al_2O_3 catalyst at reaction temperature 425 ^oC, the API gravity and viscosity of the produced oil was found to improve by 9^o API and 96 % with ultrafine particles compared to 5^o API and 79 % achieved with pelleted fixed-bed catalyst (Hart et al., 2015). However, Galarraga and Pereira-Almao (2010) investigated ultradispersed trimetallic (Ni–W–Mo) submicronic catalyst for in situ upgrading at 380 ^oC in a batch reactor, a stirring speed of 500 rpm, and reaction time 3–70 h.

The API gravity increased by 6.5^{o} and a viscosity reduction of 98 % was observed relative to the Athabasca bitumen (API gravity 9.5° and viscosity 7680 mPa s). As the size of particle decreases to nanoscale, its specific surface area increases while the diffusion path length decreases, this improves interaction with macromolecules and cracking reaction. Also, the nanoparticles (NPs) experience lower inter-particle distances that increases the probability of active phase interaction with the hydrocarbon molecules. Ultradispersed upgrading is a once-through process, hence will bypass the hurdles of pre-packing the horizontal production well with pelleted HDT catalyst, but will require the precipitation or transport of the NPs into the mobile oil zone ahead of the combustion front during THAI process. Furthermore, utilising a once-through process deploying NPs could potentially reduce production line blockages due to coke deposition (Hashemi et al., 2014; Krishnamoorti, 2006). Moreover, incorporating commercial supported catalysts and hydrogen with in-situ upgrading could be challenging, hence the search for a cost effective substitute for expensive hydrogen (H_2) is required. Methane (CH_4) is one of main sources of hydrogen (H_2) and direct use of CH_4 instead of hydrogen during heavy oil upgrading could be economically attractive to generate hydrogen indirectly rather than using expensive pure hydrogen gas (Egiebor and Gray, 1990). Also, water could be used as an alternative source of hydrogen during heavy oil upgrading in-situ (Watanabe et al., 2010; Dutta et al., 2000). Furthermore, injecting a hydrogen donor solvent during the THAI process could be quite a promising solution to inhibit coke formation in the THAI process and also, eliminate further cost of using hydrogen gas. The objectives of this study and the thesis organisation are described in detail in the next two sections.

1.2 Objectives of study

The main goal of utilising NPs catalysts with the THAI processes is not only to improve the physical properties of heavy oil, such as API gravity and viscosity, but also to modify the product quality to produce a more valuable product and to minimise coke formation in product distribution. The following are more specific objectives that were investigated during the current study:

1) To understand the overall thermal upgrading mechanism as well as the catalytic upgrading mechanism using dispersed catalysts.

2) To examine the activity and selectivity of different types of dispersed catalysts (inorganic transition metal oxide, transition metal in sulphide form) at hydroconversion conditions: Temperature > 300 °C, high hydrogen pressure and long reaction time (1 hour). To study the products of the reaction including:

   a) Product distribution (coke formation, light hydrocarbon formation, middle distillate formation).

   b) Product quality (sulphur, metal and nitrogen removal).

   c) Physical properties (API gravity and viscosity).

3) To utilise Taguchi's design of experiment method to study:

   a) Effect of reaction parameters such as reaction temperature, initial hydrogen pressure, reaction time speed of mixing and catalyst concentration upon heavy oil upgrading.

   b) Optimum reaction conditions.

4) To evaluate the effect of tetralin and different hydrogen sources upon the inhibition of coke formation.

1.3 Thesis organisation

The laboratory investigation into heavy oil upgrading by NPs is illustrated through seven technical chapters. The current study examined the effect of NPs in down-hole upgrading of heavy oil as well as focusing on the inhibition of coke formation and increasing level of heavy oil upgrading. The level of upgrading was evaluated in terms of physical properties (API gravity, viscosity), product distribution and product quality.

Chapter 1 delivers the detailed introduction and motivations of the current study. In addition, it illustrates the necessity to sustain oil as a major source of energy as well as showing the regional distribution of unconventional oil and identifying the considerable drawbacks and challenges in previous studies, which need further modifications and solutions. Chapter 2 provides details about the chemistry of heavy oil and bitumen, the mechanism of thermal and catalytic upgrading, enhanced oil recovery technology as well as upgrading technology for heavy oil and bitumen using dispersed catalysts, and the fundamental technical background to down-hole catalysis and the emerging technologies, such as CAPRI add on THAI. Furthermore, the chapter discusses the dispersed catalysts types, form and application in down-hole catalytic upgrading. Chapter 3 presents the methods and materials in detail, and describes the analytical instruments that were used to measure the physical properties (API gravity, viscosity), product distributions and product quality. Chapter 4 describes the optimisation study of catalytic upgrading of heavy oil using NPs iron oxide catalysts to identify the effect of process parameters upon heavy oil upgrading, and to achieve the maximum production of middle distillate as well as inhibit coke formation. The investigation in Chapter 4 is based on the orthogonal array described in Chapter 3. Signal-to-Noise ratio (SN) was employed to study the impact of control levels on response variables. ANalysis Of VAriance (ANOVA) was employed to determine significant control factors. Chapter 5 examines the effectiveness of different types of unsupported

dispersed catalysts, such as inorganic transition metal oxide, transition metal sulphide. In Chapter 5, the evaluation and selection of proper catalysts is carried out based upon levels of upgrading in terms of physical properties, product distributions, product quality and type and quality of formed coke. Chapter 6 tests the effect of different hydrogen sources as well as effect of tetralin upon the inhibition of coke formation and heavy oil upgrading. Additionally, Chapter 6 shows effect of tetralin and different hydrogen source on type and quality of formed coke after upgrading of heavy feed. Chapter 7 provides the conclusion of this study along with further recommendations and future work

.

Chapter 2
Literature Review

2.1 Introduction

Oil can be defined as chemical organic compound that is obtained from living organisms. Oil mainly consists of carbon and hydrogen and can be found in gaseous, liquid, semisolid and solid states. The oil in gas and liquid states is known as conventional oil. However, oil that tends to be found in a solid or waxy state is known as unconventional oil (Riazi, 2005; Gray, 1994). Heavy oil, extra heavy oil and bitumen are common types of unconventional oil. They are found in shallow deposits and are formed from conventional by the effects of weathering and bacteria (Clarke, 2007).

Heavy oil, extra heavy oil and natural bitumen are characterized by low American Petroleum Institute (API) gravity, high viscosity, are deficient in hydrogen and rich in carbon and sulphur elements. Additionally, they have a high concentration of oxygen, nitrogen and metals such as nickel and vanadium. Oil with API gravity between 20^o and 10^o and a density above 1.00 g/cm^3 is classified as heavy oil. Extra heavy oil is usually defined as having an API gravity of less than 10^o and a viscosity at reservoir conditions of no greater than 10,000 cP (Ancheyta, 2013). Natural bitumen tends to be more viscous in comparison with extra heavy oil, where its viscosity is over 10,000 cP at reservoir conditions, and a lower API gravity of 5^o (Speight, 2005; Meyer et al., 2007).

Table 2.1 shows details about the chemical and physical properties of heavy crude oil and natural bitumen.

Table 2.1. Physical and chemical properties of heavy crude oil and natural bitumen (Meyer et al., 2007).

Properties	Unit	Heavy Oil	Natural Bitumen
API gravity (at 15°C)	degrees	16.3	5.4
Viscosity (at 25°C)	cP	100,947.0	1,290,254.1
Viscosity (at 38°C)	cP	641.7	198,061.4
Asphalt	wt%	38.8	67
Carbon	wt%	85.1	82.1
Hydrogen	wt%	11.4	10.3
Nitrogen	wt%	0.4	0.6
Oxygen	wt%	1.6	2.5
Sulphur	wt%	2.9	4.4

2.2 Chemical composition of heavy oil and bitumen

Generally, reservoir fluids (e.g. light oil, heavy oil) are believed to be degraded chemically and biologically by the action of micro-organisms (Santos et al., 2014; Clarke and Trinnaman, 2004). As a result of oil degradation phenomenon the chemical and physical nature of oil changes. The oil form after degradation phenomenon could tend to be more viscous, deficient in a paraffinic group and has a high concentration of heteroatoms relative to original reservoir fluid. For example, due to chemical and biological degradation the conventional oil (e.g. light oil) can be transferred to unconventional oil (e.g. extra heavy oil). Additionally, the degree of complexity of reservoir fluids can be classified based on the combination of hydrocarbon groups (e.g. aromatic, paraffin), presence of heteroatoms and the level of isomer presence in the reservoir fluids (Gray, 1994). The following sections illustrate and explain the main constituents which are combined together to form heavy oil and bitumen.

2.2.1 Hydrocarbon groups

Chemistry simply classifies the chemical compound into two main groups, namely organic and inorganic, depending on their origin. The origin of inorganic compounds is from minerals, whereas carbon is the main component of organic compounds, as well them being derived from living organisms. Hydrocarbons are the largest group of organic compounds, and only contain hydrogen and carbon atoms. Hydrocarbons have the general formula of C_xH_y where x and y are integers. Also, hydrocarbons are classified into four main groups, namely paraffins, olefins, naphthenes and aromatics. In general, oil may contain a vast number of different hydrocarbon groups (Speight, 2014; Riazi, 2005). Paraffins, also known as alkanes, are a large group of hydrocarbons, with methane (CH_4) being the first compound in the homologous series. Paraffins may account for up to 20% by volume in crude oil and, because of their saturated characteristic, paraffins could remain stable during long periods of geological time (Riazi, 2005; Danesh, 1998). Examples of both normal paraffins and isoparaffins are shown below in Figure 2.1.

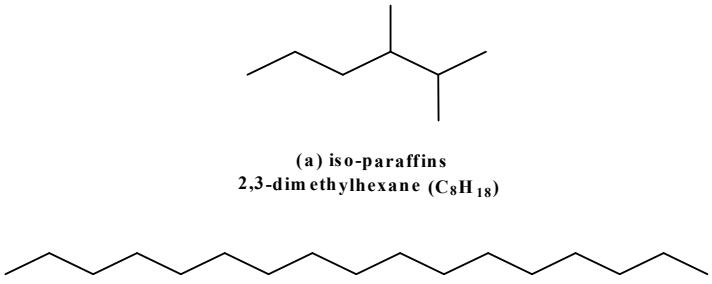

Figure 2.1. Examples of both normal paraffins and isoparaffins.

Olefins are unsaturated non-cyclic hydrocarbons which have at least one double bond between carbon atoms. In comparison with paraffins (saturated), olefins (unsaturated) are more reactive. Olefins are mainly produced from oil cracking reaction in the refinery and they are a valuable products of the petrochemical industry where they are used as feedstock

to produce different types of polymers, such as polyethylene (Cook and Graham, 2008; Danesh, 1998). Naphthenes are defined as saturated hydrocarbon rings with a general formula of C_nH_{2n}, and are also known as cycloalkanes. The volume percentage of naphthenes in crude oil may reach 60%, and polycycloparaffins may be available in heavier oil (Riazi, 2005; Gray, 1994; Boduszynski, 1988). Figure 2.2 shows the common types of naphthenes.

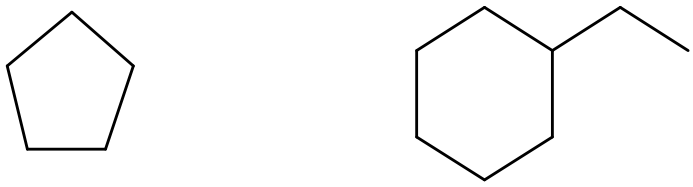

cyclopentane (C_5H_{10})

Ethylcyclohexane (C_8H_{16})

Figure 2.2. Common types of naphthenes.

Aromatics are cyclic unsaturated hydrocarbons which include carbon to carbon double bond, also, they are known by their fragment odours and benzene is the first compound in the aromatic family. Generally, heavy oil has a high content of aromatics relative to light oil. As an example, the percentage by weight of aromatics in coal liquid reaches as high as 98%. Moreover, polyaromatics are rich with heteroatoms such as sulphur and nitrogen. Different examples of polyaromatics are shown below in Figure 2.3 (Speight, 2014; Cook and Graham, 2008; Riazi, 2005).

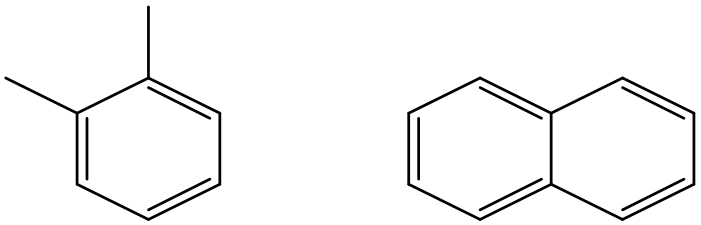

O-xylene
C_8H_{10}

Naphthanlene
$C_{10}H_8$

Figure 2.3. Examples of polyaromatics.

2.2.2 Heteroatoms

Sulphur, nitrogen, oxygen and metals (Ni and V) are the main heteroatoms which can be found in all the different types of oil in different concentrations. The main target is to minimize the concentration of heteroatoms when upgrading the oil. This reduction plays an important role in controlling undesired emissions, such as nitrogen oxide and sulphur oxide. Furthermore, metals (Ni and V) are considered a major reason for catalyst deactivation during oil upgrading (Speight, 1997).

The most important heteroatom is sulphur; it can be found in natural gas in the form of hydrogen sulphide (H_2S) as well as in oil in cyclic and non-cyclic compounds. Mercaptans (R-S-R) and sulphide (R-S-R′) are common examples of sulphur compounds in oil, where R and R′ are alkyl groups. Also, hydrogen sulphide can be associated with the natural gas and its amount could reach 30% by volume of gas. Additionally, the sulphur content in liquid oil varies between 0.05% and 6 % by weight (Riazi, 2005; Gray, 1994; Gray, 2015). Table 2.2 shows the range of heteroatoms on a weight basis in heavy oil (liquid).

Table 2.2. The range of heteroatoms on a weight basis in heavy oil (Speight, 2014).

Heteroatoms	Range (wt%)
Nitrogen (N)	0.1-2.0 %
Oxygen (O)	0.05-1.5 %
Sulphur (S)	0.05-6.0 %
Metal (V, Ni and Cu)	< 1000 ppm (0.1 %)

In general, as oil tends to be heavier (low API), the heteroatoms and carbon content increases; however, the quality of oil and hydrogen content decreases. The vanadium level should be controlled below 2 ppm to avoid severe corrosion and deterioration. Figure 2.4 shows examples of heteroatoms in heavy crude oil.

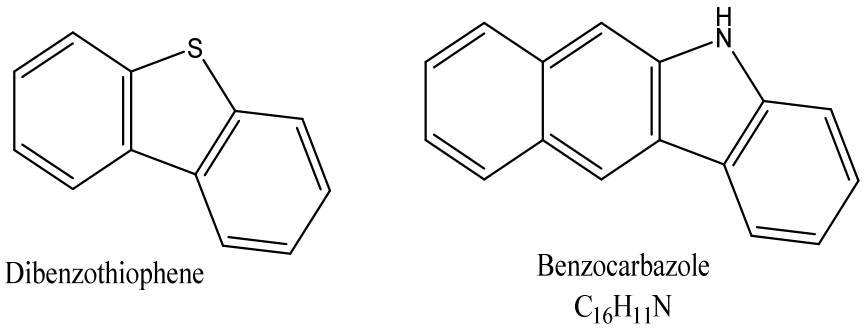

Figure 2.4. Examples of heteroatoms in heavy crude oil.

2.2.3 Asphaltene

Asphaltene is a complex group of compounds with a high boiling point of more than 500°C; which is rich with polyaromatic groups. Moreover, an asphaltene compound contains sulphur and nitrogen elements which are presented in benzothiophene and pyrrole respectively. Also, asphaltene contains heavy metals, such as nickel and vanadium, that attach to pyrrole nitrogen atoms in a porphyrinic ring (Merdrignac and Espinat, 2007;

Demirbas, 2002). Extensive studies were undertaken in order to understand and model asphaltene structure (Ancheyta, 2013). The most conventional definition of asphaltene is based upon its solubility properties, where it is defined as a fraction that is soluble in aromatic solvents such as benzene or toluene, and insoluble with excess of n-pentane or n-heptane, (Sharma et al., 2007; Andersen, 1994). Figure 2.5 shows structure of the asphaltene molecule.

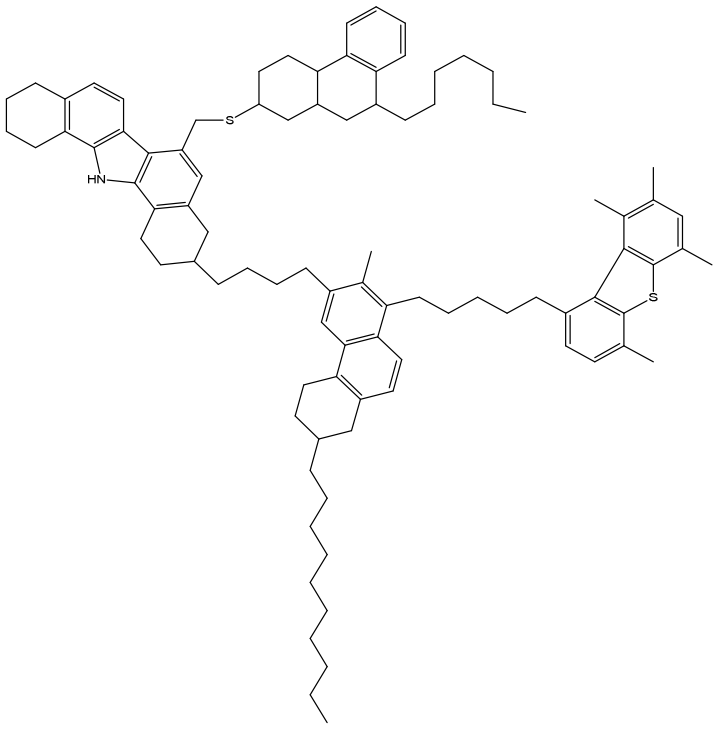

Figure 2.5. Structure of asphaltene molecule (Speight, 2014).

2.3 Heavy oil and bitumen extraction technology

Reservoir production involves three main stages in the extraction and production of crude oil for different applications. During the production process, multiple techniques are used to improve the production of reservoir fluids as well as to maintain the reserves. In this section, primary, secondary and enhanced oil recovery will be discussed in detail.

2.3.1 Primary and secondary methods for heavy oil and bitumen recovery

The first stage in oil production is primary recovery, during which oil production is controlled by natural drive mechanisms, such as the force of gravity and associated gas evolution from reservoir fluids. Primary recovery efficiency is low, differing from the various natural drive mechanisms involved. Primary production efficiencies vary between 5 and 20% of the original oil in place (OOIP) (Aurel, 1992).

The secondary production stage begins when the energy from the natural driving mechanisms declines. The main goal of the secondary recovery stage is to raise and maintain the reservoir pressure. In order to achieve this, external energy, usually water injection (i.e. water flooding) is used. The net efficiency of both primary and secondary methods combined is less than 40% of the OOIP (Dong et al., 2009; Butler and Mokrys, 1993).

The dominant methods for heavy oil and natural bitumen in the earlier production stages are open pit surface mining and cold production (Tüzünoğlu and Bağci, 2000; Greaves et al., 2000a). Recently, the oil industrial sector started concentrating on thermal energy as an external force to improve recovery of heavy oil and natural bitumen. Steam flooding and in situ combustion are the most important techniques in thermal extraction for unconventional oil; however, extensive studies and research were conducted to develop those techniques in order to improve the recovery rate (Shah et al., 2010; Greaves et al., 2012). THAI and steam-assisted gravity drainage (SAGD) are the most recent techniques created to overcome the difficulties for production of heavy oil and bitumen.

2.3.1.1 Surface mining

Surface mining is a reliable and economical method for very shallow oil reservoirs. It excavates the oil reservoir to produce oil sand and then the oil sand is treated with hot water and caustic soda (NaOH) to extract natural bitumen. It is a very efficient method where the total recovery of bitumen from a shallow oil reservoir can reach 90% of the original bitumen

in place; however, it is limited because it only works for shallow deposits. However, surface mining may be considered as an unfavourable method if the environmental impacts are considered, where rivers, lands and trees can be destroyed by implementation of surface mining method due to excavation (Shah et al., 2010).

2.3.1.2 Cold heavy oil production

The cold production method can be applied to recover heavy oil at reservoir conditions by drilling networks of horizontal wells in an oil reservoir. The cold production method operates without an external source of energy, such as heat, to improve the production (Huang et al., 1997). In order to maximize the production the horizontal wells are supported by multiple lateral branches where most of the oil reservoir area is covered. During the production processes, diluents such as naphtha are injected to reduce oil viscosity and different types of pumps are used to lift the oil to the surface. The cost of the cold production technique is low in comparison with other technologies, such as the thermal method (steam-assisted gravity drainage). However, the cold production recovery factor is low; it varies from 8 to 12% of OOIP (Villarroel and Hernández, 2013; Dusseault, 2008). This method is used in Venezuela as well as the North Sea to recover heavy oil. Figure 2.6 shows a well configuration of the cold production method.

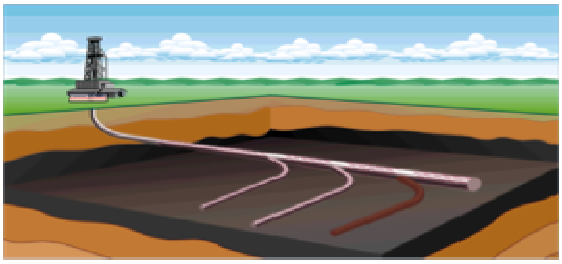

Figure 2.6. Cold production well configuration.

2.3.1.3 Water flooding

Water flooding can be considered as a useful production technique, especially for conventional oil. The implementation of water flooding starts at the secondary stage for conventional oil; however, it can be employed as a primary technique in unconventional oil deposits for limited cases (Romero-Zerón, 2012; Buckley and Leverett, 1942). The main objective of water flooding is to supply pressure to the reservoir to displace oil towards the production well. The process can be summarized as follows: first, the water is injected into the injection well (vertical and horizontal well) where the injected water provides a more uniform pressure in the oil reservoir and therefore, pushes the oil towards the producing well. Then, the submersible pumps are used to lift oil to the surface. Also, the water flooding technique further enhances the production of water from oil reservoir which can then be used in production processes to reduce the quantities of injected water. The effectiveness of the water flooding method tends to be low in deposits without underling water, where the injected water is dispersed and chanelled along the reservoir before it reaches the production well (Hawkins, 1991; Donaldson et al., 1985).

2.3.1.4 Cold heavy oil production with sand

Cold Heavy Oil Production with Sand (CHOPS) is a non-thermal recovery technique which has been successfully applied to the heavy-oil belt in Eastern Alberta, Canada. However, it has been reported that only between 5 and 15% OOIP can be produced by CHOPS (Istchenko and Gates, 2014; Du et al., 2015; Zhao et al., 2014). The production of heavy oil using CHOPS technique starts by deliberate initiation of sand influx into a perforated oil well and, as a consequence of that, the oil in place will be produced with the sand influx (Dusseault, 2002). Under CHOPS processes the major driving force which can maintain the deliberated sand influx are foamy oil flow phenomena and gravitational force (vertical stress generated by overburdened strata) (Dusseault, 2002). In this method, the production well is designed in such a manner that allows the sand and crushed rock to flow

up to the surface at the same time as the oil. The CHOPS technology depends on a vertical well which is equipped with an artificial lift system to lift the sand and oil to the surface. The implementation of this technique creates wormholes through the reservoir (Rivero et al., 2010). The wormholes play an important role in increasing the permeable flow paths which improve the production rate up to 30 times in comparison with cold heavy oil production alone. CHOPS is highly recommended for poorly consolidated sandstone reservoirs (Dusseault, 2002; Clarke, 2007). It is implemented extensively in Canada where the majority of the heavy oil deposits have a high porosity (poorly consolidated sandstone reservoirs). The effectiveness of CHOPS is related to the gas evolved during the heavy oil production. The high gas-oil ratio helps to disturb and set the sand particles in motion (Shah et al., 2010). Figure 2.7 shows a schematic diagram of the CHOPS well.

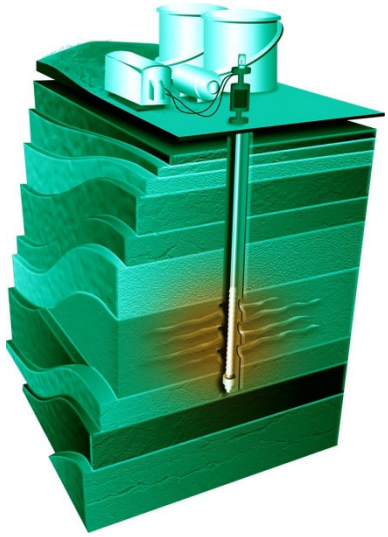

Figure 2.7. Cold heavy oil production with sand well schematic (CHOPS) (Dusseault, 2008).

The major challenge in CHOPS is in separating the produced sand, which needs special equipment, and is expensive. The expansion of wormholes is an important issue that should be taken into consideration during the production processes; it allows the stored water to migrate from its sources to fill the production well, which force the producer to shut down

the production wells later. Recent studies recommend filling the wormholes with clay or some gel foam in order to solve the water immigration problem (Clarke, 2007).

Table 2.3 summarizes commercial primary production methods for heavy oil and bitumen.

Table 2.3. Summary of commercial primary production methods for heavy oil (Clarke, 2007).

Method	Current usage	Remarks
Surface mining	Used in Canada for shallow oil sand	High recovery factor High environmental impact
Cold heavy oil production (Horizontal well and multilateral well)	Used in Venezuela, some used in North Sea	Low recovery factor Low capital expenditure relative to thermal technique
Water flooding	UK Continental shell	Considerable cost Cause Channelling in absence of underling water
Cold heavy oil production with sand	Used in Western Canada	Low recovery factor Requires good gas-oil ratio Unconsolidated sandstone reservoir

2.3.2 Enhanced recovery technologies for heavy oil and bitumen

Enhanced Oil Recovery (EOR) is classified as the last stage in reservoir production. In this phase, external thermal energy, gas injection or chemical injection are used to stimulate production. EOR processes are selected based on the fluid characteristics, such as oil viscosity, the geology of the reservoir and the OOIP (Taber et al., 1997). The main goals for EOR technologies are to improve the displacement of heavy oil by reducing its viscosity, decrease interfacial tension and increase the contact area of the reservoir during the extraction processes, which known as the improvement of sweep efficiency. Thermal technology is highly recommended to improve the production of extra heavy oil and bitumen, while the injection of gas and chemical material is more suitable for heavy oil (Ghoodjani et al., 2012;

Donaldson et al., 1985). Details of the commercial technologies used to enhance heavy oil and bitumen recovery will be discussed in the following sections.

2.3.2.1 Miscible displacement

The principle of miscible displacement is similar to water flooding. Gases such as carbon dioxide (CO_2), nitrogen (N_2) and light hydrocarbons (CH_4) are used to stimulate production (Sheng, 2015; Torabi et al., 2012; Miller and Hamilton-Smith, 1998). In this technique, gases are injected into the reservoir to reduce the interfacial tension of oil as well as maintain the reservoir pressure. A limited miscible zone is formatted between the displacing fluid and oil; this zone can be considered as a piston pushing the oil towards the production well (Monger and Coma, 1988). On the other hand, the used gases have a low density in comparison with the reservoir oil which can create good sweep efficiency. In general, the gas injection technique is categorized as a low-cost process relative to the thermal methods, because CO_2 and N_2 gas are abundant. The gas injection technique is not recommended for shallow deposits as displacement efficiency for gas injection decreases for high viscosity oil (Zuo et al., 1993; Thomas, 2008).Table 2.4 shows a comparison between major gases used in miscible displacement technique (Clarke, 2007).

Table 2.4. Comparison between major gases used in miscible displacement technique (Clarke, 2007).

Gas	Minimum Miscible Pressure	Cost	Extracts	Comment
Carbon dioxide	Low	High, due to separation of CO_2 and pressurizing recycled gas	Light to intermediate components (C_5-C_{30})	Causes asphaltene precipitation
Nitrogen	High	Low	Light components (C_2-C_6)	
Methane	High	High	Light components (C_2-C_6)	Enriches gas drive or dry gas drive

2.3.2.2 Chemical flooding

Similar to the miscible displacement principle, chemical flooding concentrates on reducing the interfacial tension of oil as well as improving sweep efficiency (Dong et al., 2009). The technique relies on polymers, surfactants and alkalis to enhance oil recovery by up to 40%. The major problem with chemical flooding is the adsorption of chemicals by the reservoir, especially the carbonate and clay. Also, it is considered a high cost process, due to the high cost of chemicals. Extensive studies were conducted to optimize this technology either by mixing polymers, surfactants and alkalis to form the emulsions, or by developing foams and microbes which form an in situ surfactant from biological processes (Shah et al., 2010; Wang and Dong, 2009; Liu et al., 2007).

2.3.2.3 Thermal technologies

Thermal technologies are the most powerful way to improve natural bitumen and heavy oil production. Steam flooding and in situ combustion are the dominant techniques in thermal methods to enhance unconventional oil recovery (Ghoodjani et al., 2012). All the thermal methods rely on external sources of heat to reduce oil viscosity which increases the mobility of heavy oil (Greaves et al., 2000a). In spite of thermal technologies' high energy cost, they are a feasible choice for enhanced heavy oil recovery. Details about several thermal methods, such as steam injection, in situ combustion and Toe to Heal Air Injection (THAI) will be discussed in the following sections.

2.3.2.3.1 Steam injection

Under this process, continuous steam injection supplies heat to the reservoir in order to stimulate production of heavy oil (Ali, 1974; Romero-Zerón, 2012). There are different patterns that the injection wells can be arranged in to supply heat for the reservoir; however, the highly recommended pattern is one which arranges the injection wells to surround the oil layer (Shah et al., 2010). Continuous steam injection through the surrounding pattern creates a steam zone which reduces the heavy oil's viscosity, as well as providing the driving force

pressure to help the heavy oil move towards the production well (Farouq Ali, 1982; Ali and Meldau, 1979). The recovery factor under the steam injection method is normally up to 60% OOIP (Clarke, 2007). On the other hand, the disadvantages of the steam injection process can be concluded as the heat loss in earth formation and high cost of generating steam.

2.3.2.3.2 Cyclic steam stimulation

Cyclic Steam Stimulation (CSS) is an older thermal technology also known as "huff and puff" which consists of three stages. Figure 2.8 shows the stages of CSS process. The first stage of CCS starts by injecting high-pressure steam through a single well for durations of between three weeks and one month. The second stage of CCS is "soaking" where steam stays in the reservoir to allow the heat distribute before the well turns to production mode (third stage) (Bera and Babadagli, 2015; Shah et al., 2010). The injection of high pressure steam during CCS process creates a fracture in the oil formation and as a consequence, injected steam rises rapidly in the reservoir due to its lighter density. Also, under CCS the concentrated steam injected on one side of the reservoir which provides incoherent heating, which pushes oil to the surface through the wells (Ho and Morgan, 1990). The CCS records a high recovery factor in the beginning of production stage and the obtained recovery factor remains within a narrow range of target level for a short period before it becomes gradually depleted. A new cycle of periodic of steam injection in the production well alternating with production is then implemented to boost the production rate towards the target level. However, more cycles could be needed to maintain the recovery factor at the same level during the CSS process. The recovery factor range of CSS varies from 10% to 40% (Alvarez and Han, 2013; Alikhlalov and Dindoruk, 2011).

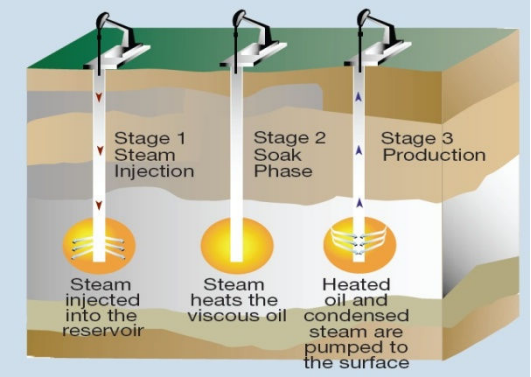

Figure 2.8. Cyclic steam stimulation process (Shah et al., 2010).

2.3.2.3.3 Steam-assisted drainage gravity

Steam-Assisted Gravity Drainage (SAGD) relies on continuous steam injection to provide the required heat to stimulate production of reservoir fluid. The SAGD well configuration consists of two parallel horizontal wells where the steam injection well is set about 5 meters on the top of the production well as illustrated in Figure 2.9 (Bera and Babadagli, 2015; Clarke, 2007). This source of heat (steam) reduces the heavy oil's viscosity and makes the heavy oil move downwards to the production well (see Figure 2.9). The success of SAGD relies on different issues, such as the geology of reservoir, the rate of the injected steam and operation conditions. In addition, the SAGD method provides a good recovery factor of 50% OOIP (Jimenez, 2008). However, it has been reported that SAGD is not a feasible choice for a thin reservoir (For example the depth of some of the Canadian reservoirs are only 6 meters) where the reservoir depth is not sufficient to set up SAGD well configuration (two horizontal well). Additionally, SAGD is considered an expensive method where two to ten barrels of water are needed to produce one barrel of heavy oil. Furthermore, as a result of the steam generation, greenhouse gases are formed and emitted. On the other hand, Expanding Solvent Steam Assisted Gravity Drainage (ES-SAGD) technology was developed in order to optimize SAGD costs as well as increase energy efficiency. The ES-SAGD method depends on

injecting steam with a solvent to enhance oil recovery. The ES-SAGD method recovery rates fluctuate from 40% to 60% OOIP (Dong et al., 2015; Shah et al., 2010; Yang et al., 2006).

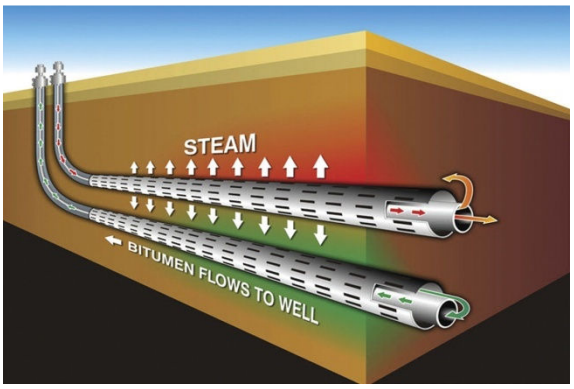

Figure 2.9. Steam Assisted Gravity Drainage (SAGD) well configuration (Tonn, 2010).

2.3.2.3.4 Conventional in situ combustion (fire flooding)

The conventional in situ combustion process relies on heat displacement using oxygen gas (or air) in order to improve heavy oil recovery (Liu et al., 2011; Guerra Aristizábal and Grosso Vargas, 2005; Moore et al., 2012). Similar to the water flooding method, air or oxygen-enriched air is injected into the target formation through the injection well for several days to a few weeks. The injected air is then burned using either an electrical heat source or down-hole gas burners. In the presence of oxygen, fuel (a portion of reservoir oil) and a source of ignition, the exothermic reaction taking place in the target formation produces steam, water and flue gases, which form the combustion zone. The steam provides a large amount of heat where the temperature rises up to 600^{o}C near the combustion zone (Castanier and Brigham, 2003; Bagci and Kok, 2001; Moore et al., 1995). As a result of the combustion reaction in the reservoir, heavy oil viscosity is reduced due to heat generated and the oil recovery becomes stimulated. Also the heavy oil displacements could be further improved by assistance of the formed gas from combustion reaction. Generally, in comparison with other thermal methods, such as steam injection, conventional in situ combustion has effective thermal displacement with less environmental impact due to the in situ generation of thermal

energy. However, low densities of flue gases, as well as rock heterogeneity, restrain the success of the process where gas channelling and overriding occurs (Castanier and Brigham, 2003).

The combustion front progression of conventional in situ combustion produces different zones between the injection and producer wells due to heat, mass transfer and chemical reaction (Shah et al., 2010). Those zones can be summarized as follows:

1. Burn zone: traces of solid as well as unburned residual oil are found in this zone. Also, the temperature profile directly increases from burn zone to front burn zone due to the continuous air injection.
2. Front combustion zone: in this zone the temperature reaches its peak value where oxidization reaction of heavy hydrocarbon initiate in the presence of oxygen
3. Downstream of the front combustion zone: due the high temperature of the combustion zone, further treatment of crude oil is achieved by thermal cracking as well as light ends (C_1-C_4) are produced. Also, as results of thermal cracking of heavy hydrocarbon organic solid formed which deposit on the rock.
4. Steam plateau: the temperature reduces in this zone and OOIP may undergo mild thermal cracking where the oil viscosity reduces; mild thermal cracking is known as visbreaking.
5. Water bank: in this zone the temperature decreases under the steam saturation temperature which leads the water to condensate next to the steam plateau zone.
6. Oil bank: the displaced light oil from the downstream zone is collected in this zone including the obtained light ends.
7. Beyond layer: the rest of the reservoir which is not affected by the in situ combustion process.

2.3.2.3.5 Toe to Heel Air Injection

Toe to Heel Air Injection (THAI) is classified as an advanced thermal technology which combines horizontal well technology with conventional in situ combustion technology. THAI could play two important roles by enhancing the production of heavy oil and partially upgrading it in situ, which is beneficial for transportation and further downstream upgrading (Xia and Greaves, 2002; Greaves et al., 2000a). Mainly, the producer well is placed horizontally in the direction of the driving force, near the combustion zone and air is injected, either through the horizontal well (HIHP) or vertical well (VIHP). There are different well arrangements; more horizontal wells are added for production and injection or more vertical wells are placed for injection (Greaves, 2004). Basically, steam is injected for around three months to create a suitable hot environment around the horizontal well and reservoir formation, as well as the vertical well. Compressed air is then injected to initiate the combustion. It generates a high temperature (between 400 and 600^{o}C) at reservoir pressure (30 to 50 bar) where thermal cracking reactions take place in the mobile oil zone (Guan et al., 2011; Greaves et al., 2008). The thermal cracking reaction partially upgrades the bitumen and heavy oil through carbon rejection. Normally, the bitumen API gravity value increases by several orders and light ends are produced from heavy hydrocarbons, as well as the viscosity of heavy oil decreasing (Greaves et al., 2000b). In comparison with conventional in situ combustion, THAI is characterized by the combustion and oil displacements taking place in a small section, which known as short displacement process (Greaves et al., 2012; Xia and Greaves, 2006).

Using THAI technology as a short displacement process creates several advantages for enhancing the recovery of bitumen and heavy oil. First, a short displacement process controls gases overriding where the flue gases from the combustion are forced to leave the formation through a horizontal well. Secondly, it increases the sweep efficiency because the

combustion propagation through the horizontal well leads to a high recovery factor of 80% OOIP. In addition, this technology is not affected by reservoir conditions or geology of the reservoir like other thermal techniques. It is feasible at low pressure, deeper reservoirs and thinner reservoirs, (Liang et al., 2012; Shah et al., 2010; Clarke, 2007; Xia et al., 2003). Figure 2.10 illustrates the THAI process.

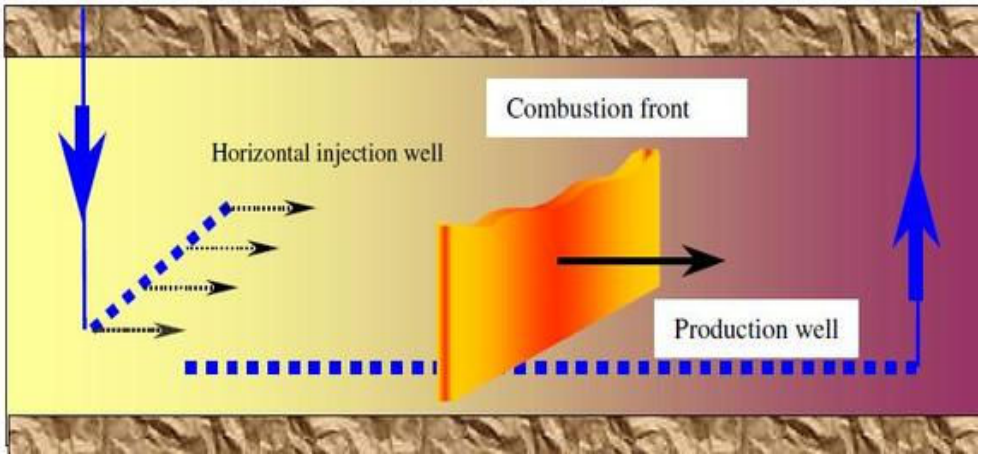

Figure 2.10. Toe to Heel Air Injection (THAI) processes (Xia and Greaves, 2006).

2.4 Chemistry of upgrading heavy oil and bitumen

Within this section, the chemical mechanism of heavy oil and bitumen upgrading will be discussed in order to explain the findings and observed experimental results. The ultimate chemical and physical objectives of upgrading heavy oil and bitumen can be summarized by the following points (Timko et al., 2015; Schacht et al., 2014; Chao et al., 2012; Gray, 1994) to:

1. Enhance production of middle distillates which have a boiling point below 525°C by breaking carbon to carbon and carbon to sulphur bonds of high molecular weight components in heavy oil and bitumen.
2. Maximize Hydrogen to Carbon mol ratio (H/C) of middle distillate products to meet market desirable value of 1.8 (mol/mol).

3. Suppress formation of undesired products, such as coke, to prevent catalyst deactivation.
4. Reduce heteroatom concentrations, such as sulphur and nitrogen, down to very low levels to avoid emission of undesirable gas such as nitrogen oxide and sulphur oxide.
5. Improve physical properties of produced oil after upgrading, such as API gravity and viscosity.

Generally, heavy oil and bitumen undergo simultaneous series reactions under thermal and catalytic upgrading. Gray (1994b) suggests the terms "primary upgrading" and "secondary treatments" to facilitate understanding of the chemistry of heavy oil upgrading. Primary upgrading is the first step towards converting large molecules in heavy oil and bitumen into light and more valuable products (middle distillates). This step mainly depends on a significant breaking of carbon to carbon (C-C) bonds in heavy oil by using thermal energy. In addition, C-C bond breaking can be promoted by prober catalysts in the presence of hydrogen gas (H_2). Thermal cracking and hydroconversion are the commercial terminologies for primary upgrading (Speight, 2013; Gray, 1994). In the secondary step, the products after primary upgrading are further treated in the presence of prober catalysts and H_2, where further improvement in the products' quality (sulphur and metal removal) is the ultimate target in this step. Hydrotreating is the most common commercial process to conduct the secondary treatments (Edwards et al., 1986; Wailes et al., 1980; Tang et al., 2014).

Primary upgrading and secondary treatment are different steps; however the two steps share implied chemistry (Gray, 1994). At primary upgrading, the thermal reaction is dominant over the catalytic reaction due to the high temperature however, at milder reaction temperatures the secondary treatment leads to (Hsu and Robinson, 2007).

2.4.1 Thermal reaction

At high temperatures, even without catalysis, the primary upgrading of heavy oil can be achieved by breaking chemical bonds to produce light oil. Carbon to carbon (C-C), Carbon to Hydrogen (C-H) and Carbon to –Sulphur (C-S) bonds are the main bonds affected by thermal reaction. In order to achieve a moderate rate of C-C bond breaking, the temperature of the order of 420°C is required in the absence of a catalyst (Gray, 1994). Furthermore, the C-C and C-H bonds in the aromatic groups are much stronger than other hydrocarbon groups, due to resonance stabilization and that the aromatic bonds are unbreakable at temperatures of less than 600°C (Gray, 2015). Primary upgrading at temperatures below 400°C are limited and it needs an initiation by a very active catalyst, such as zeolite, to promote C-C bond breakage (Gray, 2015). In conclusion, the primary upgrading should be operated at a temperature above 420°C to promote C-C bond breakage; also the contribution of catalyst at high reaction temperature is limited. Table 2.5 shows the required energy to initiate bond breaking in different hydrocarbons groups.

Table 2.5. Bond dissociation energy for different hydrocarbon groups (Benson, 1976; Gray, 2015; Gray, 1994).

Chemical bond	Energy (kcal/mol)	Reaction Temperature °C
C-C (aliphatic)	85	< 420
C-H (n-Alkanes)	98	< 420
C-H (aromatic)	110.5	< 600
C-S (methyl sulphide)	77	< 420

2.4.1.1 Cracking of paraffins

Thermal reaction of paraffins is considered as a base line to understand and develop a reaction mechanism of other types of hydrocarbons groups under high reaction temperature. In the absence of catalysts, the cracking of paraffins molecules is initiated by thermal energy. As a consequence, highly active free radicals form and the cleavage of C-C bonds proceeds

via free radical chain reactions (Chen and Yan, 2008; Gray, 1994; Magaril, 1967). The thermal reaction stages of paraffins are as follows (Gray, 1994):

Initiation:

$$M \xrightarrow{k1} 2R^{\cdot} \quad 2.1$$

Propagation:

Chain transfer

$$R^{\cdot} + M \xrightarrow{k2} RH + M^{\cdot} \quad 2.2$$

β-scission

$$M^{\cdot} \xrightarrow{k3} R^{\cdot} + Olefin \quad 2.3$$

Termination:

$$Radical + Radical \xrightarrow{k4} Product \quad 2.4$$

where M is the parent compound, and $R^{\cdot}$ is the smaller alkyl radical.

The chain reaction takes place when reactions 2.2 and 2.3 are more frequent relative to reactions 2.1 and 2.4. Also, reaction pressure plays an important role in directing the reaction pathway, where paraffins thermal cracking at low pressure (101.3 KPa) tends to form lighter olefins such as ethylene (Gray, 1994). However, at high pressures (≥ 10 MPa) both hydrogen abstraction reactions (equation 2.2) as well as radical addition reactions (equation 2.4) become more frequent. Additionally, at elevated pressure the thermal cracking of paraffins can be illustrated in terms of a single-step mechanism where the β-scission reaction (equation 2.3) is less important (Kissin, 1987; Ford, 1986; Fabuss et al., 1964). Moreover, it has been reported that thermal cracking of paraffins under moderate reaction pressure (3-7 MPa) can be described in terms of a two-step cracking (equation 2.2 and 2.3) (Zhou et al., 1987; Zhou and Crynes, 1986; Mushrush and Hazlett, 1984). The heavy oil and

bitumen constituent is deficient in paraffins; however, the side chains of the heavy molecules tend to react according to the paraffins thermal cracking (Gray, 1994).

2.4.1.2 Olefins reaction

The hydrogenation reaction of olefins takes place in the presence of catalysts and hydrogen to form saturates. However, in the absence of H_2 or catalysts, olefins are involved in free radical reactions to form either more olefins or diolefins as follows (Gray, 2015; Gray, 1994):

Hydrogen abstraction:

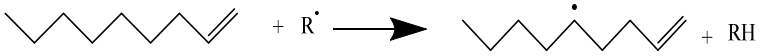

2.5

β-scission:

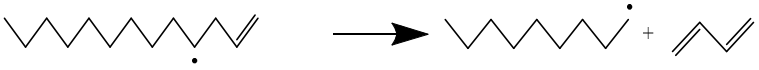

2.6

Addition:

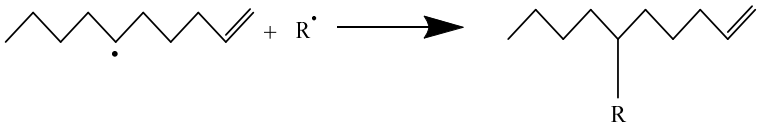

2.7

2.4.1.3 Naphthene reactions

The naphthenes rings are linked with other groups via the paraffinic bridge. Under high reaction temperatures (in the absence of catalysts) the naphthenes rings follow a similar mechanism to paraffins thermal reaction, however naphthenes can also follow additional pathways, such ring opening and dehydrogenation. The reaction chemistry of naphthenes shows that the products released are mainly naphthenic groups and the associated chains which consider more readily than breaking up of naphthenic aggregates. The naphthenes' thermal reaction is illustrated in the following equations (Gray, 1994; Savage and Klein, 1988):

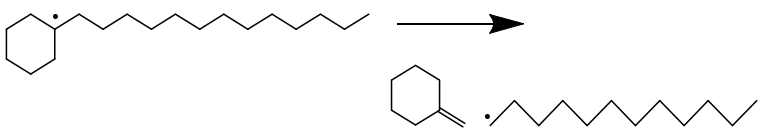

2.8

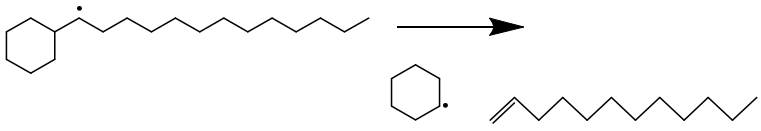

2.9

Naphthenes can be hydrogenated to form aromatics in the absence of hydrogen and catalysts. For example, tridecylcyclohexane could be hydrogenated at a high reaction temperature (450°C) to form an aromatic and toluene. Additionally, in the presence of catalysts in a rich hydrogen atmosphere, the reverse reaction can take place, where the naphthenes are produced from aromatics. The hydrogenated reaction of tridecylcyclohexane is presented as follows (Gray, 1994):

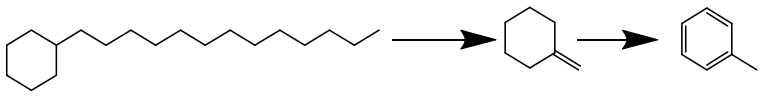

2.10

2.4.1.4 Alkylaromatic and aromatic reactions

Aromatic groups, such as benzene, are not cracked thermally at temperatures below 600°C. However, the thermal reaction mechanism of alkylaromatics is similar to alkylnaphthanes, where the thermal cracking removes the side chains and gives the following distributions: alkylaromatic with shorter side chains, alkanes and olefins (Gray, 2015; Savage and Klein, 1987). The produced alkylaromatic radicals due to thermal cracking of alkylaromatics tend to participate in condensation reactions which give dense fused aromatics and eventually coke (Towfighi et al., 2002). Poutsma (1990) suggested that the following radical reaction forms the bridge aromatic compounds. The bridge aromatic compounds

could then propagate via addition reactions to form a cluster of aromatic rings that can lead to coke formation (Poutsma, 1990).

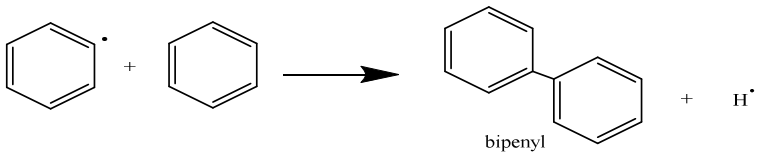

2.11

2.4.2 Catalytic reactions

Thermal reaction (primary upgrading) is dominated by the conversion of heavy molecules to form more valuable products, such as middle distillates. However, catalysts play an important role during primary upgrading, where they enhance hydrogen uptake as well as inhibit condensation reactions which could lead to suppressed coke formation (Hart et al., 2015; Liu et al., 2009; Ren et al., 2004). Molybdenum, nickel, cobalt, iron and tungsten are active transition metals used for hydrogenation reactions (Panariti et al., 2000a). In addition, these metals have the ability of being active in either metallic or sulphide form. However, it has been reported that the metal sulphide form has a higher activity relative to the metallic form. High sulphur content in heavy oil can contribute to transferring metal oxide catalysts to active phase (sulphide form) under upgrading conditions (Bhattacharyya and Mezza, 2012; Panariti et al., 2000a; Derbyshire and Hager, 1992).

2.4.2.1 Reaction of aromatic compound

Hydro-aromatics and naphthenes were generated by hydrogenating the aromatic groups in the presence of proper upgrading catalysts and hydrogen gas. Hydrogenation reactions of aromatic groups are directly proportion to the number of rings; the more rings in the aromatic group, the more it thermodynamically tends to hydrogenation reaction. For example, benzene is hard to hydrogenate compared to phenanthrene and naphthalene (a polyaromatic) (Gray, 1994) The following reactions illustrate how these polyaromatics

undergo cycles of dehydrogenation and hydrogenation in the presence of proper catalysts and hydrogen gas:

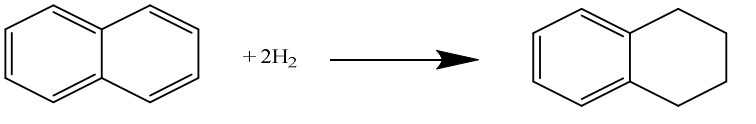

2.12

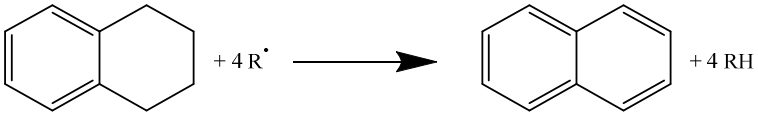

2.13

Hydrogenation and dehydrogenation reactions of aromatic group are very important in upgrading bitumen and heavy oil where these compounds are rich in polyaromatics and naphthenes. Different studies have been conducted to further understand and develop aromatic thermal reaction using deuterium as a tracer for hydrogen transfer, as well as model compound instead of heavy oil (Dwyer and Rawlence, 1993; Steer et al., 1992). According to those studies, free radical reactions, such as those in equation 2.13, occurs at temperatures of about 450°C which lead to little hydrogen shuttling.

In general, C-C bond breaking is mainly controlled by thermal reactions; however, catalysts can enhance the uptake of hydrogen in liquid hydrocarbons. This provider of hydrogen can lead to the minimizing of coke formation and produce more valuable products (Steer et al., 1992; Otterstedt et al., 1986; Miki et al., 1983).

2.4.2.2 Reaction of sulphur and nitrogen compounds

Sulphur compounds in heavy oil and bitumen show different reactivity. For example, the sulphur elements attached to aliphatic groups are readily removed during thermal reactions. However, the sulphur associated with aromatic groups, such as in thiophene compounds, needs further treatment in the presence of proper catalysts and hydrogen. The catalytic hydrodesulphurization (HDS) reaction can take place in two parallel pathways,

namely hydrogenolysis and hydrogenation. Moreover, reaction mixture, catalysts and hydrogen pressure are the key parameters affecting the two types of reactions (Gray, 1994).

The sulphur removal could be achieved via hydrogenolysis pathway where the sulphur bonds cleavage are caused by hydrogen. (Prins et al., 1989) developed the reaction mechanism of sulphur removal via hydrogenation pathway in the presence of catalysts; they found that the NiMo and CoMo catalysts are selective for sulphur heterocyclics in the preference of aromatic hydrocarbons. Also, they explained this result based on favourable energetic of coordination of the sulphur atom with active sites on a catalyst's surface. The following equations illustrate this mechanism (Prins et al., 1989):

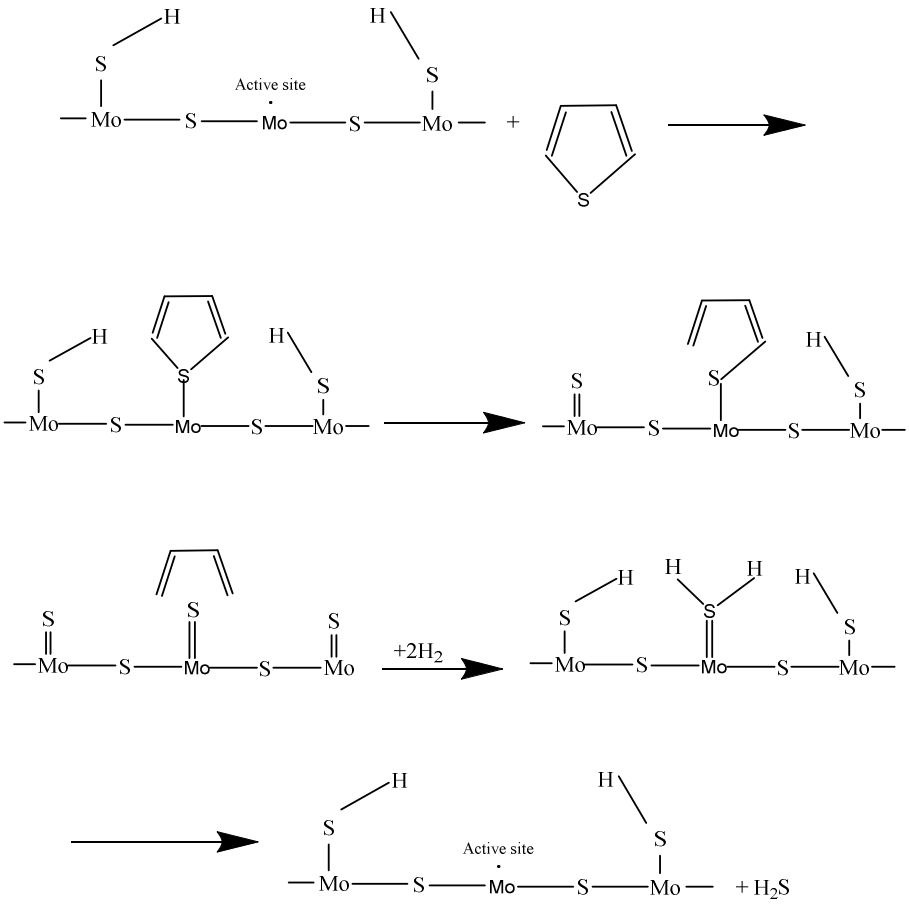

2.14

As shown above, hydrogenation of attached sulphur groups on molybdenum surface gave hydrogen sulphide and regenerate the active site on molybdenum surface (Gray et al., 1989). Eventually a new catalytic cycle will start to remove another sulphur atom following the same mechanism. However, compared with sulphur compounds, nitrogen compounds are less reactive. The lower reactivity of nitrogen compounds is thought to be due to the observation of hydrogenation pathway alone in the presence of catalysts. The following reaction illustrates the hydrodenitrogenation (HDN) reaction for a pyrrole compound:

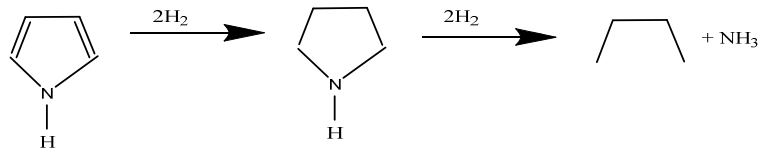

2.15

During the upgrading of heavy oil and bitumen, nitrogen compounds build up in the fraction because of the low reactivity. Gray et al. (1989) report in their study that nitrogen content doubled due to the accumulation of both pyrrolic and basic nitrogen compounds (see Table 2.6). Hydrogenation sites tend to be more acidic, which can lead to be poisoned by adsorption of nitrogen compounds because, hence HDS and HDN showed inhibition of hydrogenation of aromatic rings (Sundaram et al., 1988).

Table 2.6. Nitrogen content of pyrrolic and basic nitrogen compounds before and after hydrocraking of Athabasca bitumen (Gray et al., 1989).

Nitrogen Type (mol/kg)	Athabasca Bitumen	Hydrocracker (427°C)
Pyrrolic N	0.12	0.22
Basic N	0.09	0.16

2.4.2.3 Demetallisation reactions

Metals such as nickel and vanadium (Ni and V) are present in heavy oil and bitumen as organometallic complexes and poryphyrin types. The poryphyin types are studied and chemically defined in the literature which is used to explain upgrading of heavy oil in term of metal removal, also, metal removal of non-porphyrin types are thought to display similar trends. Metal removal can be performed during thermal reactions due to the cleavage of C-heteroatom bonds as well as via catalytic upgrading pathway. However, the metal removal completed by a catalytic reaction is called hydrodemetallization (HDM). The mechanism of catalytic removal of vanadium and probable sequence of steps was presented by (Asaoka et al., 1987). They reported that porphyrin hydrogenated to form chlorine structures, which loses the vanadium to the catalyst's surface and eventually, pyrrole groups appears in the upgraded oil. Also, they found that as catalytic removal reaction of vanadium carries on, vanadium gradually accumulates as a bulk of vanadium sulphide and forms rod-shaped deposits with the composition of V_3S_4 on the surface of catalysts.

2.5 Coke formation

The thermal and catalytic cracking of heavy molecules during heavy oil upgrading results in the deposition of carbonaceous solid and an undesired product known as coke (Carrillo and Corredor, 2013). Coke is an undesired product because it impedes the performance of the catalyst and eventually leads to deactivate the catalysts. Coke can be classified into three main types, namely: shot-type coke, sponge-type coke and associate-shot-type coke (Siskin et al., 2006; Kelemen et al., 2007). The chemical compositions of feedstock as well as natural reaction conditions greatly influence the type of coke formed (Elliott, 2000). Picón-Hernández et al. (2008) reported that sponge-type coke is formed from feedstock which has moderate asphaltene and metal content (Picón-Hernández et al., 2008). Shot-type coke texture is characterised by a smooth and concave surface, and is very hard and

more difficult to burn. Shot-type coke is low in economic value and consists of individual particles that are spherical to slightly ellipsoidal, with average diameters of about 1-4 mm (Siskin et al., 2006). The sponge-type coke texture is characterised by a highly porous microstructure with a wide variety of pore sizes. Sponge-type coke is named for its sponge-like appearance, with different sized pores and bubbles in the coke matrix. The coke which has morphology between shot-type coke and sponge-type coke is classified as an associate-shot-type coke. Also, it has sponge-like physical appearance with evidence of small, shot spheres which just starting to form as discrete particles. Compared to shot-type coke, sponge-type coke has a higher economic value with a high potential to be used as fuel (Ellis et al., 1998). The coke can be formed chemically during thermal and catalytic upgrading through three main routes, namely: (1) propagation reaction of free radicals; (2) addition between low molecular radicals and activated asphaltene precursor; and (3) asphaltene combinations of asphaltene propagation (Towfighi et al., 2002).

2.6 Inhibiting coke formation

In the presence of active catalysts, quenching free radicals by activated hydrogen can help in suppressing coke formation from routes (1) and (2). Moreover, addition of an aromatic solvent (such as tetralin) can help dilute the coke precursor which can lead to relaxing the aggregated structure and inhibit coke formation from route (3) (Towfighi et al., 2002; Watanabe et al., 2010). The following sections will provide details on inhibiting coke formation from different chemical routes.

2.6.1 Inhibiting coke formation by dispersed catalyst

Impregnation of metal sulphide as very small crystallites on a high surface area support such as ɤ- alumina (ɤ-Al_2O_3) is a conventional way to improve the level of heavy oil upgrading in terms of suppressing coke formation. Furthermore, it is well known that the combination of Ni and Mo or Co and Mo supported on ɤ-Al_2O_3 increases the activity of

catalysts for hydrogenation of heavy oil during catalytic upgrading (Prins et al., 1989; Ho, 1988). However, the gradual deactivation of catalysts during heavy oil upgrading due to the deposit of coke and metal in the porous media (γ-Al_2O_3) has been considered as the main drawback.

Unsupported dispersed catalysts (or "additive" in some references or texts) are classified into two main groups, namely heterogeneous (fine, solid powder) and homogeneous (water and oil soluble) dispersed catalysts, where the transition metals (Mo, Fe, Ni, Co or Cr) are the essential constituents in both groups (Sahu et al., 2015; Zhang et al., 2007). The most common form of heterogeneous unsupported dispersed catalyst which can be used for upgrading heavy oil are inorganic metal compounds, such as metal oxides, $FeSO_4$ and metal alloys (Angeles et al., 2014; Del Bianco et al., 1993). Additionally, the following are examples of common homogenous oil-soluble unsupported dispersed catalysts for heavy oil upgrading: metal salts of organic acids such as naphthenates, multi-carbonyl and resonates (Liu et al., 2010; Ren et al., 2004; Lee et al., 1996; Del Bianco et al., 1993). Also, phosphomolybdic acid and ammonium molybdate are common examples for water-soluble unsupported dispersed catalysts (Angeles et al., 2014; Ortiz-Moreno et al., 2012; Lee et al., 1996).

Unsupported dispersed catalysts can be an alternative option which can eliminate susceptibility of catalyst deactivation. The high catalyst dispersion can be related to the high surface area of the reaction, which increases the accessibility of active sites for reaction, minimizing diffusion control during heavy oil reaction (Angeles et al., 2014; Panariti et al., 2000a). Unsupported dispersed catalysts are not bifunctional in nature as they do not promote cracking of C-C and C-heteroatom bonds by the acidic sites present on zeolites and alumina (Wu et al., 2010; Hongfu et al., 2002; Gray, 1994). However they are mainly responsible for activation of H_2 and interfere with free radicals which are produced from a

condensation reaction between aromatic clusters (Rezaei et al., 2012; Breysse et al., 2002). Eventually, that can lead to inhibition of coke formation and produce more valuable products (coke formation from routes (1) and (2), see section 1.5). It has been reported in the literature that the utilization of dispersed catalysts showed high activity in terms of coke reduction during heavy oil upgrading, even at severe reaction temperatures. However, at severe reaction temperatures, a few problems have been observed with particle agglomeration during heavy oil upgrading using unsupported dispersed catalysts (Angeles et al., 2014). Additionally, the properties and types of unsupported dispersed catalysts, as well as reaction conditions, are key factors for improving the level of heavy oil upgrading and inhibiting coke formation (Panariti et al., 2000b).

Extensive studies have been conducted to investigate the efficiency of unsupported dispersed catalysts' activity in terms of product distribution, physical properties and product quality during heavy oil upgrading. Using ultrafine particles and a pelleted Co-Mo/Al_2O_3 catalyst at a reaction temperature of 425^{o}C, the API gravity and viscosity of the produced oil was found to improve by respectively 9^{o} and 96 % viscosity reduction with ultrafine particles compared to 5^{o} and 79 % viscosity reduction achieved with pelleted fixed-bed catalyst (Hart et al., 2015). Similarly, Galarraga and Pereira-Almao (2010) investigated an ultradispersed trimetallic (Ni–W–Mo) submicronic catalyst for in situ upgrading at 380^{o}C in a batch reactor, with a stirrer speed of 500 rpm and a reaction time of 3–70 h. The API gravity increased by 6.5^{o} API and a viscosity reduction of 98% was observed relative to Athabasca bitumen (API gravity 9.5 and viscosity 7680 mPa s) (Galarraga and Pereira-Almao, 2010). Also, as the size of the particles decreases to nano-scale, its specific surface area increases while the diffusion path length decreases; this improves interaction with macromolecules and cracking reaction (Del Bianco et al., 1993).

Compared to HDT catalysts such as Ni-Mo/Al_2O_3 and Co-Mo/Al_2O_3, Nano Particles (NPs) of iron oxide (Fe_2O_3) are potentially cost effective, as hematite (α-Fe_2O_3) is one of the most abundant iron oxide minerals and is also nontoxic (Khalil et al., 2015). Additionally, nanoparticles of iron oxide do not require rigorous and special methods of preparation. Iron NPs can readily be separated using magnetic separation. Adding silica (SiO_2) and maghemite (γ-Fe_2O_3) NPs to in situ combustion substantially increases the fuel distillates produced and decreases the activation energies of the thermocatalytic conversion of heavy oil (Rezaei et al., 2013). Ovalles et al. (2003) showed that iron-dispersed catalyst upgrade Hamaca extra-heavy oil from 500 to 1.3 Pa.s viscosities, 14% sulphur content reduction, and 41% conversion of > 500^{o}C fraction relative to the original oil at 420^{o}C, 11 MPa, and a residence time of 1 h using a stirred batch reactor (Ovalles et al., 2003).

Panariti et al. (2000a) investigated the role of organic groups for homogenous unsupported catalysts and whether the presence of particular elements, such as phosphorous or sulphur, have a large effect on the upgrading process. They conclude that the upgrading process is independent of the presence of organic groups. However, the transient elements play an important role in the performance of catalysts where the molybdenum base catalyst shows a high performance in the heavy oil upgrading process (Panariti et al., 2000a). Furthermore, the operation conditions (reaction temperature, hydrogen pressure, reaction time and catalyst loading) and their effect on the upgrading of bitumen and heavy oil has been studied, and several observations can be noticed from the literature as follows (Shuyi et al., 2008; Panariti et al., 2000b; Panariti et al., 2000a; Fixari et al., 1994; Del Bianco et al., 1994): (1) The conversion of heavy hydrocarbons to distillates is thermally controlled (2) coke formation is decreased by introducing a dispersed catalyst; and (3) hydrodemetallization is a function of hydrogen partial pressure and catalysts presence, where it shows a high HDM % using Mo with a high hydrogen partial pressure.

2.6.2 Inhibiting coke formation by different hydrogen sources and aromatic solvents

Incorporating commercial supported catalysts and an alternative hydrogen source with in situ upgrading could be desirable in the search to find a cheaper substitute for expensive hydrogen gas (H_2). Natural gas (methane, CH_4) is one of main sources of H_2 and the direct use of CH_4 instead of H_2 during heavy oil upgrading can further minimize the cost of the intermediate step of H_2 production from CH_4 (Egiebor and Gray, 1990). Also, water can be used as an alternative source of hydrogen during heavy oil upgrading in situ (Watanabe et al., 2010; Dutta et al., 2000). In addition, the free-radical reaction mechanism can lead to incorporating CH_4 and H_2O (in the absence of catalysts) into hydrocarbon molecules via production of methyl (CH_3) and hydroxyl (OH) groups by free radicals ($R^{\cdot}$) (Ovalles et al., 1995; Dutta et al., 2000), and that can reduce coke formation products (coke formation from routes (1) and (2), see section 1.5) during thermal upgrading under CH_4 and H_2O. Moreover, the sulphidation reaction between the dispersed catalysts and the sulphur contained in the heavy oil can lead to the generation of active metal sulphide (Liu et al., 2009; Ovalles et al., 2003). This active phase also could be fulfil the function of activation of CH_4 (Ovalles et al., 2003; Egiebor and Gray, 1990), and that can participate in a further reduction in coke yield, as well as an increase in produced liquid after heavy oil upgrading. The reaction stages for upgrading under CH_4 are as follows (Ovalles et al., 1995):

Initiation:

$$R - R' \rightarrow R^{\cdot} + R'^{\cdot} \qquad 2.16$$

Propagation:

$$R^{\cdot} + CH_4 \rightarrow RH + CH_3^{\cdot} \qquad 2.17$$

$$CH_3^{\cdot} + R - R' \rightarrow R'CH_3(RCH_3) + R^{\cdot}(R'^{\cdot}) \qquad 2.18$$

Termination:

$$R^{\cdot} + CH_3^{\cdot} \rightarrow RCH_3 \qquad 2.19$$

$$CH_3^{\cdot} + CH_3^{\cdot} \rightarrow CH_3CH_3 \quad 2.20$$

$$R^{\cdot} + R'^{\cdot} \rightarrow R - R' \quad 2.21$$

where $R\ and\ R'$ are hydrocarbons.

Much research has explored the upgrading of heavy oil in the presence of CH_4, steam, H_2 and solvents such as tetralin. Ovalles et al. (2015) reported that extra heavy oil upgrading using tetralin as a hydrogen donor under steam injection conditions at 280-315°C, 1600 psi and silica-supported nano-iron oxide (Fe_2O_3), led to an 8° API increase for produced oil and 26% in sulphur reduction. Hart et al. (2014b) investigated the effect of steam on the CAtalytic upgrading Process In situ (CAPRI) process in the presence of commercial Co-Mo/AlO_3 at 425°C, and 20 bar of N_2. It was found that the coke yield was significantly reduced relative to upgrading in a free steam atmosphere. Egiebor and Gray (1990) studied pyrolysis and liquefaction of Highvale (Alberta subbituminous) coal under methane and tetralin in the presence and absence of Fe_2O_3 as a catalyst at 450°C reaction temperature and 19-24 MPa. It was reported that both non-catalysts and catalysed coal liquefaction under CH_4 showed a higher coal conversion compared to analogue reaction conducted under inert gas (Argon) (Egiebor and Gray, 1990).

It has been reported that coke formation can be promoted during thermal and catalytic upgrading of heavy oil by large molecules such as asphaltene (Rahmani et al., 2002). Wiehe (1993) suggested the phase separation reaction kinetic model (PSK) to explain coke formation during thermal and catalytic upgrading of heavy oil (coke formation from route (3), see section 1.5) (Wiehe, 1993). The stages of coke formation shown by the Wiehe (1993) model are as follows:

$$A^{+} \overset{k_A}{\rightarrow} aA^{*} + (1-a)(M^{*} + volatile) \quad 2.22$$

$$M^{+} \overset{k_B}{\rightarrow} bA^{*} + (1-b)(M^{*} + volatile) \quad 2.23$$

Equations 2.22 and 2.23 show that both reactive maltenes (M^+) and reactive asphaltene (A^+) produce non-reactive maltenes (M*) as well as an asphaltene core (A*) where k_A and k_B are rate constants and "a" and "b" are stoichiometric constants. The oil mixture (M^+, M* and volatile) has the ability to dissolve a portion of produced A*. However, if A* exceeds the solubility limit, the excess amount of asphaltene core could be precipitated (A^*_{ex}) as follows:

$$A^*_{ex} = A^* - A^*_{max} = A^* - S_L(M^+ + M^* + volatile) \quad 2.24$$

where A^*_{max} is the maximum amount of soluble A* in the oil mixture and S_L is the solubility coefficient, eventually the A^*_{max} is transfer to coke (C) is as follows:

$$A^*_{ex} \xrightarrow{k_C} C \quad 2.25$$

The coke formation during thermal and catalytic heavy oil upgrading can be reduced by slowing down the rate of reaction of equations 2.22, 2.23 and 2.25 by utilizing solvents. The solvents fulfil the following functions: (1) increase solubility limits, S_L; and (2) improve hydrogen transfer reaction and therefore inhibit coke formation (Savage et al., 1988; Rahmani et al., 2003; Rahmani et al., 2002; Wiehe, 1993). Rahmani et al (2002) tested the effect of liquid solvents such as tetralin upon thermal upgrading of heavy oil at a reaction temperature of 430°C in the batch mode. They found that the coke formation was reduced in consistency with the PSK model (Rahmani et al., 2002).

2.7 Surface upgrading technology of heavy oil and bitumen using dispersed catalysts

It has been reported that non-conventional oil (heavy oil and bitumen) is available in large quantities which can compensate for the shortage in fulfilling the world's energy demands. However, the chemical and physical nature of heavy oil imposes many hurdles during the upgrading and treatment processes (Sahu et al., 2015; Bellussi et al., 2013). In the

last few decades, several industrial and academic research centres have studied and developed different surface technologies to convert heavy oil to high-quality desired products which meet market requirements (economical and environmental). Among the different heavy oil upgrading technologies, hydroconversion in a slurry reactor is considered as the prominent technology to treat and upgrade heavy oil (Sahu et al., 2015). Hydroconversion of heavy oil in a slurry reactor rely on using once-through variant types of homogenous and/or heterogeneous dispersed catalysts. Additionally, hydroconversion in a slurry reactor can operate in the presence of inexpensive catalysts, such as iron-based catalysts, or low concentrations of very active metals such as molybdenum, which minimize costs (Hashemi et al., 2014; Angeles et al., 2014; Khalil et al., 2015).

VEBA-combi-cracking (VCC) was developed in Germany for coal liquefaction. A combination of fine coke powder from Bovey coal and red mud (iron-containing material) is used as a catalyst. It has been reported that the coal conversion was in the range of 90-94%, and the total produced product was 4,000 barrels/day. However, a high operating pressure (15-27 MPa) as well as large amount of catalysts (5 wt %) have been identified as major drawbacks of this process (Sahu et al., 2015; Ancheyta, 2013; Doehler et al., 1987).

The ExxonMobil group has developed the M-coke process for unconventional oil upgrading. They found that the M-coke process achieved 90% conversion at a reaction temperature of 440°C and a pressure of 17 MPa in the presence of phosphor-molybdenum acid and molybdenum naphthenate as dispersed catalysts. The ExxonMobil group has noticed that utilizing dispersed catalysts in the M-coke process showed a high activity as well as a high production rate (1 drum/day in lab scale); however, the high cost of catalysts prevent the use of this process (Schuetze and Hofmann, 1984; Bearden Jr and Aldridge, 1980; Bearden Jr and Aldridge, 1979). The ExxonMobil group also developed the MICROCAT-RC process for heavy residues. In this process, oil-soluble manganese and molybdenum were

used as homogenous dispersed catalysts (the particle size was less than 1 μm). They observed that coke formation was inhibited; however, catalyst recovery has been reported as an issue in the MICROCAT-RC process (Castañeda et al., 2012; Bearden, 1997).

Commercial scale application of hydroconversion of heavy oil in a slurry reactor in started with Eni Slurry Technology (EST) which was developed by R&D laboratories at Eni in the early 1990s (Bellussi et al., 2013). An organic oil-soluble molybdenum compound was used as a catalyst, and the upgrading reaction was performed at 400-450°C and a pressure of 150 bar of hydrogen (Bellussi et al., 2013; Montanari et al., 2003). It was reported that under the EST operating conditions, highly dispersed MoS_2 formed in situ, and that they also found that the shape and the size of the formed catalysts remained constant with a long reaction time (Sahu et al., 2015; Bellussi et al., 2013). However, it was reported that the catalyst's activity was impeded by the formed coke precipitated asphaltene and metals deposited. Separations of asphaltene as well as metal were recommended ahead of the hydrocracking reaction to mitigate this challenge (Sanfilippo, 2009; Marchionna et al., 2002). EST technology has been used to upgrade various types of heavy oil across the world. In 2005, Eni designed a reactor with a capacity of 1,200 Barrel Per Stream Day (BPSD) for upgrading Venezuela Zuata and Athabasc bitumen, and by 2012, the reactor capacity reached 23,000 BPSD. Additionally, in Italy, since the EST process started in 2005, around 23,000 bbl of feedstock has been successfully upgraded in the commercial demonstrating plant (Sahu et al., 2015; Bellussi et al., 2013).

The extensive research of CANada Centre of Mineral and Energy Technology resulted in the CANMET process. The CANMET process shows high activity in terms of feed conversion, as well as demetallization during heavy oil upgrading. The CANMET process operates at 440-460˚C reaction temperature and a pressure of 100-150 bar of hydrogen (Bellussi et al., 2013). Additionally, the upgrading of heavy oil was conducted by

the CANMET process in the presence of iron sulphate as an additive (1-5 wt% of $FeSO_4$) (Rana et al., 2007). Moreover, the CANMET process has been used at a commercial level, where 5,000 barrels were treated daily. However a few hurdles have been reported with separating the product from unconverted bottom oil, as well as the lack of desulphurization and denitrogenation reactions (Sahu et al., 2015; Khulbe et al., 1981). In 2006, Universal Oil Product (UOP) developed and modified the operating conditions of the CANMET process, and they eventually created a new version of CANMET called the UOP uniflex process. Using UOP uniflex processes, the upgrading reaction of heavy oil takes place in an up-flow reactor in the presence of new nano-scale catalysts (V_2O_5) which boost conversion of heavy oil to above 90% (Sahu et al., 2015; Rana et al., 2007).

2.8 Down hole catalytic upgrading

The difficulties and problems recorded during the dealing with bitumen and heavy oil do not stop after their production. The problems extend during the transportation and surface upgrading process (Shah et al., 2014; Rad et al., 2014; Lee et al., 2011; Weissman et al., 1996). Those challenges open many windows for researchers to investigate how to mitigate those obstacles. Appling down-hole catalytic upgrading could be a potential approach to facilitate transportation and upgrading of bitumen and heavy oil. In situ catalytic upgrading involves the use of the reservoir as a reactor, which offers cost, energy and environmental benefits as it utilizes heat energy from in situ combustion to drive the catalysis; most of the impurities, such as sulphur, vanadium, iron and nickel, are left behind in the reservoir, thus lowering the environmental footprint and impact on downstream refining processes, and reduce the cost of diluents to improve pipeline transport (Hart et al., 2014; Hoshyargar and Ashrafizadeh, 2013; Hashemi et al., 2013).

2.8.1 CAPRI add on THAI process

Catalytic upgrading process in situ (CAPRI) added on to the THAI method was studied extensively for more than fifteen years after the first work of Greaves et al. (Xia and Greaves, 2002; Hart et al., 2014; Greaves et al., 2012; Xia and Greaves, 2006; Xia et al., 2003; Greaves et al., 2000a). The THAI method is classified as an advanced thermal technology to enhance the recovery of heavy oil, where compressed air is injected to initiate the combustion and thermal cracking occurring at the mobile oil zone ahead of the combustion front. Further details about the THAI process have been reported in section 1.3.2.3.5. The CAPRI add on to the THAI process delivers two works together: first, it enhances unconventional oil recovery; second, it upgrades heavy oil using an in situ thermal source and catalytic bed. The THAI/CAPRI process is a modified version of the THAI process which equips it with a catalytic bed fitted in the perforation of the horizontal well. In order to simulate and create the CAPRI process conditions, the THAI process takes place to provide a reaction temperature between 400 and 600^{o}C at a reservoir pressure of 30 to 50 bar due to the combustion reaction (Thomas 2008). The thermal cracking reaction then takes place due to the high temperature in the mobile oil zone, which creates precursor conditions for catalytic upgrading. Finally, the bitumen and heavy oil are further upgraded through a hydroconversion reaction which takes place in the CAPRI section. Furthermore, during the THAI process, a water gas shift reaction and/or gasification reaction takes place, and as a result of this reaction, hydrogen gas is formed. In the presence of hydrogen, the CAPRI process can also be used as an in situ hydro-treating process to upgrade heavy oil and bitumen (Shah et al., 2010).

The CAPRI process has been tested experimentally by Greaves and Xia (2001), and the obtained results demonstrated the potential of THAI/CAPRI during upgrading of Wolf Lake heavy oil. It was observed that the THAI process alone increased the API gravity by

10° points, as well as a further increase in the range of 4-7° points by the addition of CAPRI. Additionally, Xia and Greaves (2002) simulated the THAI/CAPRI process at the laboratory scale using a series of 3-D combustion cell experiments at reaction temperatures between 500 and 550°C using a Co-Mo/alumina HDS catalyst. They reported that the oil recovery factor was 79% OOIP and API gravity increased to 23° relative to 11.9° for the feed oil (Lloydminster heavy crude oil), with a low viscosity of 20-30 mPas. These results demonstrate that the THAI/CAPRI process has the potential to enhance oil recovery, as well as upgrade heavy oil to almost light crude oil in a single step without resorting to an expensive surface upgrading process (Xia and Greaves, 2002). Moreover, Petrobank Energy and Resources Ltd implemented the THAI/CAPRI process in a well (P-3B) located at Whitesands near Conklin, Alberta, Canada. Additional upgrading has been noticed by analysing the oil produced from the P-3B well which can be attributed to the ability of the CAPRI section. This observation was in agreement with the laboratory-scale experiments conducted by (Xia and Greaves, 2002; Greaves and Xia, 2001). Petrobank Energy and Resources Ltd has operated the P-3B well in continuous production, with an oil production level of up to 400 barrels per day on a low air injection rate and limited sand produced from the sandstone reservoir encountered at Whitesands.

As a part of a large project delivered by the University of Birmingham for in situ upgrade of bitumen and heavy oil, the CAPRI process with supported catalysts was tested at laboratory scale to investigate the bitumen and heavy oil upgrade. Shah et al (2011) investigated the following factors in order to mitigate the catalyst deactivation hurdle: testing different types of commercial catalysts at a reaction temperature of 400 °C and a pressure of 20 bar of N_2 he found that the deactivation time of $CoMo/Al_2O_3$ was 95 hours, which was the longest period of catalyst deactivation. Also, in the same study, they found that the catalyst pre-treatment with hydrogen step showed a slight improvement in physical properties (API

and viscosity) of produced oil. Furthermore, the effect of a short run time was performed in the same study and Shah noticed that coke was formed and deposited on the catalysts, even with a short reaction time (2-4 hours) (Shah et al., 2011).

Hart et al. (2013) studied optimization of the CAPRI process using a micro-scale flow reactor with a range of commercial supported catalysts (e.g. Co-Mo/Al_2O_3), a temperature range of 350−425°C, a pressure of 20 bar (H_2, N_2) and a residence time of 9.2 min. They found that the CAPRI process reduced oil viscosity up to 82% relative to feed oil, as well as the upgrading of heavy oil in terms of API gravity in the range of 2°-7° points above feed oil (Hart et al., 2013). However, they observed that the CAPRI process was a good example of catalyst deactivation by coke formation due to thermal cracking of bitumen and heavy oil. Hart et al (2013) modified the CAPRI flow reactor by introducing a guard bed (activated carbon) ahead of the catalytic bed. Hart et al (2013) found that the amount of coke deposited on the catalysts after reaction was reduced to 40 wt% in comparison to 57 wt% in the absence of a guard bed, which can help extend catalyst life. Macromolecules such as asphaltenes could be absorbed by the guard bed and that can contribute to the reduction of coke deposition where asphaltenes are known to promote coke formation during thermal and catalytic upgrading (Hart et al., 2013).

Introducing unsupported dispersed catalysts during THAI processes could be an alternative option which can eliminate the susceptibility of catalyst deactivation. The nano-particles experience shorter inter-particle distances that increase the probability of active phase interaction with the hydrocarbon molecules. Ultra-dispersed NPs could be deployed in a once-through process, hence could avoid the hurdles of pre-packing the horizontal production well with pelleted HDT catalyst. However, this will require the precipitation or transport of the NPs into the mobile oil zone ahead of the combustion front during the THAI process. Also, high dispersion could be achieved by introducing homogenous unsupported

catalysts (oil soluble or water soluble) during THAI processes. However, using homogenous dispersed catalysts have a few challenges with the active form of catalyst generates in situ which later form fine solid particles or slurry phase due to the thermal decomposition (Del Bianco, Panariti, Di Carlo, Elmouchnino, Fixari and Le Perchec 1993; Panariti, Del Bianco, Del Piero and Marchionna 2000a). Furthermore, THAI processes could be further modified by considering substituting expensive hydrogen (H_2) by a low cost hydrogen source such as CH_4, where the intermediate step of H_2 production from CH_4 could be eliminated. Also, solvent injection during THAI processes could be quite a promising approach to suppress coke formation and eventually avoid blockage in the production well.

Chapter 3
Experimental, Materials and Methods

3.1 Introduction

In this chapter, an overview of feedstock properties, materials used and the properties of different types of unsupported dispersed catalysts are provided. Additionally, details of experimental protocols and instruments employed to perform upgrading of heavy oil, as well as minimising coke formation, are described in detail in Chapter 3. Moreover, analytical methods used to determine the level of heavy oil upgrading and the efficiency of the nano-dispersed catalysts are explained in detail through this chapter. Furthermore, the chapter covers design of experiments using the Taguchi method as a systematic approach to identify the most significant reaction parameters and determine the optimum reaction conditions in order to increase the level of heavy oil upgrading and inhibit coke formation.

3.2 Materials

3.2.1 Feedstock and its properties

Heavy crude samples were collected from Whitesands THAI pilot trial at Christina Lake, Alberta, Canada by Petrobank Energy and Resources Ltd. The samples were supplied to the reaction laboratory at the University of Birmingham, where numerous experiments and analyses were conducted to complete the research goals. The supplied crude samples were primary upgraded during the thermal recovery stage of the THAI process. The heavy feed is a mixture of partially upgraded crude produced by the THAI process from eight different wells. Following the validation, the samples were transferred from the Petrobank Energy and Resources Ltd barrel to the reaction laboratory-owned preserved barrel and zero-grade nitrogen gas was used to fill the rest of the barrel to avoid sample oxidation during storage. The chemical and physical properties of the crude samples were measured and are detailed in Table 3.1.

Table 3.1. Properties of THAI feedstock Crude.

Properties	Results	Units
Density @ 25 °C	0.9776	(g/cm^3)
API° gravity @ 15 °C	13.4	
Dynamic viscosity @ 20 °C	1482	(cP)
Asphaltene Content	14	(wt %)
Elemental analysis		
C	84.72	(wt %)
H	10.77	(wt %)
N	0.08	(wt %)
S	3.09	(wt %)
Ni	30	(ppm)
V	102	(ppm)
(Ni + V)	132	(ppm)
Simulate distillation		
Naphtha Fraction (Initial boiling point-177 °C)	0.68	(wt %)
Distillate Fraction(177 °C–343 °C)	28.18	(wt %)
Heavy Fraction (343 °C+)	71.60	(wt %)

3.2.2 Gases, solvents and dispersed catalysts

Table 3.2 shows the commercial gases, solvents and unsupported dispersed catalysts that were used during this study as received without further purification.

Table 3.2. Commercial gases, solvents and unsupported dispersed catalysts.

Item	Technical specification	Supplier
Nitrogen	Grade: Zero N4.8 (99.998%) Cylinder size: L (50L water capacity) Pressure (bar): 200	BOC
Hydrogen	Grade: Chemically pure zero grade N5.0 (99.999%) Cylinder size: L (50 L water capacity) Pressure (bar): 200	BOC
Methane	Grade: Zero N4.8 (99.998%) Cylinder size: L (50L water capacity) Pressure (bar): 200	BOC
1,2,3,4-Tetrahydronaphthalene (Tetralin)	Purity (GC) ≥ 98.5 %	Sigma Aldrich
Distilled water	Purity 100	
Iron(III) oxide	Nanopowder, <50 nm Particle size Powder, <5 μm, ≥99%	Sigma Aldrich
Nickel(II) oxide	Nanopowder, <50 nm particle size , 99.8% trace metals basis	Sigma Aldrich
Molybdenum(VI) oxide	Nanopowder, 100 nm ,99.5% trace metals basis	Sigma Aldrich
Molybdenum(IV) sulfide	powder, <2 μm, 99%	Sigma Aldrich
Iron(II) sulfide	−100 mesh, 99.9% trace metals basis	Sigma Aldrich

3.3 Experimental setup and procedures

3.3.1 Experimental setup

During this study, a 100-mL batch reactor was employed (Baskerville Reactors & Autoclaves Ltd, United Kingdom) to evaluate the effect of the following factors on heavy oil upgrading in term of product distribution, physical properties, product quality and quality and type of formed coke.

- Reaction factors and their levels, Table 3.4 provides the factors and their varied level
- Various kinds of unsupported dispersed catalysts containing transition metals oxide and transition metal sulphide, details about the catalysts type are tabulated in Table 3.2; and
- Other type hydrogen sources such as water and methane as well as tetralin as solvent.

Figure 3.1 and Figure 3.2 show respectively a schematic diagram and a picture of the batch reactor parts respectively. As shown in Figure 3.1, the 100-mL batch reactor is equipped with a high-efficiency inline agitator, a temperature thermocouple, a digital pressure gauge, two high-pressure bellows-sealed valves and a relief valve. In addition, the 100-mL batch reactor is attached to a high-powered heating mantle that supplies heat to perform the reaction at temperature up to 550 °C. A control cabinet connected to the batch reactor was employed to control both the speed of mixing and the heating rates during the reaction. Furthermore, a specific 60-mL stainless steel sleeve with baffles was designed to fit inside the reactor to allow the formed coke to be easily collected for weighing and thus to perform mass balance . The baffles also served to improve mixing by diverting the flow towards the agitator. Details of the batch reactor parts and functions are provided in Table 3.3.

Table 3.3. Batch reactor parts details.

Part Name	Supplier	Function	Operating Range
Furnace	Baskerville reactors & autoclaves ltd	Heating	Temperature up to 550 °C
Inline agitator with propeller impeller	Parvalux	To ensure thorough and continuous dispersion and mixing	Mixing speed 100–1000 RPM
Temperature thermocouple K type	RS Components	Measure actual temperature during the heating stage as well as during the reaction period	Temperature from 0 °C to 1000 °C
Stainless steel sleeve with baffles in the wall	University of Birmingham workshop	To allow the coke to be collected to perform mass balance and improve mixing	Service up to 60 mL as well as hold back or turn aside the flow
Digital pressure gauge	Keller	Measure actual pressure inside the batch reactor during the heating stage as well as during the reaction period	Measure pressure from 0 bar to 300 bar
High-pressure bellows-sealed inlet valve	Swagelok	Feed the gas to the reactor	Service up to 340 bar
High-pressure bellows-sealed outlet valve	Swagelok	Purge and collect the product gas from the reactor	Service up to 340 bar
Relief valve	Swagelok	Open gradually when the pressure increases beyond the operation limit	Open when system pressure reaches 120 bar
Control Cabinet			
Proportional-integral-derivative temperature controller PID controllermodel 2216e	Eurotherm	Control the heating rate during the heating stage as well as during the reaction period to maintain the temperature at the desired value	Adjust input and output power to hold the temperature at the required value
Agitator controller model 2216e	Eurotherm	Control the heating rate during the heating stage as well as during the reaction period to maintain the temperature at the desired value	Adjust input and output power to hold the speed of mixing at the required value

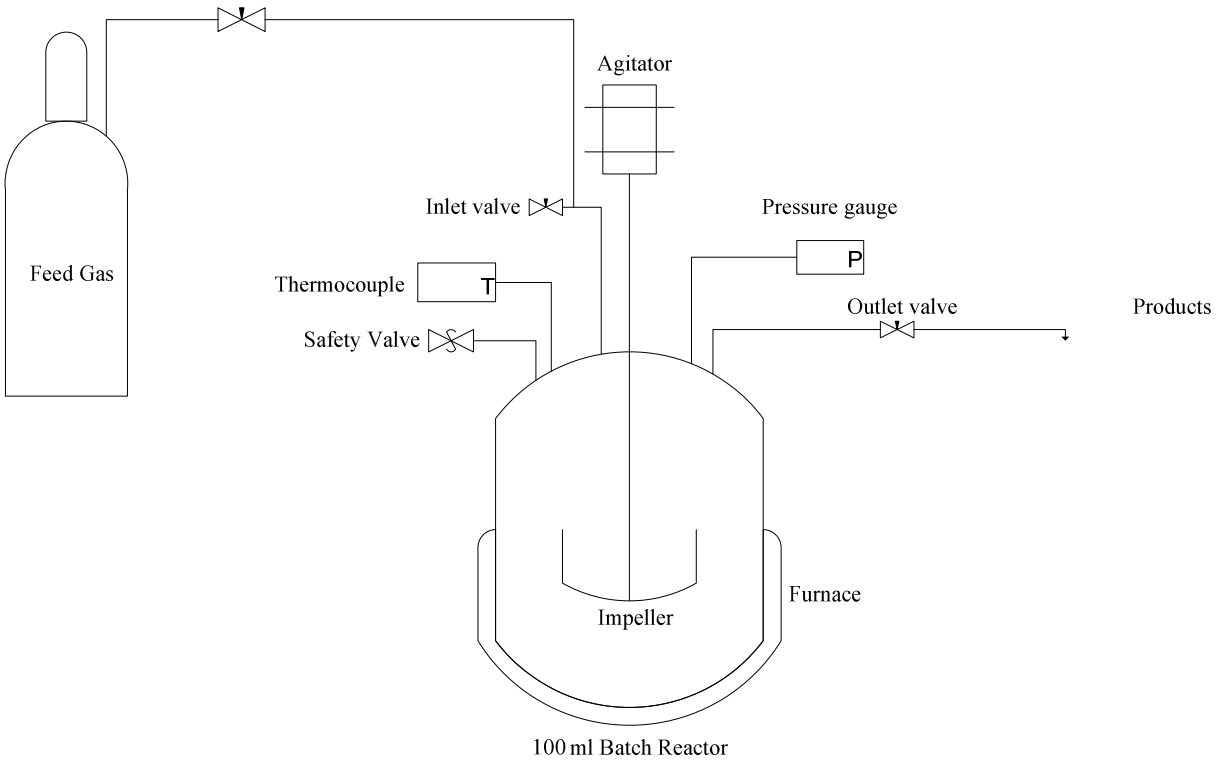

Figure 3.1. Schematic diagram of the batch reactor (Baskerville Reactors & Autoclaves Ltd, United Kingdom).

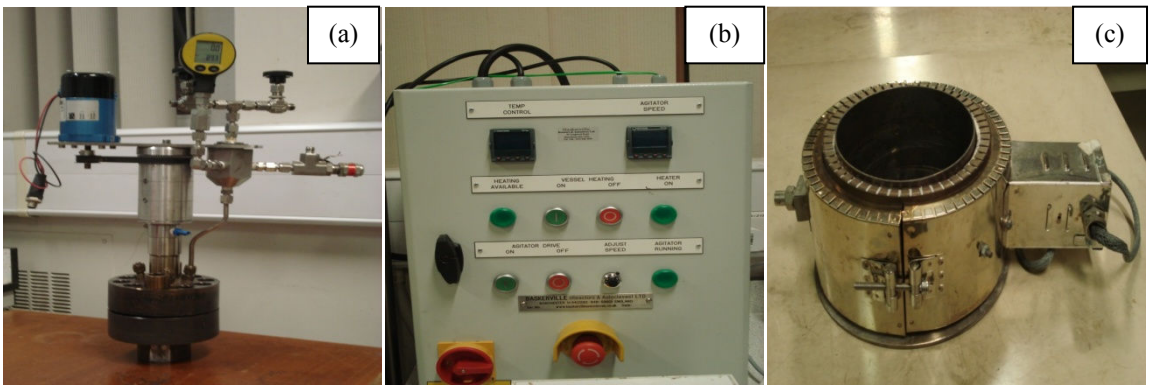

Figure 3.2. Batch reactor parts (a) 100 ml batch reactor (b) cabin controller (c) furnace.

3.4 Experimental procedures

The heavy oil upgrading experiments were carried out on THAI feedstock as reference oil (see Table 3.1) using a 100-mL batch reactor with the following procedures. Typically, 30 g of THAI feedstock and known amount of tetralin (free tetralin atmosphere in the case of studying effect of different hydrogen sources and selectivity and activity of unsupported

catalysts) was placed in a 60-mL stainless steel sleeve. The mass of the empty sleeve, THAI feedstock and tetralin were recorded in order to perform mass balance. The unsupported dispersed catalysts for catalytic upgrading were transition metal oxides and transition metal sulphide (see Table 3.2). Initially, a known amount of dispersed catalysts (no catalyst was used in the case of thermal upgrading) was placed into 30 g of THAI feedstock in a 60-mL stainless steel sleeve. The sleeve was then fitted inside the batch reactor, and the top and the bottom of the batch reactor were coupled using 10 stainless steel bolts. In a typical experiment, the batch reactor was pressurised to around 30 bar with the feed gas (e.g. nitrogen) and purged. The previous step was repeated three to four times to evacuate air from the batch reactor. The reactor then was pressurised with feed gas to the required value. Agitation was performed at the required speed using the agitator. In order to ensure that the unsupported dispersed catalysts were activated during the catalytic upgrading due to the high sulphur content of the THAI feedstock, a reaction was carried out at a milder temperature for certain time than the reaction temperature and time themselves, the batch reactor was then heated to the required temperature by the furnace to ensure activation of unsupported dispersed catalysts (Bhattacharyya and Mezza, 2012; Liu et al., 2009; Ren et al., 2004; Ovalles et al., 2003). The proportional-integral-derivative controller (PID controller) was programmed to adjust the input and output power of the furnace to quickly obtain the desired temperature. Once the reactor temperature reaches the required value, the reaction time is started. After the reaction is complete, the reactor is cooled down quickly to around room temperature using high-efficiency fans. During the reaction, the heavy fraction converts into light oil, light ends and coke fractions. The gas was collected using a gas bag while, the upgraded oil was left for 2 hr to facilitate the precipitation of the coke fraction and dispersed catalysts. Additionally, the upgraded oil was vacuum filtered using Whatman filter paper grade 6 with 6 μm pore size and 4.5 cm diameter to separate out any suspended coke fraction. The filter

paper was washed with tetrahydrofuran until colourless tetrahydrofuran was observed, and vacuum filtration was carried out to circulate air through the filter paper to completely dry the filter paper. Also, the coke left in the wall and bottom of sleeve was recovered and the dried filter paper was measured before and after the filtration in order to determine the total mass of the coke fraction. The mass of gas produced was calculated as the mass remaining after subtracting the masses of the light oil, catalysts and coke fraction in the reactor from the mass of THAI feedstock that was fed. The mass balances of the three products, light liquid, gas and coke, were calculated and reported as a percentage of the mass of feed oil fed using the following equation:

$$\boldsymbol{Yield}\ (\boldsymbol{wt}\%) = \frac{\boldsymbol{m_i}}{\boldsymbol{m_{feedstock\ THAI\ crude\ (B)}}}\ \boldsymbol{X\ 100} \qquad 3.1$$

where m_i is weight of component i.

After upgrading reaction under tetralin, the upgraded oil and tetralin were homogeneous mixture making it difficult to separate them because of the high boiling point of tetralin (207 °C at 1 atm). Hence, separating the tetralin from produced upgraded oil will affect the upgraded oil composition since some hydrocarbons can evaporate or escape in the process. Therefore, the physical properties (API° gravity and viscosity) reported here are those of the produced mixture (upgraded oil and tetralin). Summary of upgrading reaction experiments and conditions are presented in Table 3.4.

Table 3.4. Summary of upgrading reaction experiments and conditions [a].

Feedstock	Gas (Slovent)	Dispersed catalysts (size)	Dispersed catalysts Loading (wt%)	Reaction Temperature (°C)	Initial Pressure (bar)	Reaction Time (min)	Speed of mixing (rpm)
THAI	H_2	Fe_2O_3 (≤ 50 nm)	0.03-0.4	355-425	10-50	20-80	200-900
THAI	N_2	No catalysts	0	425	50	60	900
THAI	N_2	No catalysts	0	425	50	60	900
THAI	H_2	Fe_2O_3 (≤ 5 μm)	0.1	425	50	60	900
THAI	H_2	Fe_2O_3 (≤ 50 nm)	0.1	425	50	60	900
THAI	H_2	FeS (≤ 140μm)	0.1	425	50	60	900
THAI	H_2	MoO_3 (≤ 100 nm)	0.1	425	50	60	900
THAI	H_2	MoS_2 (≤ 2 μm)	0.1	425	50	60	900
THAI	H_2	NiO (≤ 50 μm)	0.1	425	50	60	900
THAI	CH_4	No catalysts	0	425	50	60	900
THAI	CH_4	Fe_2O_3 (≤ 50 nm)	0.1	425	50	60	900
THAI	N_2 (H_2O, 0.11 W/O)	No catalysts	0	425	50	60	900
THAI	N_2 (H_2O, 0.11 W/O)	Fe_2O_3 (≤ 50 nm)	0.1	425	50	60	900
THAI	N_2(tetralin 0.03 T/O)	No catalysts	0	425	50	60	900
THAI	N_2(tetralin 0.03 T/O)	No catalysts	0	425	50	60	900
THAI	N_2(tetralin 0.11 T/O)	No catalysts	0	425	50	60	900
THAI	N_2(tetralin 0.11 T/O)	Fe_2O_3 (≤ 50 nm)	0.1	425	50	60	900

[a] (W/O) is water to feedstock mass ratio, (T/O) is the tetralin to feedstock mass ratio

3.5 Taguchi method

Kinetic studies are considered as a powerful tool for performing reactor design, simulation and process optimisation. In particular, it has been reported in the literature that the kinetic study of hydrocracking of heavy oil is difficult due to heavy oil composition (owing to the large number of hydrocarbon compounds involved). However a body of research has been conducted to facilitate the kinetic study of heavy oil upgrading. It is complex since suitable consideration must be given to each compound and all the possible reactions during study kinetic of hydrocracking of heavy oil (Ancheyta et al., 2005; Yui and Sanford, 1989). Additionally, studying kinetics of hydrocracking of real feeds is also difficult because of analytical complexity and computational limitations, whereas the more compounds that are involved in the model, the more kinetic parameters that need to be estimated and as a consequence extra experimental investigation is needed (Ancheyta et al., 2005). During this study a simple systematic statistical approach (Taguchi method) was used instead of kinetic studies to understand the reaction mechanism as well as optimise reaction factors affecting upgrading of heavy oil during the THAI process.

The overall effectiveness of statistical method such as surface response methodology, full factorial and Taguchi method are somewhat similar. However, the Taguchi method is a more simple, systematic, low cost and comprehensive approach which attempts to provide a useful understanding and optimisation about the complex multi variable system with a limited number of experiments. These aspects show the effectiveness of Taguchi method as an attractive and alternative choice among the rest of the methods for studying optimisation of heavy oil upgrading during the THAI process when cost and simplicity are considered (Kowalczyk, 2014; Tansel et al., 2011; Simpson, 1998; Phadke et al., 1983).

The Taguchi method is a systematic approach to process optimisation. Here, optimisation means minimising the process variance while keeping the mean of the response

at the required value (Kowalczyk, 2014; Pignatiello Jr, 1993). The major advantages of Taguchi method are orthogonal array and signal-to-noise ratio (S/N). The orthogonal array is an economical way of simultaneously studying the effect of many variables on the mean of response (Section 3.5.1). In the Taguchi method, the signal-to-noise ratio is used to explore process variability (for more details see Section 3.5.2). By optimising a process with respect to signal-to-noise ratio, it is ensured that the resulting optimum process conditions are robust and stable, meaning that they have minimum process variation (Mukherjee and Ray, 2006). Figure 3.3 shows how the Taguchi method procedures are applied.

Extensive investigation of THAI process over the last decade has been conducted by Improved Oil Recovery (IOR) research group at University of Bath. A 3-D combustion cell has been used to simulate the THAI process to provide the useful understanding about the combustion front temperature sweeping efficiency. It has been reported that the combustion front temperature efficiency varied with the time and oil layer thickness. Also, they noticed after long simulation of THAI process using 3-D combustion cell (time = 480 min) about 90 % of sandpack was swept by temperature front higher than 400 °C. During this study the range of reaction temperature were selected based on the temperature front at short and long times of the THAI process(Hart et al., 2013; Shah et al., 2011; Xia et al., 2002; Greaves and Xia, 2000). Reaction temperature (°C), H_2 initial pressure (bar), reaction time (min), iron metal loading (wt %) and mixing speed (RPM) were selected as controllable factors. Table 3.5 shows the controllable factors and their levels.

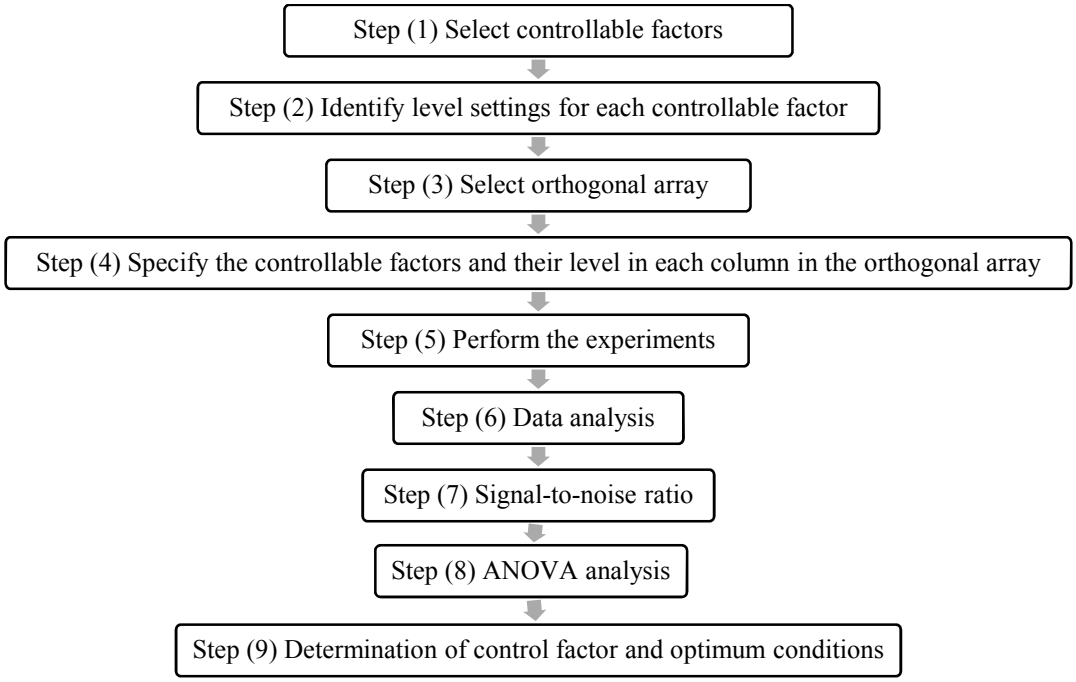

Figure 3.3. Taguchi method procedure (Kowalczyk, 2014).

Table 3.5. Selected controllable factors and their levels.

Factors	Control level			
	Level (1)	Level (2)	Level (3)	Level (4)
Reaction temperature (°C)	355	370	395	425
H_2 initial pressure (bar)	10	25	40	50
Reaction time (min)	20	40	60	80
Iron metal Loading (wt %)	0.03	0.06	0.1	0.4
Mixing speed (RPM)	200	400	600	900

3.6 Orthogonal array

The orthogonal array is a powerful tool proposed by the Taguchi method to generate a number of experiments to examine the effect of different controllable factors, with each factor having a different level (Kowalczyk, 2014; Athreya and Venkatesh, 2012; Ghani et al., 2004; Phadke et al., 1983; Kolahan et al., 2011). Selecting the right orthogonal array depends on the number of controllable factors and their levels. In this study, five controllable factors were select with four levels in order to generate the proper orthogonal array. Minitab 16

software was used. Table 3.6 shows the generated orthogonal array L_{16} from Minitab 16 software. The orthogonal array consists of five columns, which represent the control factors and their corresponding levels. In addition, every single row in the orthogonal array includes the experiment that should be performed at the given level of each control factor.

Table 3.6. Orthogonal array used to determine experimental conditions that were tested in the upgrading experiment.

Experiment Number	Factors and their level				
	Reaction Temperature (°C)	Initial H_2 pressure (bar)	Reaction Time (min)	Iron metal loading (wt %)	Speed of mixing (RPM)
1	355	10	20	0.03	200
2	355	25	40	0.06	400
3	355	40	60	0.1	600
4	355	50	80	0.4	900
5	370	10	40	0.1	900
6	370	25	20	0.4	600
7	370	40	80	0.03	400
8	370	50	60	0.06	200
9	395	10	60	0.4	400
10	395	25	80	0.1	200
11	395	40	20	0.06	900
12	395	50	40	0.03	600
13	425	10	80	0.06	600
14	425	25	60	0.03	900
15	425	40	40	0.4	200
16	425	50	20	0.1	400

3.7 Signal-to-noise ratio

The Taguchi method suggests a convenient approach to select optimum conditions for response variables using the signal-to-noise ratio (S/N) function. In its elemental form, the signal-to-noise ratio is the ratio between the desired values of a response variable and the undesired values of a response variable (Tansel et al., 2011). It is used to measure the quality characteristic of deviation from a desired variable and it should always be maximised in order to allow the response variable to approach optimum conditions (Kowalczyk, 2014; Mukherjee and Ray, 2006; Ghani et al., 2004). The Taguchi method proposes three main types of signal-to-noise ratios for the selection of optimum conditions. Table 3.7 shows the type, application and formula for each type. Details about the selection of optimum condition reported in section 4.6 where the proper signal to noise ratio function employed.

Table 3.7. Signal-to-noise ratio (S/N) type and application.

Signal-to-noise ratio type	Application	Formula
Smaller the better	Minimum response variable	$\left(\frac{S}{N}\right) = -10log\left(\frac{1}{n}\sum_{i=1}^{n} y_i^2\right)$
Larger the better	Maximum response variable	$\left(\frac{S}{N}\right) = -10log\left(\frac{1}{n}\sum_{i=1}^{n} \frac{1}{y_i^2}\right)$
Nominal the best		$\left(\frac{S}{N}\right) = -10log\left(\frac{1}{n}\sum_{i=1}^{n} \frac{1}{\bar{y}_i^2}\right)$

where

n: number of measured value

y_i^2: measured value

S^2: standard deviation

$\bar{y}^2$: mean of measured value

3.8 Data analysis

Following the Taguchi method, the analysis was conducted in two parts, namely mean analysis and signal-to-noise ratio analysis. As shown in Table 3.6, each experiment is a combination of different levels. In order to identify the main effect of each controllable factor, the Taguchi method suggests calculating the mean value of the measured response variable for the corresponding level setting. For example, the main effect of setting the reaction temperature to Level (3) is evaluated by calculating the mean of the measured response variables of Experiments (9, 10, 11, and 12). Similarly, the main effect of the initial H_2 pressure at Level (1) was evaluated by calculating the mean of the measured response variables for the corresponding level setting experiments (1, 5, 9, 13), and so on. Once all the mean values were calculated for each level of each controllable factor, the mean values for each controllable factor were plotted against the proper signal-to-noise ratio, the type was selected and the calculation of mean signal-to-noise ratio was performed following the previous procedure. Details of raw data of all run are tabulated in Appendix A.

3.9 Analysis of variance

ANalysis Of VAriance (ANOVA) is a statistical technique that is used to compare the means of at least three levels of different variables. The F-value and P-value were computed using one-way ANOVA to determine which variables have a significant influence upon heavy oil upgrading (Athreya and Venkatesh, 2012). One-way ANOVA was conducted using the following five steps:

1. State Hypotheses.

- H_o = all means of all level is same.
- H_1 = at least one difference among the means.

2. Analysis of degrees of freedom between different levels ($Df_{between}$), within each level (Df_{within}) and the total degrees of freedom (Df_{Total}).

3. Calculate the mean of the square between the different levels ($SS_{between}$), within each level (SS_{within}) and the total mean (SS_{Total})
4. Compute the variance between different levels ($\mu s_{between}$) and within each level (μs_{within}).
5. Determine F and compare with $F_{critical}$ to either accept or reject the hypotheses in Step 1.

The following equations are used to conduct the one way ANOVA:

$$\boldsymbol{Df_{between} = \kappa - 1} \quad 3.2$$

$$\boldsymbol{Df_{within} = N - \kappa} \quad 3.3$$

$$\boldsymbol{Df_{Total} = Df_{between} + Df_{within}} \quad 3.4$$

$$\boldsymbol{SS_{Total}} = \sum \left(\chi - \frac{G}{N}\right)^2 \quad 3.5$$

$$\boldsymbol{SS_{within}} = \sum(\chi - \bar{\chi}_1) \quad 3.6$$

$$\boldsymbol{SS_{between} = SS_{Total} - SS_{within}} \quad 3.7$$

$$\boldsymbol{\mu s_{between}} = \frac{\boldsymbol{SS_{between}}}{\boldsymbol{Df_{between}}} \quad 3.8$$

$$\boldsymbol{\mu s_{within}} = \frac{\boldsymbol{SS_{within}}}{\boldsymbol{Df_{withon}}} \quad 3.9$$

$$\boldsymbol{F} = \frac{\mu s_{between}}{\mu s_{within}} \quad 3.10$$

$$\textbf{Percentage contribution } \% = \frac{\mathbf{SS_{within}}}{\mathbf{SS_{Total}}} \quad 3.11$$

where:

κ: Number of levels.

N: Total number of response values.

G: Sum of all response at all levels.

χ: Value of response.

$\bar{\chi}_i$: Mean of all responses at each level.

3.10 Analytical instruments

The main products of the upgrading reactions are upgraded oil (i.e., liquid), non-condensable gas and coke. The feed and collected upgraded oil samples were analysed for API gravity, viscosity, and True Boiling Point (TBP) distribution, using the following analytical instruments an Anton Paar DMA 35 density meter, an Advanced Rheometer AR 1000 (TA Instruments Ltd, United Kingdom) and simulated distillation by Agilent 6850N gas chromatography (GC) in line with ASTM D2887 method. Product quality in term of sulphur and metal content and the upgraded oil samples were determined by Warwick Analytical Service, United Kingdom, using Inductively Coupled Plasma–Optical Emission Spectroscopy (ICP–OES) and nitrogen content was measured by a CE 440 elemental analyser. The asphaltene content was determined in accordance with method ASTM D2007-80 using n-pentane in order to evaluate the level of heavy oil upgrading. The surface morphology analysis was conducted on the produced coke as well as the spent dispersed catalysts using a Philips XL 30 SEM (XL 30 ESEM-FEG) equipped with a LaB5 emission source and operating at 15 kV. X-ray diffraction (XRD) analyses was conducted on fresh and spend dispersed catalysts using a Bruker D2 PHASER Diffractometer with a scan range from

0° to 160° and Co Kα radiation with a wavelength of 1.54056 Å. Details about analytical method and instruments will discussed in the following sections.

3.10.1 Density and API gravity

Density of the feedstock and upgraded oil was measured at 15 °C and reported in g/cm^3 using an Anton Paar DMA 35 (Anton Paar GmbH, Austria) digital density meter. The Anton Paar density meter consists of four major parts, namely: pump lever, U-shaped glass tube, temperature sensor and digital monitor. The Anton Paar density meter conducts density measurement based on the oscillating U-tube concept. The U-shaped glass tube was filled with the sample using the pump lever. The filled U-shaped glass tube was then agitated to measure the sample density based on the oscillating u-tube concept. The sample density and temperature results were displayed on the digital monitor. Calibration of the Anton Paar density meter was performed using distilled water to validate the density measurements of the feedstock and the upgraded samples. The calibration result shows that the density of distilled water is 0.9999 g/cm^3 at 15 °C, which almost matches the density of distilled water reported in the literature 1.0 g/cm^3 at 15 °C. Figure 3.4 shows the Anton Paar density meter and its parts.

Figure 3.4. Anton Paar Density meter.

American Petroleum Institute (API) gravity is a criteria widely used to measure crude grades; the higher the API gravity, the lighter and more desirable the crude oil. API gravity was calculated using the following equations:

$$\boldsymbol{API\ gravity} = \frac{\mathbf{141.5}}{\boldsymbol{SG}} - \mathbf{131.5} \qquad 3.12$$

$$\boldsymbol{SG} = \frac{\boldsymbol{density\ of\ sammple\ @\ 15\ ^{\circ}C}}{\boldsymbol{Density\ of\ water\ @\ 4\ ^{\circ}C} \approx \mathbf{1}\ (\frac{\boldsymbol{g}}{\boldsymbol{cm^3}})} \qquad 3.13$$

where SG is the specific gravity of oil.

The density measurement was repeated upon three different upgraded oil samples at the same reaction conditions, and the data were then averaged and reported.

3.10.2 Viscosity measurements

The viscosity of the feedstock as well as the upgraded oil was measured using an Advanced AR 1000 Rheometer (TA Instruments, United Kingdom). The major component parts of the equipment, as illustrated in Figure 3.5, are a fixed plate and a moving plate. A parallel 40 mm diameter aluminium plate was used as the moving plate during this study, and the viscosity measurement mode was performed as a function of shear rate vs shear stress. Initially, the rheological behaviour was studied by placing a known amount of sample on top of the rheometer fixed plate and then lowering the moving plate. Any excess sample outside the edges of moving plate was wiped off using a standard paper tissue. The gap between the fixed plate and the moving plate was usually 750 μm, however if the viscosity of the oil was too low it caused an error in the measurements. This gap was than reduced to suit these oils and so a variable gap was used in the viscosity measurements.

The measurements show that the feedstock and the upgraded oil have constant viscosities when the shear rate in range from 0.5 to 500 s^{-1}. This means that both the feedstock and the upgraded oil follow the behaviour of Newtonian fluid. Thereafter, the

viscosity measurements were conducted at a shear rate of 200 s^{-1} and a temperature of 20 °C. The viscosity measurements were repeated on two or three different upgraded oil samples under the same reaction conditions, and the data were averaged and reported.

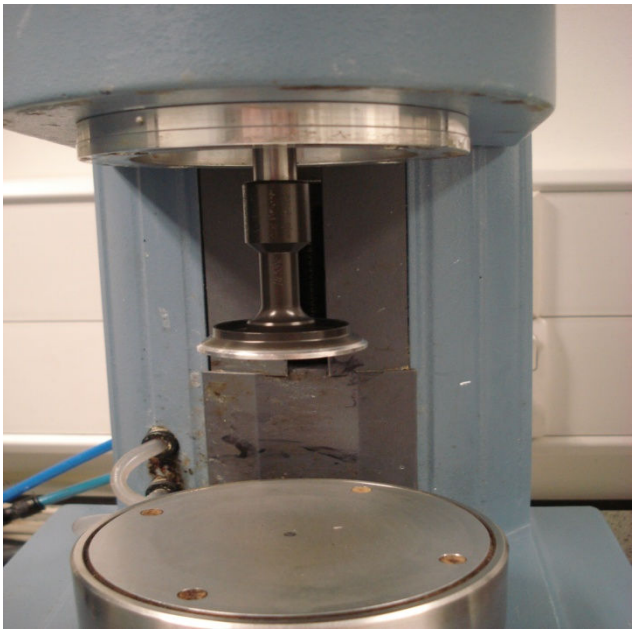

Figure 3.5. Advanced Rheometer TA 1000.

3.10.3 Elemental analysis

The nitrogen content was determined by Warwick Analytical Service, United Kingdom, using a CE 440 elemental analyser. The measurement was carried out by introducing 2 mg of accurately weighed sample into a high-temperature furnace where the combustion was performed. The products of combustion then pass through a special oxidation reagent to form CO_2, H_2O and NO gases. Furthermore, the gases are passed through a copper column to reduce nitrogen oxide to nitrogen element as well as to remove any excess oxygen. The combustion products were then detected precisely using a thermal conductivity detector. Additionally, in order to evaluate level of catalytic upgrading, the sulphur and metal contents of the feedstock and the upgraded oil were determined by Warwick Analytical Service, United Kingdom, using inductively coupled plasma–optical emission spectroscopy (ICP–OES). The sample was introduced to the ICP–OES instrument

and the intensity of the light emitted by the elements was measured. In order to determine the sulphur and metal content of the samples, the measured intensities are compared to the intensities of standards of known concentrations. The results were analysed and the sulfur removal and metal removal were calculated using equation 3.14and 3.15.

$$\%\ \boldsymbol{Removal\ of\ sulfur} = \frac{\boldsymbol{m(S_{feedstock}) - m(S_{oil\ produced})}}{\boldsymbol{m(S_{feedstock})}} \times \mathbf{100} \qquad 3.14$$

where m (*S)* is amount of sulphur in feedstock and oil produced respectively

$$\%\ \boldsymbol{Removal\ of\ metal\ (V + Ni)} = \frac{\boldsymbol{m(V+Ni)_{feedstock} - m(V+Ni)_{oil\ produced}}}{\boldsymbol{m(V+Ni)_{feedstock}}} \times \mathbf{100} \qquad 3.15$$

where *m* is amount of metal (V+Ni) in feedstock and oil produced respectively.

3.10.4 Simulated distillation analysis (true boiling point distribution)

Simulated distillation analysis was carried out using an Agilent 6850N (Agilent Technologies, Inc., Germany) gas chromatograph (GC, Figure 3.6) in accordance with method ASTM-D2887. Note that the calibration mix of the Agilent 6850N GC contains hydrocarbons from C_5 to C_{40} and also the maximum oven temperature is 280 ^oC, hence macromolecules such as resins and asphaltenes outside this carbon range cannot be accounted for by this method. The method quickly determines the boiling point distribution of various petroleum fractions. The Agilent 6850N GC was equipped with a J&W 125-10 DB-1 10 m length, 530 μ m ID and 2.65 μ m film thickness capillary column. Carbon disulfide (CS_2) was selected as the dilution solvent for the oil samples for the following reasons: low boiling point, low response factor in flame ionisation detector (FID) and high miscibility with the oil samples. A mixture of CS_2 and oil sample was prepared in a ratio of 1 to 10 by volume. An accurate volume of 1 µL of mixture was taken by GC syringe and measurement was carried

out by introducing that amount into the GC. The GC was operated at the following conditions:

- The flame ionisation detector was maintained at 260 °C.
- Helium was used as the eluent gas for the GC column at a flow rate of 20 mL min^{-1}.
- Air gas was provided with flow rate of 450 mL min^{-1}.
- Hydrogen flow rate 40 mL min^{-1}.
- Nitrogen as the make-up gas with a flow rate of 32.3 mL min^{-1}.
- Programmed column temperature gradient of 20 °C min^{-1} from 40 to 260 °C.
- Maximum GC oven temperature is 280 °C.

The introduced sample is analysed on a chromatographic column that separates hydrocarbons in order of their boiling points. Boiling point temperatures are assigned as a function of retention time in the column, based on a retention time standard. In accordance with ASTM-D2887, the results are calculated by Agilent Technologies Chemstation software and reported in terms of the temperatures up to 525 °C at which specified percentage weights of the sample have eluted from the column. Following the standard method ASTM-D2887 as well as the previous protocol and conditions, the GC was first calibrated with a hydrocarbon standard mixture containing C_5-C_{40}. The feedstock and the upgraded oil samples were then introduced into the GC for analysis. The data were collected and analysed, and the amounts of the following oil fractions were presented in the final results to show the level of upgrading. Light naphtha starts from initial boiling point to 177 °C; middle distillate starts from 177 °C to 343 °C; and gas oil starts from 343 °C to 525 °C (Gray, 1994).

Figure 3.6. Agilent 6850N gas chromatograph (Simulated distillation).

3.10.5 Asphaltene content

As part of the evaluation level of heavy oil upgrading, the asphaltene content was determined in accordance with method ASTM D2007-80. Saturated straight chain alkanes, such as n-pentane or n-heptane, were used as solvents to precipitate the asphaltene fraction. A mixture of n-pentane and oil sample was prepared in a ratio of 1 g to 40 mL, and the mixture was then agitated for 4 hours using a magnetic stirrer. The mixture was left overnight to facilitate precipitation of the asphaltene fraction. The asphaltene fraction was separated from the mixture by vacuum filtration using Whatman filter paper grade (6) with 6 µm pore size and 4.5 cm diameter. The filter paper was washed with n-pentane until colourless n-pentane was observed, and vacuum filtration was carried out to completely dry the filter paper. The dried filter paper was measured before and after the filtration in order to determine the mass of the asphaltene fraction. The asphaltene content was calculated using the following formula.

$$Asphaltene\ wt\ \% = \frac{weight\ of\ precepetated\ dried\ asphaltene}{weight\ of\ heavy\ oil}\ x\ 100 \qquad 3.16$$

3.10.6 Scanning electronic microscopy and surface morphology analysis

Surface morphology analysis was conducted on the coke as well as the spent catalysts using a Philips XL 30 Scanning Electron Microscope (SEM) (XL 30 ESEM-FEG) equipped with a LaB5 emission source and operating at 15 KV. In addition, the elemental composition of the selected sample was determined using energy-dispersive X-ray spectroscopy (EDX). A photomicrograph was collected over the selected area from the sample surface using SEM with a resolution of 1344 × 1024 pixels, width of 10 μm and magnification of 35000×.

3.10.7 . X-ray diffraction analysis

X-ray diffraction (XRD) analysis was conducted on fresh and coked catalysts using a Bruker D2 PHASER Diffractometer with a scan range from 0° to 160° and Co Kα radiation with a wavelength of 1.54056 Å. The crystalline phase was determined using a EVA database (PDF-4+2012) provided by the International Centre for Diffraction Data (ICDD). Equation 3.17 shows how the Scherrer equation relates crystal size to wavelength.

$$\boldsymbol{d = \frac{K\lambda}{\beta \cos \theta}} \qquad 3.17$$

where

d: Crystallite size (nm)

K: Constant

λ: X-ray wavelength (nm)

β: Peak width (degrees)

θ: Bragg angle (degrees)

Chapter 4
Optimization of Heavy Oil Upgrading using Dispersed Nanoparticulate Iron Oxide as a Catalyst

4.1 Introduction

In this Chapter, a comprehensive optimization of the iron dispersed NPs for in situ upgrading during THAI process was carried out in a stirred batch reactor. Investigations include the effects of reaction temperature, iron metal loading, reaction time, mixing, and initial hydrogen pressure on the extent of upgrading in terms of API gravity increase, viscosity reduction, asphaltene content, sulphur and metals reduction, and true boiling point (TBP) distribution. The impact of these variables on the yields of liquid (i.e., upgraded oil), gas and coke after reaction was also explored. This optimization is to maximize the upgrading in the produced oil while suppressing coke formation. The Taguchi method was applied to optimize the effect of reaction factors and select the optimum values that maximize level of heavy oil upgrading while suppressing coke yield. The reaction factors evaluated were reaction temperature, H_2 initial pressure, reaction time, iron metal loading and speed of mixing. An orthogonal array, analysis of mean of response, analysis of mean signal to noise ratio (S/N) and ANalysis Of VAriance (ANOVA) were employed to analyze the effect of these reaction factors. Detailed optimization of the reaction conditions with iron oxide dispersed nanoparticles ($\leq$ 50 nm) for in situ catalytic upgrading of heavy oil was carried out at the following ranges; temperature 355 – 425 ^{o}C, reaction time 20 – 80 min, agitation 200 – 900 rpm, initial hydrogen pressure 10 – 50 bar, and iron metal loading 0.03 – 0.4 wt%.

4.2 Catalysts activity

Table 4.1 summarizes the performance of dispersed iron metal oxide (Fe_2O_3, size ≤ 50 nm) at different levels of reaction factors.

Table 4.1. Dispersed iron metal oxide performance at different levels of severity [a]. (Feedstock: API 12.8°, Viscosity 1482 cP, 0.68 wt% (IBP-177 °C), 28.18 wt% (177-343 °C)).

Catalysts	Non[a]	Fe_2O_3[a]	Non[b]	Fe_2O_3[b]	Non[c]	Fe_2O_3[c]
Product distribution						
Coke (wt %)	2.21 ± 0.15	0.89 ± 0.1	7.73± 0.21	7.94 ±0.31	12.00 ± 0.35	6.79 ± 0.11
Gas (wt %)	5.73 ±0.13	4.80 ±0.1	8.70± 0.15	9.81 ±0.2	12.00 ±0.14	10.72 ±0.2
SIMDIST Boiling point distribution (wt %)						
(IBP-177 °C)	17 ± 0.11	16± 0.16	23±0.18	22 ±0.21	25 ± 0.2	21 ± 0.3
(177-343 °C)	43 ± 0.44	44±0.4	43 ± 0.2	45 ±.31	43 ±0.14	47 ±0.1
Physical properties						
API gravity° @ 15 °C	19 ± 0.2	19 ±0.3	22 ± 0.1	21 ±0.1	24 ± 0.2	21 ± 0.1
Viscosity (cP)	203.24 ±1.7	217.61 ±1	82.4 ±1.4	112.03 ±1	53.54 ±2	105.75 ±1.5

[a] Reaction conditions: one step (410 °C, 60min, H_2 initial pressure 50 bar, mixing speed 900 rpm)

[b] Reaction conditions: one step (425 °C, 60min, H_2 initial pressure 50 bar, mixing speed 900 rpm)

[c] Reaction conditions: two steps (410 °C, 50min, H_2 initial pressure 50 bar, mixing speed 900 rpm followed by 425 °C, 60min, mixing speed 900 rpm). Errors are expressed in terms of standard deviation for triplicate experiments

Non= no catalyst

It is clear from Table 4.1 (condition b) that dispersed iron metal oxide (Fe_2O_3) has very poor activity. This is because the results were very close to those obtained in the absence of catalyst (i.e., thermal cracking) at 425 ^oC. On the other hand, at reaction condition (a) in Table 4.1 the catalyst has better activity in term of inhibiting coke formation, as the coke observed was 60 % below 2.21 wt% coke yield for thermal reaction only. The results are

consistent with literature where similar observations were reported (Kaneko et al., 2000; Derbyshire and Hager, 1992; Panariti et al., 2000a).

The activation of dispersed catalysts can be achieved in-situ due to the sulfidation reaction between the iron NPs and the sulfur contained in the heavy oil to generate active metal sulfide phase(Liu et al., 2009). Though not reported here, the analysis of the spent NPs of iron showed pyrrhotite ($Fe_{1-x}S$) which is believed to occur during the heating stage to the reaction temperature. The sulfidation of the iron NPs is also confirmed by the decreased sulfur content of the upgraded oil relative to the feed oil (discussed in Section 4.5). This process can influence the activity of the NPs as well as their upgrading performance. It has been reported that the activation of dispersed catalysts could be improved by carrying out a low reaction temperature step, consisting of catalyst reduction under a flow of hydrogen at milder temperature than the reaction itself, followed by high temperature reaction (Liu et al., 2009; Ren et al., 2004; Panariti et al., 2000a; Bhattacharyya and Mezza, 2012). It was observed from Table 4.1 that the two-step experiment helped in improving the catalyst activity under more severe conditions (425 °C, 60min) where the coke yield reduced from 12 wt% (thermal cracking) to 6.76 wt% (catalytic). In addition the middle distillate production was increased to 47 wt% (catalytic) relative to the feedstock containing 28.18 wt%, which is in agreement with literature(Bhattacharyya and Mezza, 2012; Panariti et al., 2000a). Hence, the addition of iron NPs suppressed coke formation significantly while slightly improving product distribution relative to thermal cracking (Table 4.1, reaction condition c).

4.3 Effect of reaction factors on product distribution

Heavy oil upgrading is aimed at improving the yield of middle distillate fraction while gas and coke yields are inhibited (Angeles et al., 2014). Experiments in Table 3.6 were repeated three times. The samples were analyzed and pooled standard deviations were calculated to quantify the variance of the results as follow: coke wt% ±0.14, middle distillate wt%

±0.25,light naphtha wt% ±0.22, Gases wt% ±0.46, API ±0.28°, Viscosity ±0.5, sulfur wt%±0.025, Metal (Ni+V) wt% ±0.031. The effects of reaction factors on product distribution are graphically presented (vertical point plot) in Figure 4.1.

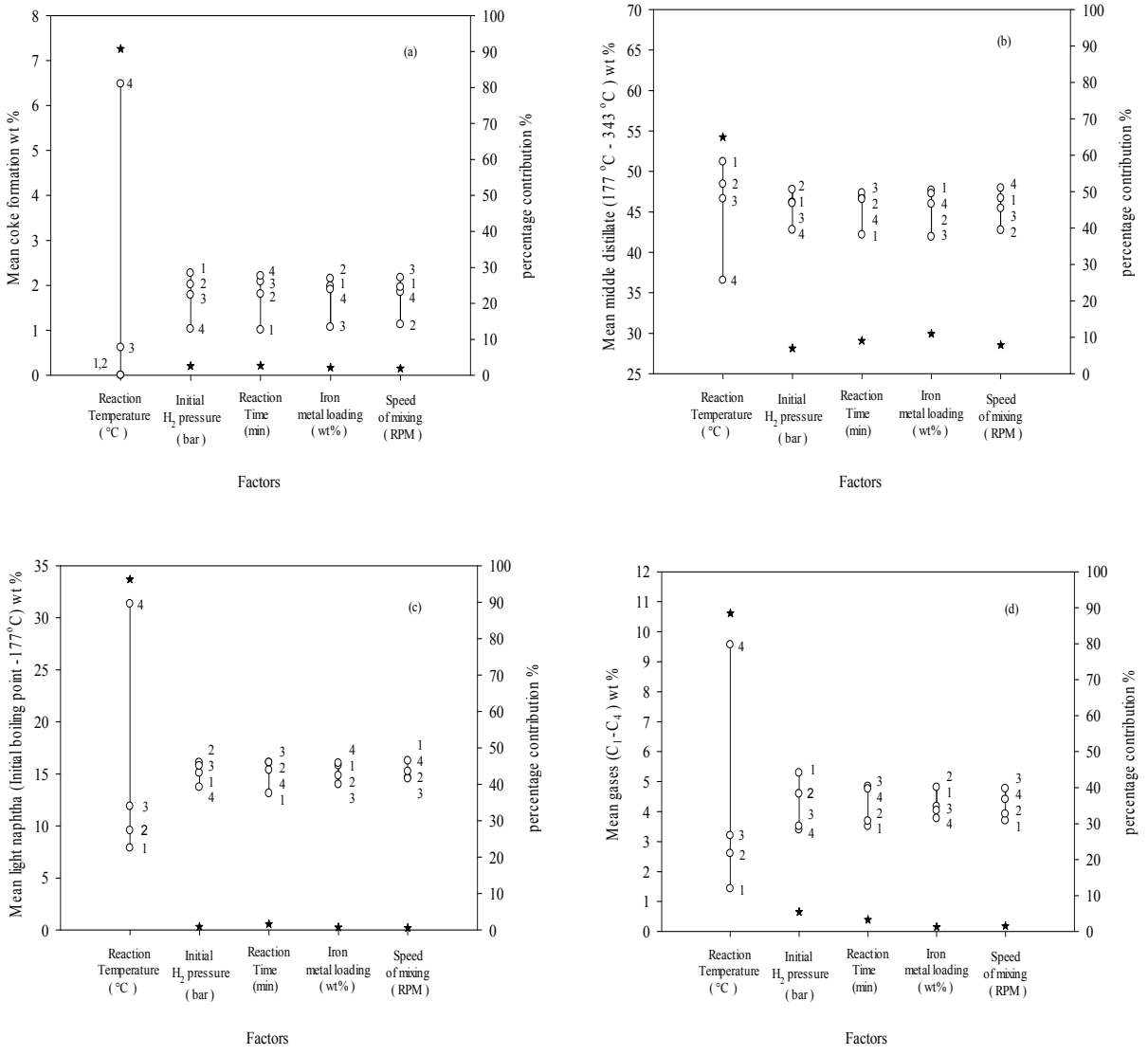

Figure 4.1. Effect of reaction factors on product distribution. (a) mean coke formation wt%; (b) mean middle distillate (177-343 °C) wt%; (c) mean light naphtha (IBP -177 °C) wt%; (d) mean gases (C_1-C_4) wt%. The mean of each factor is indicated by a circle, the number next to each circle indicates the factor level, and the percentage contribution is indicated by (*). Details of reaction factors and their levels see Table 3.5.

Qualitatively, Figure 4.1 shows that the formation of coke, light naphtha fraction (IBP – 177 °C), middle distillates fraction (177-343 °C) and gases (C_1-C_4) are highly affected by

reaction temperature for all factors. The relationships between coke, light naphtha and gas and reaction temperature are shown in Figure 4.1 (a), (c) and (d) respectively. The coke, light naphtha fraction and gas formation increases gradually at low reaction temperature Levels 1, 2 (355 °C, 375 °C respectively). However, the increased rate of mean of percentage weight for coke, light naphtha and gas becomes greater at the high reaction temperature Level 4 (425 °C). The mean of percentage weight for coke formation is negligible at Level 1 and Level 2 reaction temperature, and the coke started to form at an intermediate level where coke formation reached 0.62 wt% at Level 3 (395 °C), and it rose to its maximum value of 6.48 wt% at Level 4 reaction temperature. Furthermore, the mean percentage weights for light naphtha fraction (IBP – 177 °C) at reaction temperature are as follows 7.88 wt% (Level 1), 9.57 wt% (Level 2), 11.89 wt% (Level 3) and 31.34wt% (Level 4) respectively, relative to 0.67 wt% the light naphtha fraction in feed oil. A similar trend can be noticed in the mean of percentage weights of gases (C_1-C_4) 1.43% (Level 1), 2.6% (Level 2), 3.2% (Level 3) and 9.56% (Level 4) for reaction temperature. On the other hand, Figure 4.1 (b) shows that the middle distillate fraction (177-343 °C) gradually decreases as the reaction temperature increases levels 1, 2 and 3. However, the decreasing rate of middle distillate fraction (216-343 °C) becomes faster at the high reaction temperature Level 4. The mean of percentage weights for the mean middle distillate fraction (177-343 °C) for reaction temperature can be summarized as thus 51.18 wt% (Level 1), 48.43 wt% (Level 2), 46.62 wt% (Level 3) and 36.56 wt% (Level 4) respectively, relative to 27.59 wt% (feed oil). Similar observations have been reported in the literature (Speight, 2011; Rana et al., 2007). This is because as the reaction temperature increases, the cleavage of C-C and C-heteroatom bonds increases as well as condensation and polymerization reactions between free-radicals are favored, which are thought to be responsible for the high yield of light naphtha, gas and coke(Hart et al., 2015; Panariti et al., 2000a).

The results of experiments carried out at various levels of dispersed catalytic loading, reaction time, initial H_2 pressure, and speed of mixing are graphically presented in Figure 4.1 (a-d). It is clear that these factors do not exert as much effect as reaction temperature because the cleavages of C-C and C-heteroatom bond are dependent on temperature. However, the chemistry of hydroconversion reactions can be enhanced by these factors (Angeles et al., 2014; Fujimoto et al., 2000; Del Bianco et al., 1994).

The produced coke, light naphtha and gas appears to be inhibited slightly as H_2 initial pressure increased from Level 1 to Level 4 (10-50 bar) as shown in Figure 4.1 (a), (c) and (d). As a consequence, the mean of percentage weights for coke ranged from (2.27 to 1 wt%), light naphtha (16.27 to 13.73 wt%) and gas (5.29 to 3.5 wt%). Also, the production of middle distillate remained within a narrow range between 46 to 42 wt% as H_2 initial pressure change from Level 1 to Level 4, as shown in Figure 4.1 b. This observation is consistent with the literature where it has been reported that at moderate reaction pressure (70 bar) the yield of light product and gas is reduced (Elizalde et al., 2010). In other words, the intermediate fraction does not undergo secondary hydrocraking; hence the produced gas and light fractions are mainly products of hydrocracking of the heavy fraction. In addition, the hydrogenation reaction could be expected to be more active at moderate pressure while at high pressure the hydrocracking dominates (Elizalde et al., 2010; Elizalde et al., 2009; Ancheyta et al., 2005).

In Figure 4.1 (a-d), the effect of reaction time is also presented. It is clear that the reaction time does not have as much impact as reaction temperature. However, a long reaction time promotes cracking, secondary cracking of intermediates and more yields of coke, light naphtha, middle distillate and gas. The mean of percentage weights for coke ranged from 1 to 2.2, middle distillate 42 to 46.5 wt%, light naphtha 13 to 16 wt% and gas 3.5 to 5 wt% as the reaction time increased from Level 1 to Level 4 (20-80 min). The iron metal loading does not exact significant impact on inhibition of formation of coke, light

naphtha and gas however the middle distillate fraction is stable even in presence of low iron metal loading (Figure 4.1 (a-d)). Notably, an increase in the iron metal loading from Level 1 to Level 3 (i.e., 0.03 to 0.1 wt %) led to a reduction in mean coke (1.5 wt %), light naphtha (1 wt %) and gas (2 wt %) after reaction. In addition, the mean of percentage weights for the middle distillate fraction ranged from 42 to 47 wt% as iron metal loading changed from Level 1 to Level 4. In comparison to supported catalysts, dispersed catalyst particles in heavy oil are less susceptible to deactivation during heavy oil upgrading. Dispersed NPs offer better contact with reactants than the supported pelleted catalysts, which may lead to an increased reaction surface area as well as reduced mass transfer limitations between reactants (Liu et al., 2010; Il Yoon et al., 2003). As particle size decreases its surface area increases, therefore dispersion offers the usage of the entire surface related to pelleted counterpart. The iron NPs is pure iron oxide; hence the active phase is dispersed on the external surface after sulfidation. The process of stabilizing free radicals should be rapid in the presence of active hydrogenation catalysts to avoid fast and undesirable condensation reactions which would lead to form the mesophase then coke respectively (Fixari et al., 1994; Panariti et al., 2000a; Panariti et al., 2000b). The reduced coking observed can be attributed to the nano-dispersed iron oxide catalysts and it boosts hydrogen uptake during hydro-cracking reactions (see Figure 4.1 a). This helped to control the rate of free radical propagation via β-scission reactions and subsequently to the conversion of heavy fractions to lighter products is improved (Bellussi et al., 2013; Weitkamp, 2012). These reaction stages are as follows:

Initiation:

$$M \xrightarrow{k1} 2R^{\cdot} \qquad 4.1$$

Propagation:

Chain transfer

$$R^{\cdot} + M \xrightarrow{k2} RH + M^{\cdot} \qquad 4.2$$

B-scission

$$M^{\cdot} \overset{k3}{\rightarrow} R^{\cdot} + Olefin \quad 4.3$$

Termination:

$$Radical + Radical \overset{k4}{\rightarrow} Product \quad 4.4$$

where M is the parent compound, and $R^{\cdot}$ is the smaller alkyl radical.

On the other hand, it was observed that at Level 4 (0.4 wt %) of iron metal loading the mean of percentage weights for products tended to increase again approximately for coke (1 wt %), gas (1 wt %) and light naphtha (3 wt%). These results show that a similar trend in coke formation was observed as the use of dispersed MoS_2 (Kennepohl and Sanford, 1996; Dabkowski et al., 1991). However, the activity experienced with MoS_2 is higher compare to Fe_2O_3. It was suggested that a high level of active metal sulfide (MoS_2) could lead to a high level of hydrogenation which reduces asphaltene stability and promotes coke formation (Panariti et al., 2000b; Kennepohl and Sanford, 1996).

The flow of oil over the dispersed nanoparticles will create some sort of mixing; hence, the effect of agitation upon the level of upgrading achieved was studied. It was observed that the levels of upgrading in terms of product distribution achieved at agitation speed of 200 rpm were 1.8 wt% (coke), 46 wt% (middle distillate), 16.26 wt% (light naphtha) and 3.7 wt% (gas). At 900 rpm mixing speed, the mean of percentage weights was 1.9 wt% (coke), 47 wt% (middle distillate), 15.5 wt% (light naphtha) and 4.5 wt% (gas) (Figure 4.1 (a-d)). Since the particle size is small dispersion can be achieved with minimal mixing speed; hence minor changes were observed in the product distribution. These results are consistent with the literature where it has been reported that the yield of produced coke and gas is decreased during hydro-cracking of residua using nickel sulfate and ferrous sulfate as dispersed catalysts at the stirring rate 400-4000 rpm and reaction temperature 430 ˚C (Luo et al., 2011).

In comparison to non-catalytic (i.e., thermal) upgrading, the yield of coke and gas were reduced to 3.47 and 5.32 wt % respectively relative to yields of 10.81 % (coke) and 8.84 % (gas) reported by Luo et al. (2011) for thermal upgrading. Luo et al. (2011) also reported that the yields of coke ranged from 3.47 to 3.03%, while gas ranged from 5.23 to 3.81% as the mixing speeds increased from 500 to 2000 rpm. In addition, the same study showed that yields of both coke and gas decreases slightly with changing loading of dispersed catalysts from 0.01 to 0.06 $g.mL^{-1}$.

An important step in the hydrocracking reaction is the saturation of free radicals, which is mainly promoted by hydrogenation catalysts (Gray, 1994). In addition, the dispersion of catalysts and hydrogen gas could be improved by good mixing (Angeles et al., 2014; Rezaei et al., 2012; Luo et al., 2011). This explains why increased hydrogen pressure, increased iron metal loading and good mixing suppressed coke and gas formation as well as improving middle distillate production even at high reaction temperature (see Figure 4.1 (a-d)).

4.4 Effect of reaction factors on physical properties

The API gravity of the crude oil is one important factor for assessing the quality of crude oil. High crude oil viscosity is detrimental for extraction as well as pipeline transport. In addition, the high level of heavy oil upgrading is characterized in physical terms by an increase in the API gravity and when its dynamic viscosity is reduced by few orders of magnitude(Hoshyargar and Ashrafizadeh, 2013). The viscosity and API gravity of the crude oil is greatly influenced by its macromolecular weight constituents, such as resins and asphaltenes; chemical composition can also play a major part.

Figure 4.2 shows the effect of reaction factors such as reaction temperature, reaction time, H_2 initial pressure, mixing, and iron metal loading on the produced oil API gravity and viscosity.

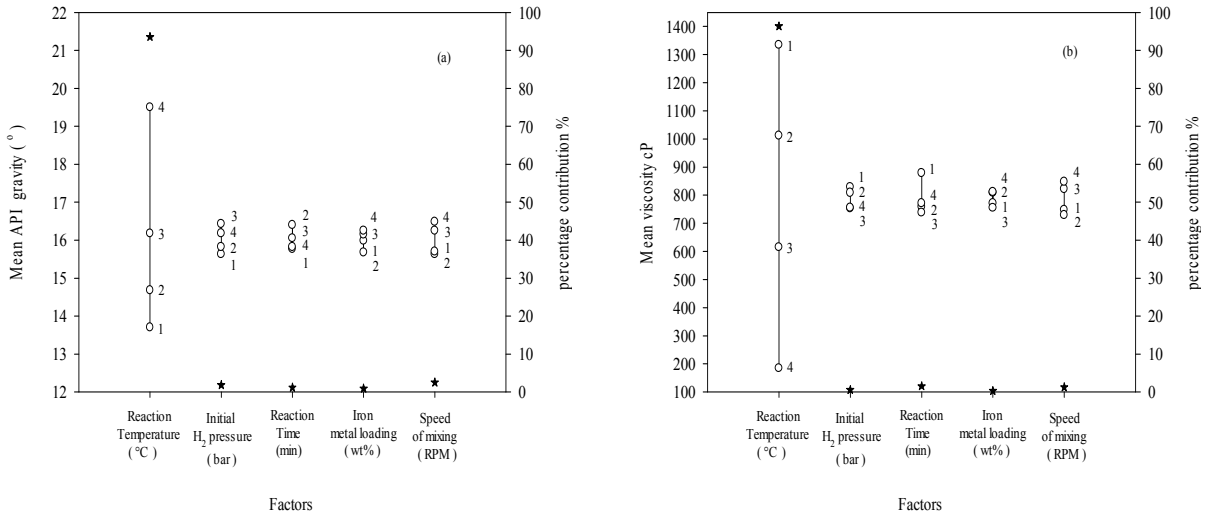

Figure 4.2. Effect of reaction factors on physical properties (a) mean API gravity (b) mean viscosity. The mean of each factors indicate by a circle and the number next to each circle indicate factor level, percentage contribution indicated by (*). For details of reaction factors and their levels see Table 3.5.

It is shown in Figure 4.2 that the API gravity of the produced oil increased as the reaction temperature increases from Level 1 to Level 4 (355 to 425 ^{o}C). The API gravity for the produced oil was 19.5^{o} (Level 4) and 13.7^{o} (Level 1), compared to 12.8^{o} for the heavy feed oil. Correspondingly, the produced oil viscosity decreased as a mirror trend of the API gravity as reaction temperature increases (see Figure 4.2 a-b). This trend in API gravity and viscosity with reaction temperature was expected as a similar observation had been reported earlier in the literature (Hart et al., 2014). This can be attributed to increased cracking reactions with temperature rise, which is re-enforced with corresponding increase in production of gas and coke as temperature increases. Hart et al. (2013) reported a similar effect of temperature on the catalytic cracking of heavy oil.

The significant influence of reaction temperature increase on the API gravity and viscosity can be noticed in Figure 4.2 (a-b). This is because an increase in temperature accelerates the rate of the three major reactions occurring in the slurry environment such as (a) free-radical formation from C-C and C-heteroatom bonds cleavage, (b) hydrogen-transfer reactions (i.e.,

hydrogen-abstraction by C-H bond scissions and hydrogen-addition capping free-radicals), and (c) condensation and polymerization reactions between free-radicals (Hart et al., 2014; Zhang et al., 2012; Weitkamp, 2012). However, in the absence of active catalysts and at reaction temperature above 420 °C, reactions (a) and (c) dominate. As a consequence of these reactions lighter oil (high yield of light naphtha fraction), gas and coke were observed. This is reflected in the increased API gravity and decreased oil viscosity noticed (Gray, 1994).

An increased hydrogen pressure increases the availability of hydrogen for hydroconversion reactions (Elizalde et al., 2010; Sambi et al., 1982), but the oil API gravity and viscosity changes slightly as the initial pressure increases from Level 1 to Level 4 (10-50 barg). An average increase of 0.85^{o} was observed for API gravity, whilst a change of 75.6 cP was observed in viscosity, respectively (Figure 4.2 a-b). Hence, initial hydrogen pressure does not achieve as much effect on API gravity and viscosity as reaction temperature. (Hart et al., 2014; Elizalde et al., 2009)) observed a similar effect of hydrogen pressure on API gravity and viscosity of the produced oil in fixed bed catalytic upgrading of heavy oil.

In Figure 4.2 (a-b), the effect of reaction time is presented. The API gravity of the produced oil increases from 15.8^{o} to 16.4^{o}API as the reaction time increased from Level 1 to Level 4 (20 to 40 min), thereafter, decreased to 15.8^{o} with further increase in reaction time to Level 4. Though reaction time does not achieve as much impact as temperature, long reaction time promotes over cracking, secondary cracking of intermediates and a greater yield of coke, which contributed to the trend observed. Also, prolonged reaction time would have promoted condensation and polymerization reactions between free-radicals resulting in the formation of larger molecular weight product, which explains the low API gravity and slightly higher viscosity of the produced oil after reaction for longer reaction time. The availability of active sites decreases with time as a result of adsorption of resins and

asphaltene, coke and metals deposits (i.e., deactivation of catalyst). This suppresses the performance of the dispersed NP catalyst and also contributes to the observed trend in API gravity and viscosity with reaction time.

It was observed that the value of API gravity decreased from 16.48^{o} to 15.7° as the agitation speed varies from 200 to 900 rpm (Level 1 to Level 4). The viscosity was 747.6 cp at Level 1 (200 rpm) and increased to 847.4 cp at Level 4 (900 rpm). An increase in agitation could lead to enhanced nanoparticle dispersion and contacting of oil-solid within the reaction medium (Jafari et al., 2012), which will decrease the mass transfer barrier between the solid-liquid-gas (Angeles et al., 2014). Nevertheless, an optimum API gravity and viscosity could be reached at agitation speed from Level 2 to Level 4 (400 – 900 rpm). This could be attributed to nano-size particles, which required intermediate mixing speed to achieve adequate suspension necessary for reaction (Angeles et al., 2014; Jafari et al., 2012). This is within the same range of agitation reported by Hart et al. (2015), who found an optimum at 500 rpm.

The iron metal is responsible for hydrogen activation and transfer reactions to moderate produced free radicals from the cracking of heavy molecules (Kaneko et al., 2000). The iron metal loading does not exact significant impact on the API gravity and viscosity of the produced oil (see Figure 4.2 (a- b)) because it is unsupported (i.e., pure iron oxide) unlike bifunctional catalyst supported on zeolites and alumina promote C-C cleavage due to their acidic sites, rather the iron NPs support hydrogen transfer reactions. This means that lack of acidic site on the iron NPs impede cracking functionality. Notably, an increase in the iron metal loading from Level 1 to Level 4 (i.e., 0.03 to 0.4 wt%) produced minor changes in API gravity and viscosity of the produced oil after reaction by 0.85^{o} and 55.9 cP.

4.5 Effect of reaction factors on product quality

The high content of sulfur and metals (i.e., Ni and V) adversely impact on downstream processes such as catalytic reforming, hydrotreating and the cost of hydrotreatment. Hence, upgrading is also aimed at decreasing the level of impurity to meet refinery feedstock specification. Figure 4.3 shows the extent of sulfur and metals reduction for the different reaction factors.

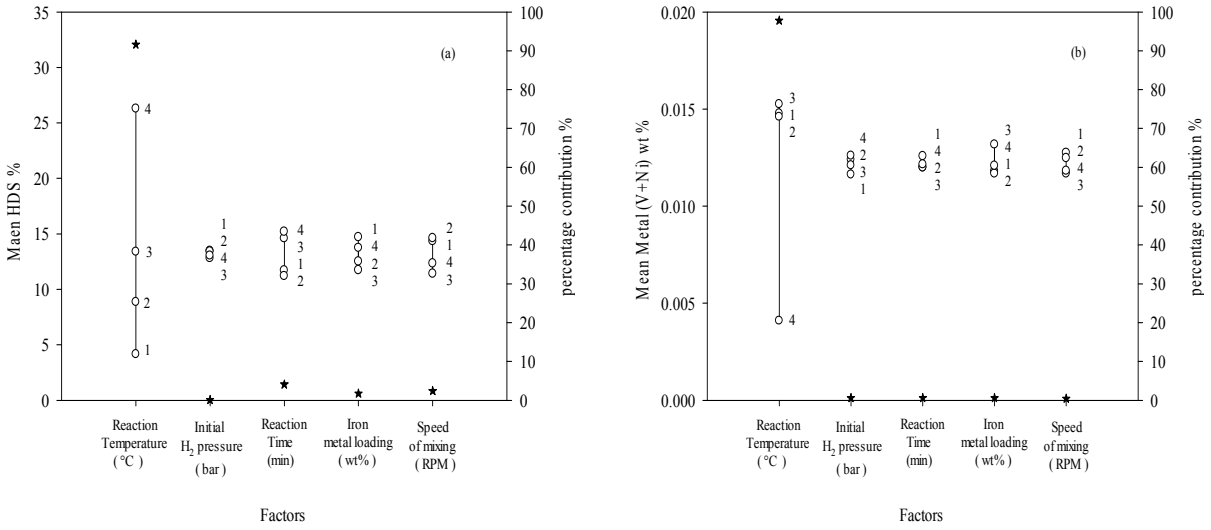

Figure 4.3. Effect of reaction factors on Product quality (a) mean HDS % (b) mean metal (V+Ni) wt %. The mean of each factors indicate by a circle and the number next to each circle indicate factor level, percentage contribution indicate by (*).Details of reaction factors and their levels see Table 3.5.

From Figure 4.3 (a), as the reaction temperature increases from Level 1 to Level 4 (i.e., 355 to 425 ^{o}C), the extent of hydrodesulfurization (HDS) increases in that order from 4.2 to 26.3%. However, it can be seen that increasing initial hydrogen pressure does not exact any influence on the extent of sulfur removal which was recorded as approximately 13.2% for all the range of H_2 initial pressures investigated. The decrease in sulfur content of the produced oil faintly increased from 11.2 to 15.2% as the reaction time increased from Level 1 to Level 4 (20 to 80 min). It was suggested that some of the sulfur in the heavy oil was removed as a result of sulfidation of the iron NPs during reaction and coke deposition (Ancheyta et al.,

2005). The sulfur content showed an average of 13.2% as the stirring speed increases from Level 1 to Level 4 (200 to 900 rpm) within standard deviation of ±0.025. Whilst the increase in iron metal loading from Level 1 to Level 4 (0.03 to 0.4 wt%) caused a similar level of sulfur removal (an average 13.2 %) within standard deviation of ±0.025 in the produced oil relative to the heavy feed oil 3.09 wt%. The above results indicate that the breaking of the C-S bond is temperature driven to overcome the bond energy, though the metal loading can also influence the interaction with the molecules and C–S bond and hydrogen to improve removal (Gray, 1994).

The removal of metals (i.e., Ni + V) was observed to be 7.6% below 0.0132 wt% for the feed oil, for the ranges of the following process variables initial hydrogen pressure, metal loading, stirring speed and reaction time investigated. The further increase of these reaction factors did not have a remarkable effect on the extent of Ni + V removal. However, increasing the reaction temperature from Level 1 to Level 4 (355 to 425 ^{o}C) increased the removal of Ni + V metals from 7.5 to 68.9 % below 0.0132 wt% for the heavy feed oil. The removed metals (Ni + V) are deposited on the NPs and with produced coke as metallic sulfides (Ancheyta et al., 2005). In reality, the sulfur and metals removed from the heavy oil will be left behind in the oil reservoir during the in situ catalytic upgrading.

Hydrogen plays two important roles in metals (V+Ni) removal which are hydrodemetallization (HDM) and hydrogenation. First hydrogen could help in hydrogenating unsaturated hetroatoms containing compounds such as quinolines and olefins and it also participates to hydrocrack the cyclic (saturated and unsaturated) compounds, which produces a metal sulfide and an organic counterpart. In general high hydrogen pressure observed in this study favored both reaction steps. In addition, the influence of hydrogen pressure as well as catalyst loading on product quality could be properly evaluated at low reaction temperature (Panariti et al., 2000b; Reynolds, 1991).

4.6 Selection of optimum factors levels

Taguchi suggests analyzing mean of signal to noise ratio as well as mean of response in order to identify the effect of process factors and optimum conditions. The optimum factor levels were selected in this section based on Taguchi method by performing ANOVA on both mean signal to noise ratio (S/N) and mean of response in addition to percentage contribution of reaction factors (section 3.5). The level of significance was measured in terms of percentage contribution (Phadke et al., 1983; Kolahan et al., 2011; Ghani et al., 2004). The percentage contribution of reaction factors, mean signal to noise ratio (S/N) and mean of response were presented graphically in Figure 4.4, 4.5, 4.6 and Figure 4.1, 4.2 and 4.3 respectively.

Reaction factors that have a significant effect on mean signal to noise ratio (S/N) are classified as control factors (Kolahan et al., 2011; Phadke et al., 1983; Simpson, 1998). It has been reported to set the level of this factor equal to the optimum level to minimize process variability (Kowalczyk, 2014; Fratila and Caizar, 2011). Secondly in order to maintain the mean responses on the target value, the Taguchi method suggested using signal factor. Ideally, the signal factor is the factor that has the most significant effect on mean response with no effect on mean S/N of the response. The percentage contribution of the different reaction factors on mean S/N ratio as well as mean of responses can be seen clearly in Figure 4.1-4.6 respectively (Ghani et al., 2004; Phadke et al., 1983; Pignatiello Jr, 1993).

It is clear from the results and Figure 4.1-4.6 that reaction temperature has the most significant effect on mean S/N ratio; hence, is the most important control factor. Also, it is evident that reaction temperature has the most significant effect on the mean of all responses. However, iron-metal loading and initial H_2 pressure have a significant effect on middle distillate fraction and gases respectively. Among the reaction temperature, iron-metal loading and H_2 initial pressure factors, the reaction temperature is the control factor and so it

is not suitable as a signal factor. The remaining two factors, iron-metal loading and initial H_2 pressure, have a moderate effect on middle distillate fraction and gas yields. Therefore, both iron-metal loading and H_2 initial pressure are assigned to be signal factors. Other factors, such as reaction time and mixing speed, could be set at an economical level where they have no significant effect on either the mean S/N ratio or mean of response.

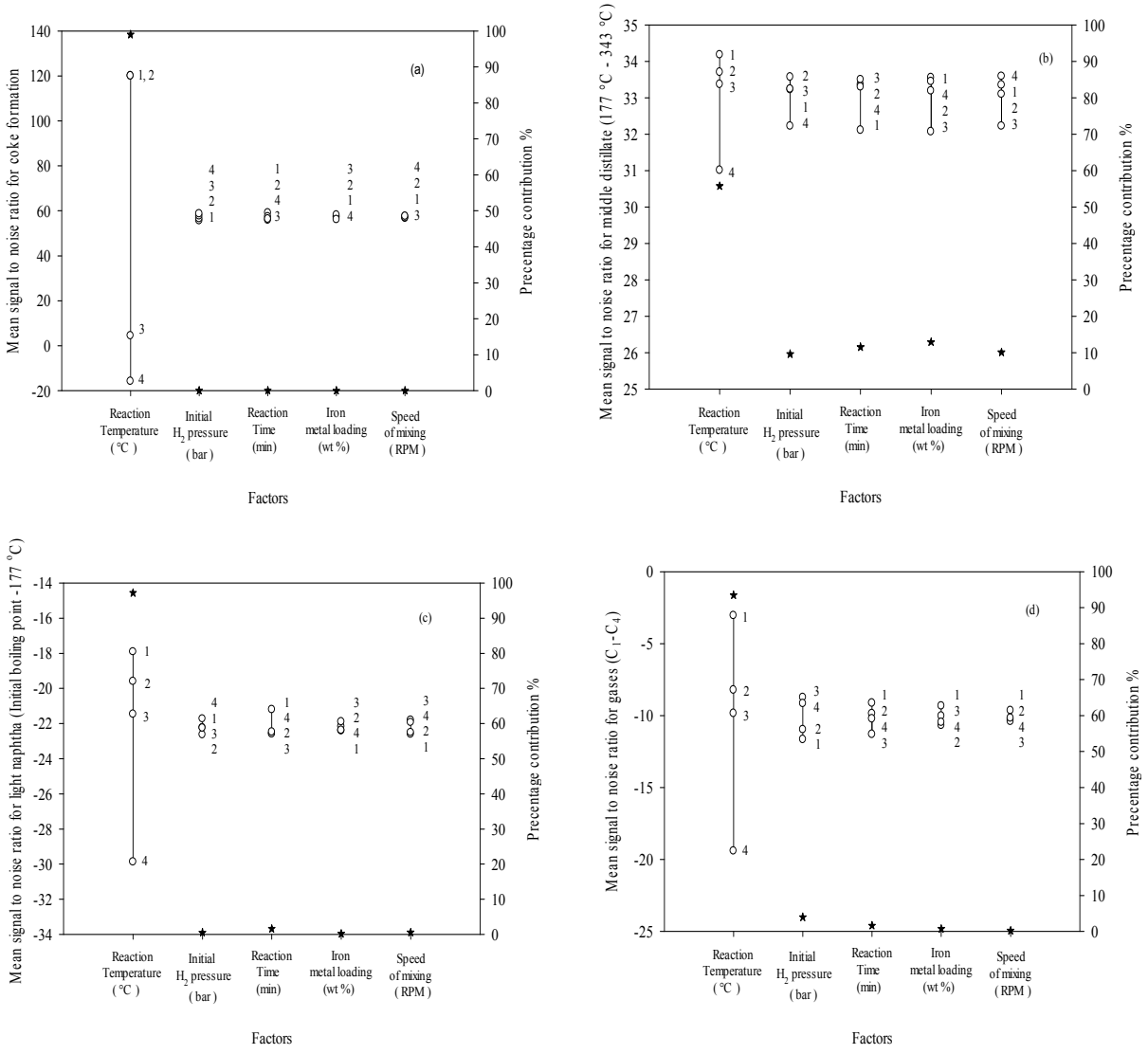

Figure 4.4. Effect of reaction factors on mean signal to noise ratio (a) coke formation (smaller the better) (b) middle distillate (177 - 343 °C) (larger the better) (c) light naphtha (IBP-177 ^{o}C) (smaller the better) (d) gases (C_1-C_4) (smaller the better). The mean of each factors is indicated by a circle and the number next to each circle indicate factor level, percentage contribution indicate by (*). For details of reaction factors and their levels and (S/N) ratio calculation see Table 3.5 and 3.7.

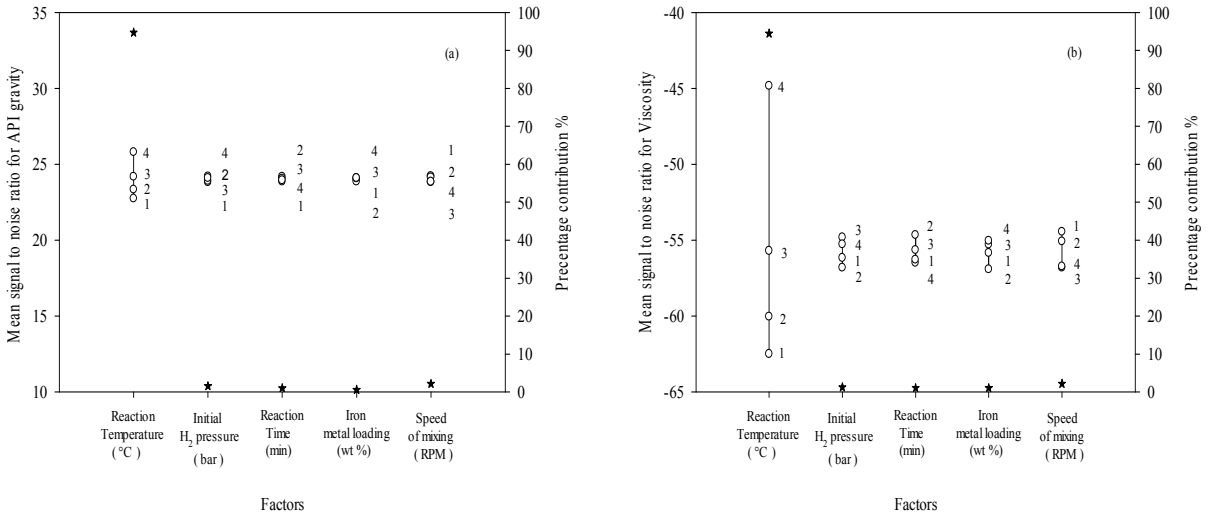

Figure 4.5. Effect of reaction factors on mean signal to noise ratio (a) API gravity (larger the better) (b) Viscosity (smaller the better). The mean of each factors indicate by a circle and the number next to each circle indicate factor level, percentage contribution indicate by (*). For details of reaction factors and their levels and (S/N) ratio calculation see Table 3.5 and 3.7.

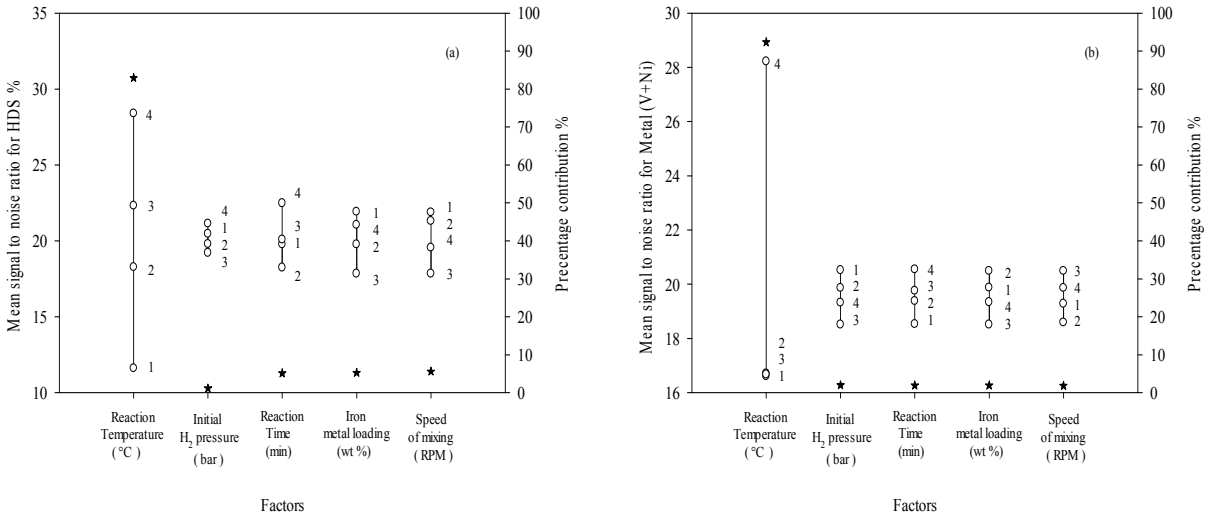

Figure 4.6. Effect of reaction factors on mean signal to noise ratio (a) HDS % (larger the better) (b) metal (V+Ni) (larger the better). The mean of each factors indicate by a circle and the number next to each circle indicate factor level, percentage contribution indicate by (*). For details of reaction factors and their levels and (S/N) ratio calculation see Table 3.5 and 3.7.

In this study, the optimum level of the control factor (reaction temperature), as well as signal factors, were selected and tested, and the results presented in Table 4.2 and 4.3 respectively. It is well known that the oxygen flux is the main driver for generating heat during THAI process. Hence, the optimum reaction temperature could be conducted by controlling oxygen flux during THAI process. Also, NPs injection needs further investigations of heavy oil formation to identify the proper layer to penetrate NPs during THAI process.

Table 4.2. Optimum factor levels and conditions.

Factor	Optimum level	Selected conditions
Reaction Temperature (°C)	4	425
Initial H_2 pressure (bar)	4	50
Reaction Time (min)	Normal	60
Iron-metal loading (wt %)	3	0.1
Speed of mixing (RPM)	Normal	400-600

Table 4.3. Results of upgrading oil at optimum conditions.

Physical properties	Results
API° gravity	21.1
viscosity (cP)	105.75
Product quality	
HDS%	37.54
Metal (Ni + V) wt %	0.062
Product distribution	
Coke formation wt %	6.79
Gases (C_1-C_4) wt %	10.72
Naphtha fraction (IBP - 177°C) wt %	21
Distillate fraction(177–343°C) wt %	47

Chapter 5

Effectiveness of Different Transition Metal Dispersed Catalysts for In-Situ Heavy Oil Upgrading

5.1 Introduction

Chapter 5 is devoted to examining the effectiveness and activity of different types of dispersed unsupported transition metal catalysts for in situ heavy oil upgrading instead of packed pellets of catalyst attached to the horizontal well. The sulfidation of the metal oxides during heating and reaction by the sulfur contained in the heavy oil was investigated using Fe_2O_3 nanoparticles. The performance of molybdenum-based, iron-based and nickel based dispersed catalysts were investigated in term of product distribution (i.e., liquid, gas and coke) and (naphtha, middle distillate and gas oil fractions), physical properties (i.e., API gravity and viscosity) and product quality (i.e., sulphur, metals and nitrogen contents) and evaluated against that achieved with thermal cracking without the addition of metal particles. Also studied is the effect of dispersed unsupported catalysts on the type of produced coke from the upgrading reactions using Scanning Electron Microscope (SEM).

5.2 Sulphidation test

The active phase (metal sulphide) of the dispersed catalysts is formed in situ during the sulphidation reaction between the unsupported metals and the sulphur contained in the heavy oil (Liu et al., 2009). This activation process can influence the activity and performance of the dispersed catalysts. The sulphidation reaction was conducted using iron-based dispersed catalysts (Fe_2O_3). The experiment was performed without adding a sulphur source at a reaction temperature of 410°C, 50 bar of initial hydrogen pressure and 900 rpm mixing speed for 50 min, followed by a reaction temperature of 425°C for 60 min. The fresh Fe_2O_3 and coke from thermal upgrading was analyzed by XRD. In addition, the spent dispersed catalyst

was recovered after the sulphidation experiment and analyzed to validate the activation reaction. Figure 5.1. (a-c) shows the result of XRD analysis of fresh Fe_2O_3, coke (from thermal upgrading) and the recovered coke and catalysts after activation reaction respectively. The presence of an active-phase pyrrhotite-5C ($Fe_{1-x}S$) can be observed (the obtained XRD data match with pyrrhotite-5C pattern using EVA database by ICDD).

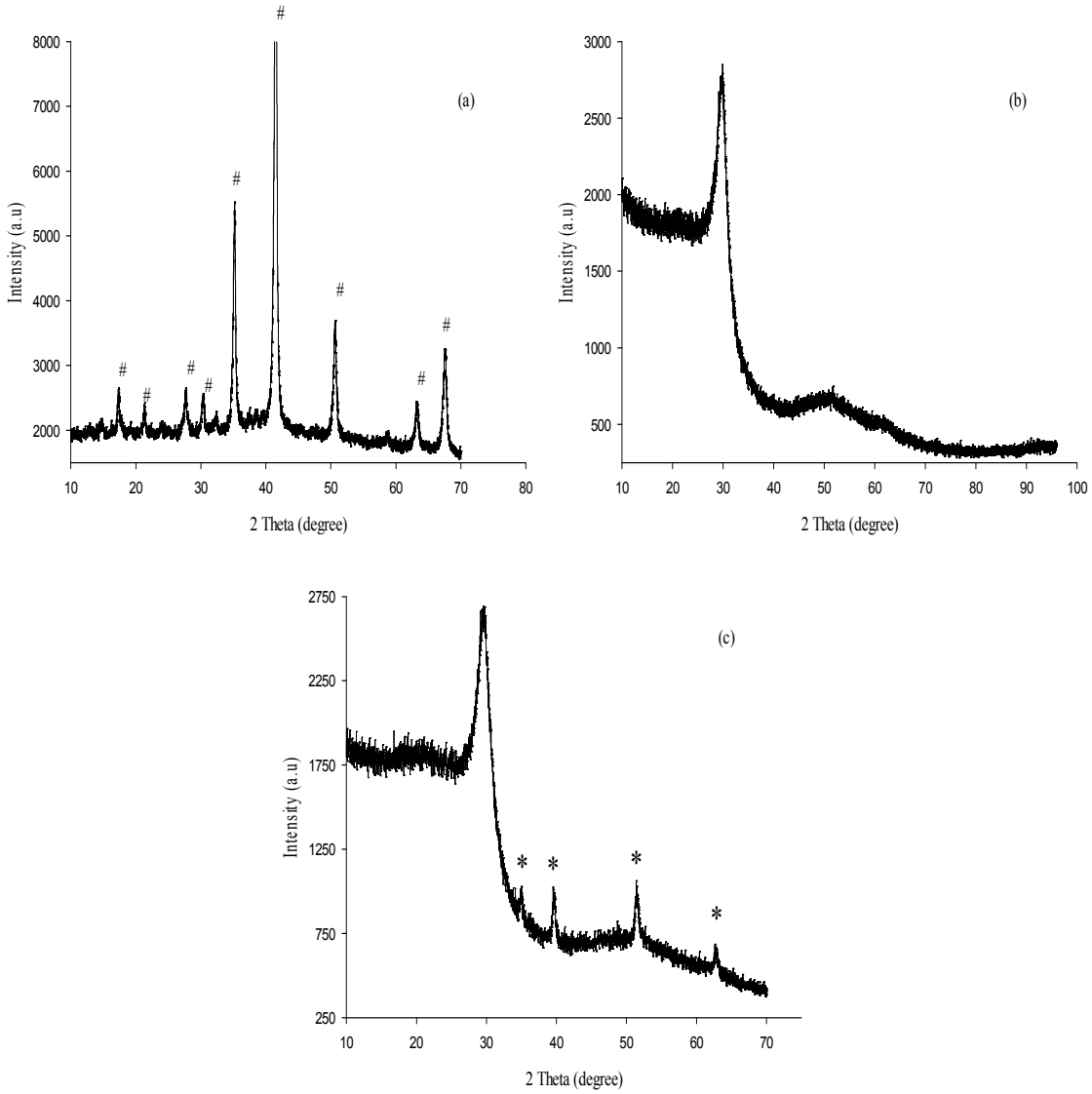

Figure 5.1. XRD pattern (a) for the fresh Fe_2O_3 catalysts (b) recovered coke from thermal upgrading (c) recovered coke and catalysts after activation reaction.

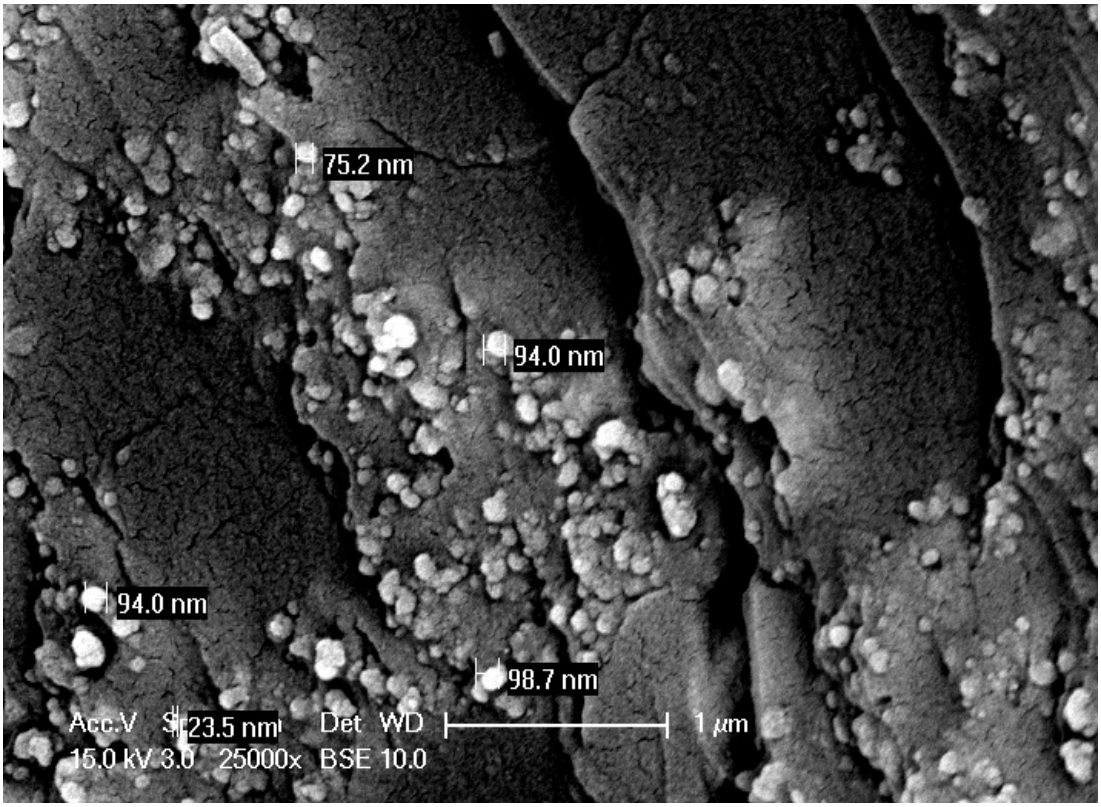

Figure 5.2. SEM micrograph of recovered Fe_2O_3 catalysts.

Figure 5.2 shows the SEM micrograph of the recovered coke and iron particles composite after reaction. The iron particle seen on SEM image has been identified by XRD (see Figure 1c) as pyrrhotite which particle size is in the nano-scale order (Figure 5.2). It is therefore clear that the unsupported catalysts are converted to their active phase (i.e., activated) during the heating and reaction stage of the experiments as shown in Figure 5.1 c. This procedure and results are consistent with that reported in the literature for activation transition metal catalyst (Mo, Ni and Fe) (Liu et al., 2009; Ren et al., 2004; Panariti et al., 2000a; Bhattacharyya and Mezza, 2012).

5.3 Effect of catalyst size on heavy oil upgrading

It has been found that the use of ultrafine catalysts could help to mitigate the challenges of coke formation during catalytic upgrading (Zhang et al., 2007). Stirred tank reactors have been widely used for the purpose of investigating the effect of dispersed catalysts on

hydroconversion of heavy oil (Speight, 2004; Pitault et al., 2004). The stirring speed used was in line with the guidelines reported in the literature to ensure suspension and adequate dispersion of the particles in the oil during reaction (Angeles et al., 2014; Jafari et al., 2012; Sahu et al., 2015).

Table 5.1 shows the effect of particle size on the extent of upgrading for experiments carried out with unsupported Fe_2O_3 particles. It can be observed that different particle sizes show similar activity in terms of their effect upon product distribution, physical properties and product quality of the produced oil at high reaction conditions (see condition a).

Table 5.1. Effect of catalysts size on product distribution physical properties and product quality [a]. (Feedstock: API 12.8°, Viscosity 1482 cP, C_5-aphaltene 14 wt%, 0.68 wt% (IBP-177 °C), 28.18 wt% (177-343 °C), 71.6 wt% 343 °C+, 3.09 wt% sulphur , 0.0132 wt% (Ni+V)).

Catalysts type /size	Non	Fe_2O_3 (≤ 50 nm)	Fe_2O_3 (≤5 μm)
Product distribution (wt %)			
Coke	12	6.79	6.64
Liquid	76	82.48	82.74
Gas	12	10.72	10.63
C_5-aphaltene	4.5	10	9.89
SIMDIST Boiling point distribution of produced liquid (wt %)			
(IBP-177 °C)	25	21	22
(177-343 °C)	43	47	47
(343 °C+)	32	32	31
Physical properties of produced liquid			
API gravity at 15 °C	24	21	21.5
Viscosity (cP) at 20 °C	53.54	105.75	92
Product quality removal % of produced liquid			
HDS	43.92	37.54	35.74
HDM	85.67	69.38	69.29
N (wt %)	0.25	0.14	0.24

[a] Reaction conditions: two steps: 410°C, 50 min, metal loading 0.1 wt % , H_2 initial pressure 50 bar, mixing speed 900 rpm, followed by 425°C, 60 min, mixing speed 900 rpm. Errors are expressed in term of standard deviation for triplicate experiments as follows: coke wt % ±0.2, liquid wt % ± 0.24, gases wt % ±0.46, asphaltene wt % ±0.8, middle distillate (177-343 °C) wt % ±0.3, light naphtha (IBP-177 °C) wt % ±0.4, gas oil (343-525 °C) wt% ± 0.5, API° ±0.28, viscosity ±1.5, HDS% ±0.4, metal HDM% ±0.31, N wt% ±0.03.

Table 5.1 shows that the coke yield reduced to 6.76 wt% for Fe_2O_3 (≤ 50 nm) and to 6.64 wt% for Fe_2O_3 (≤ 5 μm) relative to 12 wt % for thermal upgrading. In addition, the amount of middle distillate fractions increased to 47 wt % for both Fe_2O_3 (≤ 50 nm) and Fe_2O_3 (≤5 μm) relative to the 28 wt % feedstock. It is well known that the particle suspension proportional to speed of mixing (Raghava Rao et al., 1988; Myers et al., 1994). In other words, both Fe_2O_3 (≤ 50 nm) and Fe_2O_3 (≤5 μm) could be suspended adequately at the high mixing speed of 900 rpm as 500 rpm was found as the optimum mixing speed by (Hart et al., 2015), for the same feedstock and reactor, hence the effect particle size could be neglected during heavy oil upgrading at high agitation. However, particle sizes greater than the micro scale were not investigated.

5.4 Effect of molybdenum-based dispersed catalysts

Table 5.2 shows the performance of molybdenum-based catalysts in terms of product distribution, physical properties and product quality. From **Table 5.2**, thermal upgrading (in the absence of catalysts) gave a very high amount of coke and gas, and relatively low amounts of liquid and asphaltene. The product distributions after thermal cracking are as follows: coke (12 wt %), gas (12 wt %), liquid (76 wt %) and asphaltene (4.5 wt %). The distilled fractions distribution of the produced oil after thermal cracking were 25 wt % (light naphtha), 43 wt % (middle distillate) and 32 wt % (heavy fractions 343 °C+), relative to 0.68 wt % (light naphtha), 28.18 wt % (middle distillate) and 71.6 wt % % (heavy fractions 343 °C+), in the feed oil. It can be observed that while both light naphtha and middle distillate fractions of the produced oil increased, the gas oil fraction reduced after thermal upgrading. The results are in agreement with previous work on thermal upgrading of heavy oil (Carrillo and Corredor, 2013; Castañeda et al., 2012).

Table 5.2. Effect of molybdenum -based catalysts on product distribution, physical properties and product quality [a]. (Feedstock: API 12.8°, Viscosity 1482 cP, C_5-aphaltene 14 wt%, 0.68 wt% (IBP-177 °C), 28.18 wt% (177-343 °C), 71.6 wt% 343 °C+, 3.09 wt% sulphur , 0.0132 wt% (Ni+V)).

Catalysts type /size	Non	MoS_2 (≤ 2 μm)	MoO_3 (≤ 100 nm)
Product distribution (wt%)			
Coke	12	4.35	5.9
Liquid	76	85.84	83.81
Gas	12	9.81	10.29
C_5-aphaltene	4.5	9.55	7.24
SIMDIST Boiling point distribution of produced liquid (wt %)			
(IBP-177 °C)	25	17	21
(177-343 °C)	43	50	49
(343 °C+)	32	33	30
Physical properties of produced liquid			
API gravity at 15 °C	24	20	21
Viscosity (cP) at 20 °C	53.54	142.38	102.77
Product quality removal % of produced liquid			
HDS	43.92	30.55	37.08
HDM	85.67	47.33	68.89
N (wt %)	0.25	0.05	0.2

[a] Reaction conditions: two steps: 410°C, 50 min, metal loading 0.1 wt %, H_2 initial pressure 50 bar, mixing speed 900 rpm, followed by 425°C, 60 min, mixing speed 900 rpm. Errors are expressed in terms of standard deviation for triplicate experiments as follows: coke wt % ±0.15, liquid wt % ± 0.35, gases wt % ±0.45, asphaltene wt % ±0.75, middle distillate (177-343 °C) wt % ±0.25, light naphtha (IBP-177 °C) wt % ±0.45, gas oil (343-525 °C) wt% ± 0.55, API° ±0.18, viscosity ±2, HDS% ±0.55, metal HDM% ±0.31, N wt% ±0.01.

It is well known that thermal energy is responsible for the cleavage of C-C and C-heteroatom bonds, and in the absence of active catalysts the condensation and aromatization reactions between free-radicals are favoured, which are thought to be responsible for high amounts of coke and gas, as well as a relatively low amount of liquid collected compared to that observed upon the addition of an unsupported catalyst (Reyniers et al., 1994; Towfighi et al., 2002). At high reaction temperature, such as 425 ˚C, the solubility of asphaltene decreases because of the increase in aromatization by removing aliphatic side chains and hydrogenating maltenes (e.g., saturates and aromatics). As a result, the maltenes tend to be more aliphatic, causing precipitation and agglomeration of asphaltene due to their insolubility in aliphatic hydrocarbons (Gawel et al., 2005; Spiecker et al., 2003; Bartholdy et al., 2001; Bartholdy and Andersen, 2000). The lower content of asphaltene in the produced oil and

high yield of coke after thermal upgrading of heavy oil confirmed that large amounts of asphaltene were deposited (Table 5.2).

On the other hand, from Table 5.2, it can be observed that both molybdenum (IV) sulphide (MoS_2) and molybdenum (VI) oxide (MoO_3) dispersed catalysts suppressed coke formation, controlled gas production and relatively increased the amount of liquid and asphaltene in the produced oil. However, MoS_2 showed better activity than MoO_3 for heavy oil upgrading in terms of product distribution, where the produced coke was 4.3 wt % (MoS_2) and 5.9 wt % (MoO_3), and gas was 9.56 wt % (MoS_2) and 10.29 wt % (MoO_3). the liquid yield and asphaltene amount increased to 85.84 wt % and 9.55 wt % for MoS_2 and 83.81 wt % and 7.24 wt % for MoO_3 respectively relative to 76 wt % and 4.5 wt % in thermal upgrading. The observed lower asphaltene after thermal cracking relative to dispersed unsupported molybdenum catalysts can be attributed to the high carbon-rejection caused by high asphaltene deposition during thermal cracking (Gawel et al., 2005; Bartholdy et al., 2001; Bartholdy and Andersen, 2000; Gray, 1994). Furthermore, the particles lack the cracking functionality as they are unsupported, hence the upgrading is mainly by free radical mechanism with the unsupported catalyst particles aiding hydrogen uptake. Based on the distilled fractions, it can be noticed that the presence of molybdenum-based catalysts increased the amount of valuable middle distillate, while the light naphtha fraction decreased relative to thermal cracking without catalyst addition (see Table 5.2).

A similar level of upgrading in terms of product distribution was observed for Mo-based dispersed catalysts and reported in the literature (Rankel, 1994; Weissman, 1997; Bockrath et al., 1998; Castañeda et al., 2012). Also, in the hydroconversion investigation of Cold Lake vacuum residue at 415−445°C, 13.8 MPa, and a reaction time of 1 hour, Rezaei et al. (2012) found that utilizing MoS_2 suppressed coke formation from 22 wt % in the absence of catalysts (i.e., thermal cracking) to 4.8 wt % in presence of 100 ppm of Mo (Rezaei et al.,

2012). This significant suppression of coke formation could be attributed mainly to hydrogen uptake, which is a major function of the unsupported catalyst particles (Breysse et al., 2002). The hexagonal coordination exhibited by unsupported MoS_2 contributed to its activity (Kasztelan and McGarvey, 1994; McGarvey and Kasztelan, 1994; Breysse et al., 2002). During hydro-processing reactions, the corner and edge occupied by sulphur ions in MoS_2 could be easily inter-changed with hydrogen. As a result, unsaturated sites and sulphur ion vacancies formed which exhibit Lewis acid characteristics and active sites for H_2. The activation of H_2 on the surface of the catalyst particles, therefore form Mo-H and S-H moieties which helped to decrease the rate of condensation and aromatization reactions by hydrogenated free radicals (Breysse and Kasztelan, 2002; Breysse et al., 2002; Sun et al., 2004). As a consequence, the following was observed upon the addition unsupported Mo-based particles to the heavy oil upgrading: (1) suppression of coke formation; (2) control of gas formation; and (3) improvement of production of the middle distillate fraction.

Table 5.2 also shows the effect of Mo-based catalysts on physical properties as well as product quality. High viscosity and low API gravity causes major problems during the extraction and transportation process (Omole et al., 1999). Low API gravity and high viscosity for heavy oil could be attributed to high average molecular weight fractions (such as asphaltene) and the interaction strength between molecules (Wu et al., 2010; Argillier et al., 2002; Altgelt and Harle, 1975). An increase in temperature accelerates the rate of major reactions occurring in the slurry environment such as free-radical formation from C-C and C-heteroatom bond cleavage (Hart et al., 2014; Zhang et al., 2012; Weitkamp, 2012). As a consequence of molecular bond cleavage and the rupture of ring structures of heavy oil gas, coke and large numbers of smaller and less viscous products form (Wu et al., 2010; Omole et al., 1999).

The experiment on thermal upgrading of heavy oil has demonstrated that the viscosity falls drastically to 54 cP and API gravity increases to 24° relative to 1482 cP and 12.8° for the feed oil. On the other hand, it has been noticed that the produced oil after upgrading with Mo-based dispersed catalysts (MoS_2 and MoO_3) did not have the same level of improvements in both API gravity and viscosity as observed with thermal upgrading. The API gravity and viscosity were observed to be 20˚ and 142.38 cP for MoS_2, and 21.3˚ and 99.9 cP for MoO_3 respectively. Nevertheless, Hart et al. (2015) found 8.7˚ points increase in API gravity with ultradispersed Co-Mo/Al_2O_3 against 6.6˚ points increase with thermal cracking (Hart et al., 2015). The difference is that their catalyst (Co-Mo/Al_2O_3) possesses bifunctionality i.e., cracking by the alumina support and hydrogenation by the dispersed Co-Mo. It has also been reported in the literature (Wu et al., 2010; Luo and Gu, 2007; Hongfu et al., 2002; Gray, 1994; Rhoe and Deblignieres, 1979) that unsupported catalysts such as those used in this study (e.g. MoS_2) are not bifunctional in nature; as they do not promote cracking of C-C and C-heteroatom bonds by the acidic sites as present on zeolites and alumina. Further cracking was not therefore experienced with the addition of the unsupported catalyst as the main mechanism of upgrading is by free radical driven temperature. The unsupported catalyst performed hydrogenation which helped to stabilize asphaltene in the reaction medium explaining the decreased of API gravity as well as the higher viscosity relative to thermal cracking (Gawel et al., 2005; Dealy, 1979). This is again consistent with the high asphaltene content of the produced oil after upgrading with unsupported catalysts compared to thermal cracking.

In order to evaluate the performance of Mo-based catalysts, the product quality in terms of sulphur, nitrogen and metal removal was investigated and is presented in Table 5.2. It can be seen from Table 5.2 that the extent of hydrodesulphurization (HDS) and hydrodemetallization (HDM) is directly proportional to coke yield. This is because the sulphur and metals are

associated with macromolecules such as resins and asphaltenes which are the main contributors to coke formation. In the absence of the unsupported catalysts, the HDS and HDM was 43.92% and 85.67%, respectively. However, in the presence of dispersed unsupported catalysts, the HDS and HDM reduced to 30.55% and 47.33% for MoS_2, and 37.08% and 68.89 % for MoO_3. This observation is because of the high coke observed with thermal cracking. It is known that hydrogen plays a key role in HDM reactions (Reynolds, 1991; Mitchell and Scott, 1990; Mitchell, 1990). Panariti et al (2000a) observed that a high initial hydrogen pressure (160 bar) strongly affected metal removal during heavy oil upgrading using unsupported MoS_2 (Panariti et al., 2000a). In the presence of hydrogen, organometallic molecules decompose quite easily giving rise to insoluble metal sulfide. In another study conducted by Panariti et al. (2000b) showed that HDS is not affected much by a high initial H_2 pressure; however HDS was significantly improved at a high level of catalyst loading (Panariti et al., 2000b). The above findings indicate that the breaking of the C-heteroatom bond is mainly controlled by temperature to overcome the bond energy. In addition, the presence of highly active unsupported catalysts can help in stabilizing macromolecules such as asphaltene which act as stores for the sulphur and metals (Ni + V) in the reaction medium (Gawel et al., 2005; Bartholdy et al., 2001). Notably, the level of HDM was higher than HDS, because the concentration of sulphur in the feed oil was higher than the metals, and also, while metals are associated mainly with macromolecules such as asphaltenes, sulphur can exist as sulfide, disulphide and thiol.

The nitrogen content increased to 0.25 wt % and 0.2 wt % for thermal upgrading and MoO_3 respectively. These results are consistent with the literature, where (Gray et al., 1989)) reported that nitrogen compounds such as pyrroles are much less reactive which can lead to the accumulation of nitrogen compounds during the upgrading process. However, MoS_2 reduced the nitrogen amount by 46% to below 0.08 wt % in feed oil. Under hydroconversion

conditions, MoS_2 catalysts can form unsaturated sites and sulphur ion vacancies. These have Lewis acid characteristics which could adsorb molecules with unpaired electrons (e.g. N-bases) in the feed oil (Breysse et al., 2002). In summary, molybdenum-based dispersed catalysts inhibit coke formation, as well as boost production of middle distillate, during heavy oil upgrading by activating the hydrogenation reactions. However, MoS_2 and MoO_3 catalysts show different levels of upgrading in terms of product distribution, physical properties, and product quality. It has been observed (Li et al., 2004; Nath et al., 2001; Wilcoxon et al., 1997; Feldman et al., 1995; Ren et al., 2004) that the transformation of MoO_3 to the active phase (MoS_2) during the heating and reaction stage could be affected by a reducing atmosphere such as temperature and sulphur content. Feldman et al. (1995) and Nath et al. (2001) reported that if the reduction atmosphere is not sufficient it could lead to the formation of an associate intermediate such as $MoO_{2-x}S_x$, which is less active in comparison to MoS_2 (Nath et al., 2001; Feldman et al., 1995). This is the reason for the better performance of MoS_2 over MoO_3.

5.5 Effect of iron-based dispersed catalysts

Pyrite (FeS_2), troilite (FeS) and pyrrhotite ($Fe_{1-x}S$) are the most common iron sulphides and among all of these, the most active form is pyrrhotite ($Fe_{1-x}S$) (Kaneko et al., 1998; Shah et al., 1996; Nakao et al., 1984). Under hydroprocessing conditions, iron oxide (i.e.Fe_2O_3) can be converted to the sulphide form via the reaction with sulphur in heavy oil as shown in Figure 5.1 and 5.2. Hydrogen molecules are believed to be activated due to sulphur deficient sites in iron sulphide catalysts (Mochida et al., 1998). The active hydrogen can help in terminating condensation and polymerization reactions between free radicals. As a consequence, valuable products, such as middle distillate increased and coke formation was inhibited in comparison to thermal cracking.

Table 5.3 shows the activity of Fe-based dispersed catalysts on heavy oil upgrading in terms of product distribution, product quality and physical properties. It has been shown in Section 5.3 and Table 5.1 that unsupported Fe-based catalysts give similar levels of upgrading at 900 rpm under the same experimental conditions. The coke reduced from 12 wt% for thermal cracking without catalyst to 8.28 wt% for FeS and 6.79 wt% for Fe_2O_3. In addition, the produced gas yields were 9.59 wt% for FeS and 10.72 wt % for Fe_2O_3. Also, in comparison to thermal upgrading, an increase was observed for the liquid amount at 81.9 wt% for FeS and at 82.48 wt% for Fe_2O_3, respectively.

Table 5.3. Effect of iron-based catalysts on product distribution, physical properties and product quality [a]. (Feedstock: API 12.8°, Viscosity 1482 cP, C_5-aphaltene 14 wt%, 0.68 wt% (IBP-177 °C), 28.18 wt% (177-343 °C), 71.6 wt% 343 °C+, 3.09 wt% sulphur , 0.0132 wt% (Ni+V)).

Catalysts type /size	Non	Fe_2O_3 (≤ 50 nm)	FeS (≤ 140 μm)
Product distribution (wt%)			
Coke	12	6.79	8.28
Liquid	76	82.48	81.9
Gas	12	10.72	9.83
C_5-aphaltene	4.5	10	7.26
SIMDIST Boiling point distribution of produced liquid (wt %)			
(IBP-177 °C)	25	21	24
(177-343 °C)	43	47	48
(343°C+)	32	32	28
Physical properties of produced liquid			
API gravity at 15 °C	24	21	21
Viscosity (cP) at 20 °C	53.54	105.75	102.77
Product quality removal % of produced liquid			
HDS	43.92	37.54	39.57
HDM	85.67	69.38	75.18
N (wt%)	0.25	0.14	0.2

[a] Reaction conditions: two steps:410°C, 50 min, metal loading 0.1 wt %, H_2 initial pressure 50 bar, mixing speed 900 rpm, followed by 425°C, 60 min, mixing speed 900 rpm. Errors arre expressed in terms of standard deviation for triplicate experiments as follows: coke wt % ±0.3, liquid wt % ± 0.19, gases wt % ±0.6, asphaltene wt % ±0.85, middle distillate (177-343 °C) wt % ±0.4, light naphtha (IBP-177 °C) wt % ±0.35, gas oil (343-525 °C) wt% ± 0.45, API° ±0.28, viscosity ±2, HDS% ±0.65, metal HDM% ±0.38, N wt% ±0.02.

The distilled fractions from the SimDist analysis showed the following: light naphtha (24 wt %), middle distillate (48 wt %) and heavy fractions (343 °C+) (28 wt %) for FeS. However, for Fe_2O_3 the distillate fraction increased to 47 wt %, the light naphtha fraction

reduced to 21 wt %, and the heavy fractions (343 °C+), stayed constant at 32 wt %. These results are in line with the literature, where similar observations have been reported (Vasireddy et al., 2011; Kaneko et al., 2000; Kaneko et al., 1998). It was observed that the asphaltene amount in the produced oil was 7.26 wt % for FeS and 10 wt % for Fe_2O_3, relative to 4.5 wt % in thermal upgrading. This finding is consistent with the observation for MoS_2 and MoO_3 discussed in Section 5.4.

Table 5.3 shows the performance of Fe-based catalysts in terms of physical properties and product quality. As expected, the results did not show further improvement in terms of physical properties or product quality when using Fe-based catalyst relative to thermal upgrading. However, coke formation was suppressed significantly by 43.4% (Fe_2O_3) and 31.1% (FeS) which is in line with that observed with Mo-based catalysts. An API gravity of 21° and a viscosity of 102.77 ± 2 cP were observed for produced oil with FeS and Fe_2O_3 relative to 24° and 53 cP achieved with thermal upgrading. In addition, the extent of sulphur (HDS) and metal (HDM) removal was respectively 39.57 % and 75.18% for FeS and 37.5% and 69.4% for Fe_2O_3. While FeS showed slightly higher HDS activity compared to Fe_2O_3, the reverse was the case for HDM. The trend is similar to that reported in Section 3.3 and the HDM is consistent with coke yield (Table 5.3). However, Fe-based unsupported catalysts showed similar behaviour to MoO_3 in terms of removal of nitrogen. The nitrogen content was 0.2 wt % (FeS) and 0.14 wt % (Fe_2O_3), respectively and these results are similar to those of Gray et al. (Gray et al., 1989).

The observed overall performance of Fe-based catalysts was similar to Mo-based counterparts in terms of API gravity, viscosity, distillate fractions, HDS and HDM; however, Mo-based unsupported catalysts showed higher activity in suppressing coke formation. These results show the effectiveness of Fe-based unsupported catalysts as an attractive and alternative choice for in situ heavy oil upgrading when cost and availability are considered.

5.6 Effect of nickel-based catalysts

It has been shown that unsupported metal oxide catalysts are converted to their sulphide form during heating and reaction (see Section5.2), and also the performance of oxide and sulphide forms were approximately similar (Sections 5.4 and 5.5).

Table 5.4 shows the performance of nickel-based catalysts in terms of product distribution, physical properties and product quality. It can be seen that NiO-dispersed catalysts gave a low amount of coke, a moderate amount of gas and a relatively high amount of liquid and asphaltene.

Table 5.4. Effect of Nickel-based catalysts on product distribution, physical properties and product quality [a]. (Feedstock: API 12.8°, Viscosity 1482 cP, C_5-aphaltene 14 wt%, 0.68 wt% (IBP-177 °C), 28.18 wt% (177-343 °C), 71.6 wt% 343 °C+, 3.09 wt% sulphur , 0.0132 wt% (Ni+V)).

Catalysts type /size	Non	NiO (≤ 50 nm)
Product distribution (wt%)		
Coke	12	5.76
Liquid	76	84.64
Gas	12	9.59
C_5-aphaltene	4.5	8.58
SIMDIST Boiling point distribution of produced liquid (wt %)		
(IBP-177 °C)	25	21
(177-343 °C)	43	49
(343 °C+)	32	30
Physical properties of produced liquid		
API gravity at 15 °C	24	22.4
Viscosity (cP) at 20 °C	53.54	74.12
Product quality removal % of produced liquid		
HDS	43.92	35.08
HDM	85.67	65.37
N (wt%)	0.25	0.14

[a] Reaction conditions: two steps: 410°C, 50 min, metal loading 0.1 wt %, H_2 initial pressure 50 bar, mixing speed 900 rpm, followed by 425°C, 60 min, mixing speed 900 rpm. Errors are expressed in terms of standard deviation for triplicate experiments as follows: coke wt % ±0.17, liquid wt % ± 0.36, gases wt % ±0.5, asphaltene wt % ±0.67, middle distillate (177-343 °C) wt % ±0.23, light naphtha (IBP-177 °C) wt % ±0.54, gas oil (343-525 °C) wt% ± 0.25, API° ±0.3, viscosity ±2.7, HDS% ±0.35, metal HDM% ±0.45, N wt% ±0.02.

The product distributions achieved are as follows: coke (5.8 wt %), gas (9.5 wt %), liquid (84.6 wt %), and asphaltene (8.6 wt %), respectively. Notably, both light naphtha and the middle distillate fraction increased, while the heavy fractions (343 °C+), reduced in comparison to thermal upgrading. The coke yield was reduced remarkably in a similar manner to that of the Mo unsupported catalyst. Zhang et al. (2007) reported that coke yield is significantly inhibited using dispersed nickel catalysts at 425°C, 6 MPa, Ni loading 300 (μg/g) and a reaction time of 1 hour during residue hydrocracking (Zhang et al., 2007). This is because the active metals (Ni, Mo or Fe) help in moderating the rate of free radical propagation via β-scission reactions by incorporating hydrogen to the cracked active hydrocarbon fragments during heavy oil upgrading (Peureux et al., 1995; Weitkamp, 2012). This would explain the reduction in coke formation as well as the increase in liquid amount during hydroconversion in the presence of unsupported metal catalysts (Shuyi et al., 2008; Sanford, 1995). The distillate fractions of the produced oil after upgrading with unsupported Ni catalyst were 21 wt % (light naphtha), 49 wt % (middle distillate) and 30 wt % heavy fractions (343 °C+) . These results are in agreement with the literature (Zhang et al., 2007; Panariti et al., 2000a).

From Table 5.4 it can be observed that the upgraded oil with Ni catalyst produced more middle distillate than that achieved with thermal cracking; however, a reverse trend was seen for the naphtha fraction, while gas oil is similar within a marginal error of ±0.3% (standard deviation).

The upgraded oil after experiments with NiO particles achieved a viscosity value of 74.12 cP and an API gravity increase to 22.4˚ relative to 1482 cP and 12.8˚ for the feed oil. However, in comparison to thermal upgrading, the results did not show higher improvement in API gravity and viscosity (see Table 5.4). This is consistent with previous observation on the use of Mo and Fe unsupported catalysts discussed in sections 5.4 and5.5. The low API

gravity and high viscosity of produced oil after upgrading with Ni catalyst can be attributed to the high average molecular weight fractions (such as asphaltene) and the interaction strength between molecules (Wu et al., 2010; Argillier et al., 2002; Altgelt and Harle, 1975). The absence in cracking functionality of the unsupported metal particles contributed to this observation.

Table 5.4 also shows the effect of nickel oxide (NiO) dispersed catalysts on the removal of sulphur, metal and nitrogen. The immediate evaluation showed no further improvement in comparison to thermal upgrading. The HDS and HDM obtained was 35.1% and 65.4% respectively for NiO in comparison to 43.9% and 85.7 % for thermal upgrading. It has been reported that the breaking of the C-heteroatoms bond is mainly controlled by temperature (Sahu et al., 2015; Shuyi et al., 2008). In addition under reaction conditions Ni-based catalysts could be converted to sulphide phase (NiS, Ni_3S_4) (Shuyi et al., 2008; Liu et al., 2010). Nickel-based catalysts in their sulphide form are considered to be highly active for hydrogen activation and therefore, hydrogenating free radicals during heavy oil upgrading (Li et al., 2004). In terms of nitrogen removal, Ni-based catalysts showed similar behaviour to MoO_3 and Fe_2O_3. The nitrogen content increased to 0.14 wt % for NiO relative to 0.08 wt % in the feed oil. A detailed explanation has been provided in Sections 5.4and 5.5. However, NiO has very similar activity effectiveness in comparison to the metal oxides of Mo and Fe.

It has been reported in the literature that each barrel of bitumen produced by thermal production methods (e.g. SAGD, CSS), requires between 1.0 to 1.1 tonnes cubic feet (tcf) of natural gas, based on a dry steam-to-oil ratio. Additionally, the supply costs which are stated as a range, reflecting variables such as: reservoir quality, depth of the producing formation, recovery method and operating parameters has been reported as follows: (1) Cyclic Steam Stimulation (CSS) from 20 to 24 $ per barrel (2) Steam Assisted Gravity Drainage (SAGD) from 18 to 22 $ per barrel (Board, 2006; Meyer and Attanasi, 2004). In comparison to SAGD

and CSS, using the THAI method could help to further reduce the supply cost to less than $18 per barrel, since the THAI process uses little natural gas and water to produce an upgraded oil product which meets the requirement of pipeline transportation without diluents. Moreover, The CAPRI/THAI is a technique to further boost the upgrading arising from the pyrolysis of heavy oil (Dim et al., 2015) which offers the prospect of both enhancing recovery, and decreasing cost for a surface upgrading facility. In situ catalytic upgrading involves the use of the reservoir as a reactor, which offers cost, energy and environmental benefits as it utilizes heat energy from in situ combustion to drive the catalysis, most of the impurities such as sulfur, vanadium, iron, and nickel are left behind in the reservoir, thus lowering the environmental footprint and impact on downstream refining processes, and reduces the cost of diluents to improve pipeline transport (Hart et al., 2014; Hoshyargar and Ashrafizadeh, 2013; Hashemi et al., 2013).

5.7 Effect of dispersed catalysts on formed coke

High amounts of coke formed during thermal processes can be stimulated. There is a body of research directed to increase coke market value in order to use for applications such as industrial fuel or making anodes for aluminium manufacturing (Termeer, 2013; Ellis et al., 1998). A morphological investigation was conducted on coke samples obtained from thermal and unsupported catalytic upgrading in order to identify the coke quality and type.

Figure 5.3 (a) and (b) show the SEM photomicrographs of coke recovered after thermal upgrading. It can be observed that the coke texture is characterised by a smooth and concave surface (see position x in Figure 5.3 (a)) with no evidence of holes. From a morphological standpoint, the coke produced by thermal upgrading could be classified as shot-coke type, and other researchers have made similar observations in the literature (Kelemen et al., 2007; Siskin et al., 2006; Elliott, 2000).

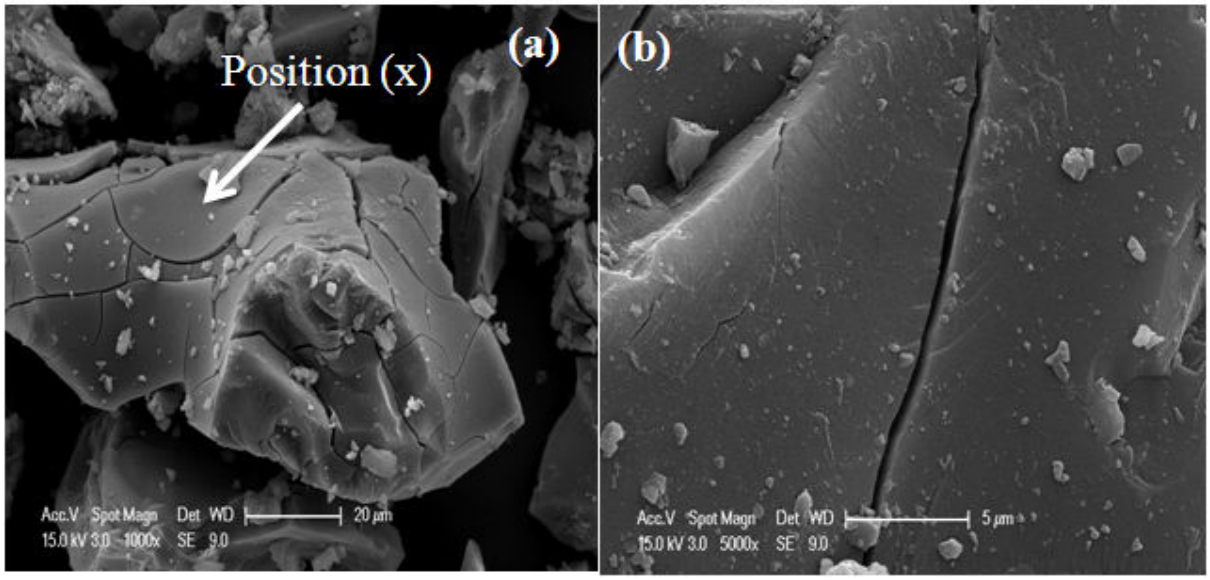

Figure 5.3. SEM photomicrograph of recovered coke from thermal upgrading. For reaction conditions see Table 5.2.

In addition, it has been reported that the type of coke formed is mainly dependent on feed properties; in particular, high asphaltene and metal content leads to shot-type coke (Picón-Hernández et al., 2008; Kelemen et al., 2007; Marsh et al., 1985). This can also be affected by Low Temperature Oxidation (LTO), producing shiny, very hard, and more difficult to burn coke. This therefore confirmed the high level of metal removal and low asphaltene content of the produced oil observed with thermal cracking (Table 5.1 and 5.2). In a similar light, Picon-Hernandez et al. (2008) observed that shot-type coke from coking processes of feed oil has an asphaltene amount of 14 wt%, as well as 600 ppm of metal (Ni+V) content (Picón-Hernández et al., 2008). The asphaltene stability in the oil mixture could be disturbed during thermal upgrading (Gawel et al., 2005), which could lead to precipitation of asphaltene and promote shot-type coke formation (Siskin et al., 2006). The asphaltene and metal content of the feed oil used in this study was 14 wt% and 0.0132 wt% (132 ppm) previously shown in Table 3.3 , which has the tendency to form shot–type coke. Shot-type coke is low in economic value and consists of individual particles that are spherical to

slightly ellipsoidal, with average diameters of about 1-4 mm (Siskin et al., 2006). Nevertheless, understanding feed properties as well as controlling upgrading reaction conditions can help in minimizing low value coke (shot-type coke) and in producing more economically valuable coke types (Elliott, 2000).

Figure 5.4 and 5.5 show the SEM photomicrographs for the coke recovered after upgrading using dispersed unsupported catalysts MoS_2 and Fe_2O_3, respectively; for reaction conditions see **Table 5.2** and 5.3. Similar micrographs were obtained for NiO, MoO_3, and FeS catalysts are presented in Appendix A.

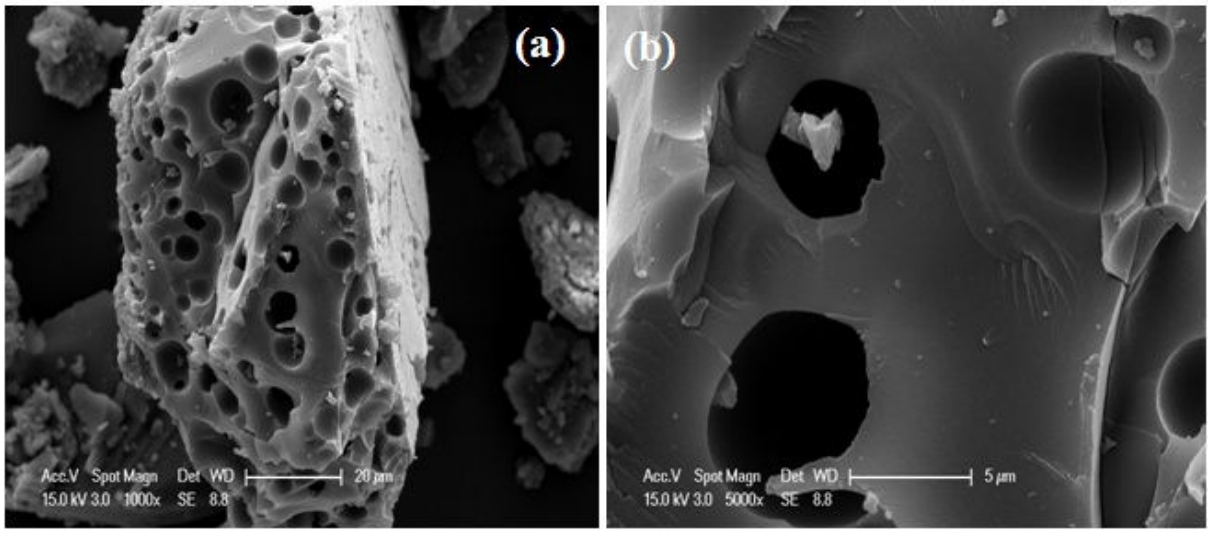

Figure 5.4. SEM photomicrograph of recovered coke from catalytic upgrading MoS_2.

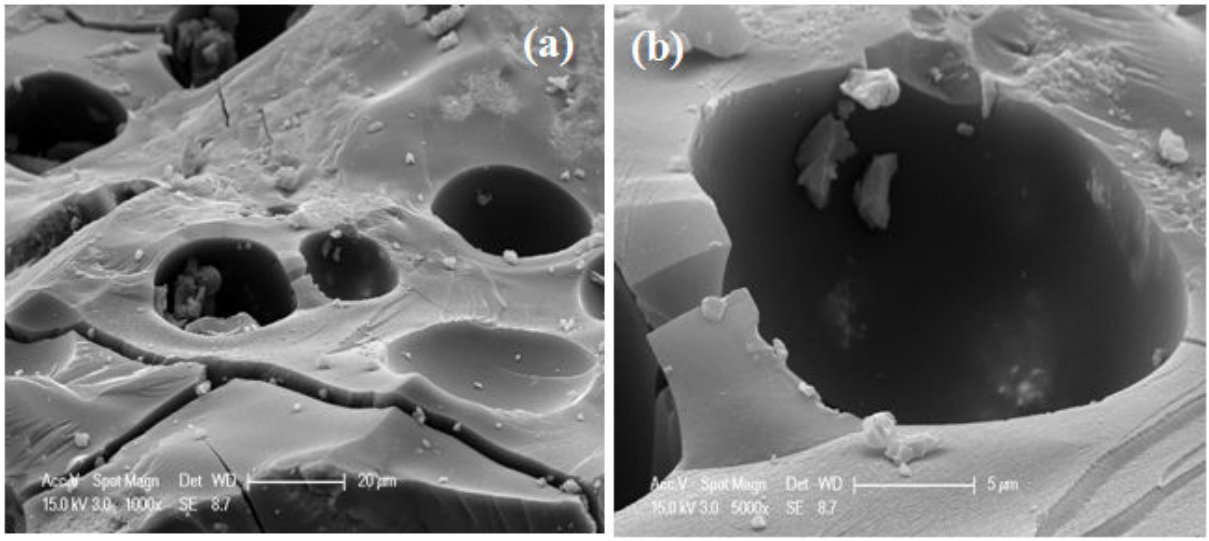

Figure 5.5. SEM photomicrograph of recovered coke from catalytic upgrading Fe_2O_3.

It is clear from Figure 5.4 and 5.5 that the coke texture is characterised by a highly porous microstructure with a wide variety of pore sizes. From a morphological standpoint, the coke produced after upgrading reactions using unsupported metals catalysts such as MoS_2 and Fe_2O_3 can be classified as sponge-type coke. Similar observations have been reported elsewhere (Picón-Hernández et al., 2008; Marsh et al., 1985). Sponge-type coke is named for its sponge-like appearance with different sized pores and bubbles in the coke matrix. Compared to shot-type coke observed for coke produced after thermal cracking (Figure 5.3), sponge-type coke has a higher economic value with a high potential to be used as fuel (Ellis et al., 1998). It was observed that the asphaltene content in feed oil is the main factor responsible for shot-type coke versus sponge-type coke formation in delayed cokers (Siskin et al., 2006; Ellis et al., 1998; Marsh et al., 1985). Moreover, Picon-Hernandez et al. (2008) observed sponge-type coke from coking processes of feed oil, which moderated asphaltene and metal (Ni+V) content (Picón-Hernández et al., 2008). It can therefore be confirmed that the active metal (Ni, Mo or Fe) actually helped in controlling the rate of addition reactions between free radicals during heavy oil upgrading by promoting hydrogen uptake by the cracked active hydrocarbon fragments (Peureux et al., 1995; Weitkamp, 2012). This stabilizes the asphaltene in the oil mixture, and explains the formation of sponge-type coke during catalytic upgrading with MoS_2 and Fe_2O_3. Furthermore, sponge type cokes are porous lumps which are surrounding by relatively thin walls with no interconnection between pores (Reis, 1975; Jakob, 1971). In the reservoir the flow of upgraded oil could crack and convey sponge-type coke to the production well and to the surface because of its physical appearance. Coke lay down ahead of the combustion front during the THAI process acts as fuel for the process.

Chapter 6
Coke Suppression by Different Hydrogen Sources during In-Situ Upgrading of Heavy oil via Dispersed Nanocatalyst

6.1 Introduction

This chapter is devoted to investigate effects of different hydrogen sources (methane, steam) instead of hydrogen in the presence and absence of unsupported dispersed catalyst ($Fe_2O_3 \leq 50$ nm) for in situ heavy oil upgrading. The performance of methane and steam with and without Fe_2O_3 were investigated in term of product distribution (i.e., liquid, gas and coke) and (naphtha, middle distillate and gas oil fractions), physical properties (i.e., API gravity and viscosity) and product quality (i.e., sulphur, metals and nitrogen contents) and evaluated against that achieved with heavy oil reaction under H_2 with and without the addition of Fe_2O_3. Also, effect of tetralin with and without dispersed catalysts were studied using the same reactor and compare with upgrading reaction achieved under different hydrogen sources with and without Fe_2O_3. Additionally, the effect of different hydrogen sources and tetralin with and without Fe_2O_3 on the type and quality of produced coke from the upgrading reactions is studied using Scanning Electron Microscope (SEM).

6.2 Effect of different hydrogen sources

Table 6.1 shows the effect of different hydrogen sources on heavy oil upgrading in the presence and absence of unsupported Fe_2O_3 NPs in terms of product distribution, physical properties and product quality.

Table 6.1. Effect of different hydrogen sources on heavy oil upgrading [a]. (Feedstock: API 12.8°, Viscosity 1482 cP, C_5-aphaltene 14 wt%, 0.68 wt% (IBP-177 °C), 28.18 wt% (177-343 °C), 71.6 wt% 343 °C+, 3.09 wt% sulphur , 0.0132 wt% (Ni+V)).

Gas (Catalyst)	Product distribution (wt %)				SIMDIST Boiling point distribution of produced liquid(wt %)			Physical properties		Product quality (wt %)	
	Coke	Liquid	Gas	C_5-aphaltene	(IBP-177 °C)	(177-343 °C)	(343°C+)	API gravity° 15 °C	Viscosity (cP) 20 °C	Sulphur	Metal (Ni+V)
N_2 (non) [b]	11.00	76.00	13.00	5.50	26	45	29	22.4	74.12	2.30	0.0031
H_2 (non)	12.00	76.00	12.00	4.50	25	43	32	24.0	53.54	2.29	0.0025
CH_4 (non)	7.16	80.57	12.28	15.43	21	30	49	21.4	112.00	2.39	0.0029
H_2O (non)[C]	7.32	78.42	14.26	14.89	26	42	32	19.3	254.60	2.45	0.0042
H_2 (Fe_2O_3)	6.79	82.48	10.72	10.00	21	47	32	21.0	102.77	2.34	0.0049
CH_4 (Fe_2O_3)	6.19	81.09	12.72	16.01	24	33	43	22.5	72.00	2.42	0.0028
H_2O (Fe_2O_3)[C]	7.48	78.85	13.67	9.47	24	45	31	20.1	140.00	2.52	0.0030

[a] Reaction conditions: two steps (410 °C, 50min, initial pressure 50 bar, $Fe_2O_3 \leq 50$ nm loading 0.1 wt % , mixing speed 900 rpm followed by 425 °C, 60min, mixing speed 900 rpm). Errors were expressed in terms of standard deviation for triplicate experiments as follows: coke wt % ±0.35, liquid wt % ± 0.45, gases wt % ±0.6, asphaltene wt % ±1, middle distillate wt % ±1,light naphtha wt % ±1.5, gas oil wt% ± 1, API° ±0.3, viscosity ±3, S% ±0.02, metal (Ni+V) % ±0.0004, [b] control experiment, [C] water to oil ratio 0.11 (g/g), N_2 was used to create desired initial pressure, non = no catalysts (thermal cracking).

It can be observed that the product distribution after upgrading of heavy oil in the absence of Fe_2O_3 NPs under N_2 (control experiment) was 11 wt % (coke), 76 wt% (liquid), 13 wt% (gas) and 5.5 wt% (asphaltene). A similar activity in terms of product distribution has been noticed with an analogous reaction performed (in the absence of catalysts) under hydrogen gas (H_2) instead of N_2 at high reaction conditions. This is because the reaction media influences the chemistry of the reaction while the C-C and C-heteroatom bonds cleavages are temperature dependent, hence, since the experimental temperature and conditions are the same this result is expected. The product distribution results from heavy

oil upgrading under methane gas (CH_4) and steam (H_2O) in the absence of catalysts, however showed lower coke formation as well as higher liquid and asphaltene yields, where the coke yield was 7.16 wt% for CH_4 and 7.32 wt% for H_2O relative to 11 wt% for the control experiment and 12 wt% for H_2. Also, from Table 6.1 it is clear that the liquid yield increased from 76 wt% for the control experiment under H_2 to 80.57 wt% for CH_4 and 78.42 wt % for H_2O. Furthermore, the amount of asphaltene significantly increased to 15.43 wt% for CH_4 and 16.01 wt% for H_2O compared to 4.5 wt% for H_2 and 5.5 wt% for the control experiments (under N_2). Hence, in the absence of catalysts the inhibition of coke formation in terms of hydrogen sources is as follows: $CH_4 > H_2O > H_2 \geq N_2$.

It can also be observed that in the presence of unsupported dispersed Fe_2O_3 NPs the inhibition of coke formation increased in terms of the hydrogen sources as follows: $CH_4 \geq H_2 > H_2O$. The coke yield reduced as follows: 6.19 wt% (CH_4+ Fe_2O_3), 6.79 wt% (H_2+ Fe_2O_3), and 7.48 wt% (H_2O+ Fe_2O_3) relative to 7.19 wt% (CH_4), 12 wt% (H_2) and 7.32 wt % (H_2O) without Fe_2O_3 NPs addition. Furthermore, the liquid yield slightly increased as follows: 81.1 wt% (CH_4+ Fe_2O_3), 82.48 wt% (H_2+ Fe_2O_3) and 78.85 wt% (H_2O+ Fe_2O_3) compared to 80.57 wt% (CH_4), 76 wt % (H_2) and 78.42 wt% (H_2O) attained when Fe_2O_3 NPs were not added. The produced gas did not show further change, it remained within a narrow range of 10 -13

wt% for all hydrogen sources in the presence and absence of Fe_2O_3 NPs. The amount of asphaltene in the produced upgraded oil samples significantly increased in the presence of Fe_2O_3 with H_2 to 10 wt % relative to 4.5 wt % for H_2 without the addition of NPs. However, the asphaltene content was almost similar in the presence and absence of Fe_2O_3 with CH_4 and H_2O (see Table 6.1). The results indicate that CH_4 and H_2O are active in terms of coke formation reduction under thermal and or catalytic upgrading and could be used as a source of hydrogen which is in agreement with the literature (Ovalles et al., 1998; Ovalles et al., 2003).

It has been reported that at reaction temperatures greater than 420 °C the free radical reaction mechanism initiated cracking C-C bonds and as a consequence free radicals (R•, where is alkyl group) are generated and chain reactions are initiated (Petrakis and Grandy, 1981; Neavel, 1976). However, a long reaction time will promote cracking, secondary cracking of intermediates and greater yields of coke, light naphtha, middle distillate and gas. The free-radical reaction mechanism can lead to incorporating CH_4 and H_2O (in the absences of catalysts) into hydrocarbon molecules via production of methyl (CH_3) and hydroxyl (OH) groups by R• (Ovalles et al., 1995; Dutta et al., 2000). This may explain why the activity of CH_4 and H_2O in terms of coke reduction was more remarkable. Moreover, the sulphidation reaction between the dispersed catalysts and the sulphur contained in the heavy oil assisted in the formation of the NPs active phase, such as metallic sulphides (Liu et al., 2009; Ovalles et al., 2003). This active phase activation can also be achieved by H_2 and CH_4 (Ovalles et al., 2003; Egiebor and Gray, 1990). The contribution of H_2 and CH_4 towards the activation of the NPs further explained the reduction in coke yield as well as the increase in produced upgraded liquid for H_2+Fe_2O_3 and CH_4+Fe_2O_3. Furthermore, the observed lower asphaltene content after thermal upgrading under N_2 and H_2 (in the absence of catalyst) with respect to upgrading under CH_4, H_2O and upgrading reaction under CH_4, H_2O and H_2 with dispersed

unsupported iron oxide catalysts can be attributed to the high carbon-rejection caused by high asphaltene deposition during thermal upgrading under N_2 and H_2 (Gawel et al., 2005; Bartholdy et al., 2001; Bartholdy and Andersen, 2000; Gray, 1994). The reaction stages for upgrading under CH_4 are as follows (Ovalles et al., 1995):

Initiation:

$$R - R' \rightarrow R^{\bullet} + R'^{\bullet} \quad 6.1$$

Propagation:

$$R^{\bullet} + CH_4 \rightarrow RH + CH_3^{\bullet} \quad 6.2$$

$$CH_3^{\bullet} + R - R' \rightarrow R'CH_3(RCH_3) + R^{\bullet}(R'^{\bullet}) \quad 6.3$$

Termination:

$$R^{\bullet} + CH_3^{\bullet} \rightarrow RCH_3 \quad 6.4$$

$$CH_3^{\bullet} + CH_3^{\bullet} \rightarrow CH_3CH_3 \quad 6.5$$

$$R^{\bullet} + R'^{\bullet} \rightarrow R - R' \quad 6.6$$

where; $R\ and\ R'$ are hydrocarbons

The upgraded oil produced after heavy oil upgrading under N_2 and different hydrogen sources in the presence and absence of Fe_2O_3 was analyzed and the distilled fractions distribution are also presented in **Table 6.1**. It can be seen that the upgrading reaction in the absence of catalyst under N_2, H_2 and H_2O has similar liquid distribution; however CH_4 notably shows a slightly higher amount of heavy fractions (343 °C+), . The light naphtha fraction (IBP-177 °C) was approximately 25 wt% , middle distillate fraction (177-343°C) and the heavy fractions (343 °C+) remained within a narrow range between 43- 45 wt% and 29-32 wt% for N_2, H_2 and H_2O in comparison to 21 wt% for the BP-177°C fraction, 30 w % for the 177-343°C fraction and 49 wt% for the heavy fractions (343 °C+) for CH_4. The upgrading reaction in the presence Fe_2O_3 under H_2O and CH_4 shows a similar trend with

upgrading without catalysts, however, H_2 with Fe_2O_3 showed a slight improvement in the 177-343 °C fraction which increased to 47 wt% relative to 43 wt% for the control experiment. The results confirmed that the hydrogen sources does not promote C-C bond cracking which is mainly controlled by reaction temperature, but may influence the reaction pathways. The increased yield of the 177-343°C fractions for H_2 + Fe_2O_3 could be attributed mainly to the capping of free radicals by hydrogen, which is a major function of the unsupported catalyst particles (Panariti et al., 2000a). Furthermore, the increase in the amount of heavy fractions (343 °C+) in the reaction of CH_4, and CH_4 + Fe_2O_3 could be attributed to the methylation of aromatic rings by CH_4 as well as cyclization and dehydrogenation reactions which may generate high boiling point aromatic derivatives (Egiebor and Gray, 1990; Giavarini and Vecchi, 1987) as follows:

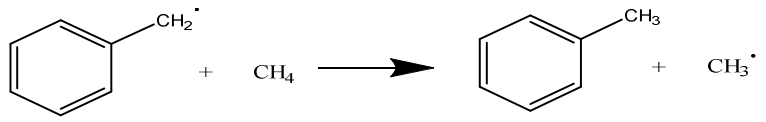

6.6

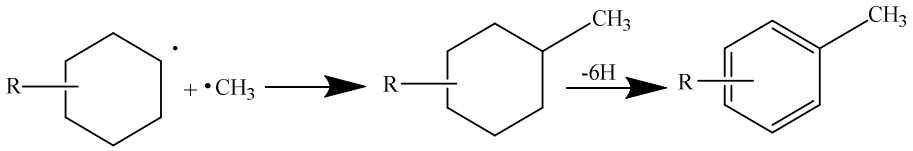

6.7

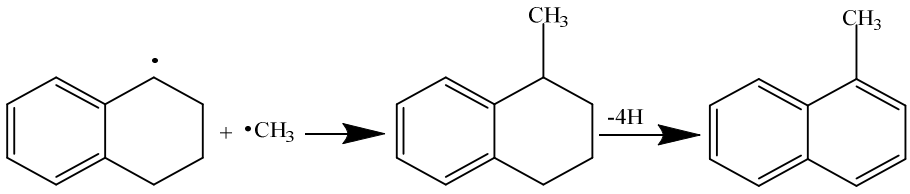

6.8

From Table 6.1, the effect of heavy oil upgrading under N_2 (control experiment) and different hydrogen sources in the presence and absence of Fe_2O_3 on the API gravity and viscosity can be seen. It can be observed in the absence of Fe_2O_3 the API gravity and viscosity increase for the hydrogen sources as follows: $H_2 > N_2 > CH_4 > H_2O$. The respective

API gravities and viscosities were (24°, 54.53 cP) for H_2, (22.4°, 74.12 cP) for N_2, (21.4°,112 cP) for CH_4 and (19.3°, 254 cP) for H_2O relative to (12.8,1482 cP) for the feed oil. On the other hand, it can be noticed that the produced oil after upgrading under H_2, CH_4 and H_2O in the presence of dispersed catalysts (Fe_2O_3) did not show the same level of API gravity and viscosity improvement as observed by thermal upgrading without Fe_2O_3 using the same hydrogen sources. The API gravity was lower by approximately 2° relative to upgrading achieved without Fe_2O_3 under different hydrogen sources. The viscosity reduced to 102.77 cP (for H_2+ Fe_2O_3), 72 cP (for CH_4+Fe_2O_3) and 140 cP (for H_2O+Fe_2O_3) relative to 1482 cP for the feed oil. The increase in API gravity and the decrease of viscosity of produced upgraded oil can be attributed to cracking of high molecular weight fractions such as asphaltene (Wu et al., 2010; Argillier et al., 2002; Altgelt and Harle, 1975; Hart et al., 2014). As a consequence of the cleavage of molecular bonds and the rupture of aromatic rings gas, coke and a large number of smaller and less viscous products were produced (Wu et al., 2010; Omole et al., 1999; Zhang et al., 2012). It has also been reported in the literature (Wu et al., 2010; Luo and Gu, 2007; Hongfu et al., 2002; Gray, 1994; Rhoe and Deblignieres, 1979) that unsupported catalysts such as that used in this study (e.g. Fe_2O_3) are not bifunctional in nature; they do not promote cracking of C-C and C-heteroatom bonds in contrast to zeolites and alumina which possess acid sites that support cracking. Hence, the viscosity reduction and API gravity improvement is mainly controlled by thermal cracking and the presence of Fe_2O_3 with different hydrogen sources would not contribute to cracking. However, H_2 + Fe_2O_3, CH_4, CH_4 + Fe_2O_3 and H_2O are known to contribute towards hydrogenation reactions of free radicals (Watanabe et al., 2010; Dutta et al., 2000; Sahu et al., 2015; Loser et al., 1989) which helped to stabilize asphaltene in the reaction medium and would explain the decrease of API gravity as well as the increased viscosity relative to thermal cracking (Gawel et al., 2005; Dealy, 1979). This is consistent with the high

asphaltene content of the produced oil after upgrading with H_2 + Fe_2O_3, CH_4, CH_4+Fe_2O_3 and H_2O compare to thermal cracking under N_2 and H_2.

In order to evaluate the effect of different hydrogen sources on heavy oil upgrading with and without dispersed catalyst the product quality of the upgraded oil was studied and the data are also presented in Table 6.1. It can be noticed that the sulphur content of the produced upgraded oil samples from thermal upgrading under N_2 (control experiment) and H_2 in the absence of Fe_2O_3 were 2.30 wt% and 2.29 wt%, respectively relative to 3.09 wt% in the fed oil. However, upgrading reactions under CH_4 and H_2O without dispersed catalyst (Fe_2O_3) show a slight increase in the sulphur content relative to reaction with N_2 and H_2, where the sulphur content was 2.39 and 2.45 wt%, respectively. The upgrading reaction under different hydrogen sources in the presence of Fe_2O_3 show a slight increase in the sulphur content with respect to upgrading under H_2, CH_4 and H_2O (without Fe_2O_3). The sulphur content was 2.34 wt % (H_2 + Fe_2O_3), 2.42 wt% (CH_4 + Fe_2O_3) and 2.52 wt% (H_2O+ Fe_2O_3). These results are in agreement with literature (Dutta et al., 2000; Gray, 1994), where noncatalytic desulphurization was achieved by the cleavage of the weak C-S bonds (compared to aromatic sulphur bonds) of aliphatic sulphides, and further increase in the sulphur due to upgrading with CH_4, H_2O, H_2 + Fe_2O_3 , CH_4 + Fe_2O_3 and H_2O + Fe_2O_3 can be attributed to high asphaltene content in the produced upgraded oil as discussed in the previous paragraph. In a similar manner, the metal content (Ni+V) followed a similar trend as the sulphur content where it can be noticed that the amount of metal (Ni+V) increased from 0.0025 wt% (H_2) to 0.0049 wt% (H_2 + Fe_2O_3). Higher asphaltene content was observed after upgrading heavy oil under CH_4, H_2O, H_2 + Fe_2O_3, CH_4 + Fe_2O_3 and H_2O + Fe_2O_3 which would explain the increased metal content as they are associated mainly with macromolecules such as asphaltene and resins (Gawel et al., 2005; Bartholdy et al., 2001). The C-hetroatoms cleavage is mainly controlled by the reaction temperature while the hydrogen source

influence the reaction pathways, however, the addition of the dispersed NPs catalysts did not show further reduction in sulphur and metal content.

6.2.1 Effect of tetralin

After the upgrading reactions tetralin and upgraded oil formed a homogeneous mixture making it difficult to separate compound by the high boiling point of tetralin (207°C at 1 atm). Separation of tetralin from the produced upgraded oil will affect the composition of the upgraded oil since some hydrocarbons would evaporate in the process. Therefore, the physical properties (API° gravity and viscosity) reported here are those of the produced mixture (upgraded oil and tetralin). Also, the reported data points on the following figures are average values taken from triplicate experimental runs and standard deviation were calculated and plotted to quantify the variance of the results.

6.2.2 Effect of tetralin to oil mass ratio

Figure 6.1 shows the coke yield and asphaltene content of the produced upgraded oil at different tetralin to oil mass ratios (T/O) at 425 °C reaction temperature, 10 bar initial pressure of nitrogen and 60 min reaction time. The initial N_2 pressure was selected as 10 bar to maintain tetralin in the liquid phase at the high reaction temperature, and maximize the interface between tetralin and oil during upgrading (Johannes et al., 2012).

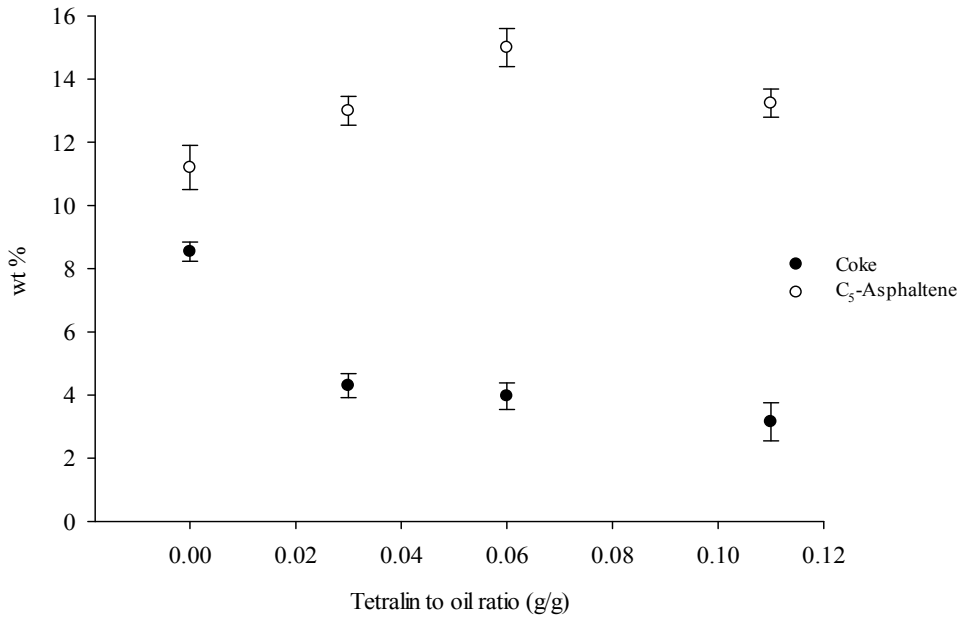

Figure 6.1. Coke yield and asphaltene content after upgrading of heavy oil at different tetralin to oil mass ratios (T/O) at 425 °C reaction temperature, 10 bar initial pressure of nitrogen (N_2) and 60 min for reaction time.

It can be observed that the coke yield drastically decreased in the presence of tetralin, however, as T/O ratio increased beyond 0.03 the decreased rate of coke yield becomes less. The asphaltene content of the upgraded oil samples gradually increased as the T/O ratio increased. At low T/O ratio (0.03 g/g) the coke yield dropped to 4.3 wt% relative to 8.54 wt% without the addition of tetralin (thermal upgrading under nitrogen N_2.). Furthermore, at 0.06 T/O ratio (g/g) the coke yield was 3.97 wt % and it decreased to its minimum value of 3.15 wt% at 0.11 T/O ratios (g/g). Moreover, the asphaltene content in the produced oil increased to 13.5 wt% for 0.03 T/O ratio (g/g), 15 wt% for 0.06 T/O ratio (g/g) and 13 wt % for 0.11 T/O ratio (g/g) relative to 11 wt % for thermal upgrading under N_2. These results are in line with literature where a similar observation has been reported (Rahmani et al., 2002; Johannes et al., 2012).

Table 6.2 shows the liquid and gas yield as well as the distillate fractions of produced upgraded oils (i.e., liquid) at different T/O ratios at 425°C reaction temperature, 10 bar initial N_2 pressure and 60 min reaction time.

Table 6.2. Distillate fractions of upgraded oil, liquid, and gas yield after upgrading at different tetralin to oil mass ratio [a]. (Feedstock: API 12.8°, Viscosity 1482 cP, C_5-aphaltene 14 wt%, 0.68 wt% (IBP-177 °C), 28.18 wt% (177-343 °C), 71.6 wt% (343 °C+), 3.09 wt% sulphur , 0.0132 wt% (Ni+V)).

Reaction media	SIMDIST D2887 ASTM of produced liquid (wt %)			Yield (wt %)	
	(IBP-177 °C)	(177-343 °C)	(343 °C +)	Liquid	Gas
N_2	22	43	35	81.34 ±0.47	10.68 ±0.6
0.03(g/g) (T/O) + N_2	27	45	28	85.89 ±1.1	9.81 ±0.38
0.06(g/g) (T/O) + N_2	20	50	30	85.10 ±0.85	10.93 ±0.4
0.11(g/g) (T/O) + N_2	21	47	32	84.38 ±0.55	12.47 ±1

[a] Reaction conditions 425°C for reaction temperature, 10 bar initial N_2 pressure 60 min, mixing speed 900 rpm. Errors were expressed in terms of standard deviation for triplicate experiments

In the presence of tetralin the liquid yield slightly increased compared to thermal upgrading under N_2, however, the gas yield was approximately the same. Consequently, as T/O ratios vary from 0.03 to 0.11 (g/g) the liquid yields did not show further improvement. The respective liquid and gas yields were almost 85 wt% and on average of 11 wt% for all T/O ratios relative to 81 wt% and 10.5 wt% for thermal upgrading under N_2. The middle distillate fraction results vary with different T/O ratio and were slightly higher than thermal upgrading under N_2. The middle distillate fraction was 45 wt% (0.03 T/O), 50 wt% (0.06 T/O) and 47 wt% (0.11 T/O) relative to 43 wt% for thermal upgrading under N_2. The slight increase of middle distillate fraction can be attributed to the presence of tetralin in the final mixture as the boiling point of tetralin overlaps the middle distillate fraction boiling point range (177-343 °C) (Alemán-Vázquez et al., 2012)., It is clear, therefore from Figure 6.1 and Table 6.2 that the 0.11 tetralin to oil mass ratio could be selected as optimum value to minimise coke formation as the coke reduced from 8.54 wt% to 3.15 wt% .

The obtained coke yield, asphaltene content and liquid yield from heavy oil upgrading at different ratios (T/O) confirm the cleavage of C-C bonds mainly controlled by reaction temperature. This cleavage of C-C bonds is believed to proceed by a free radical chain mechanism with the hydrogen donor solvent (i.e., tetralin) continually supplying active hydrogen to moderate coke precursors while producing low boiling fractions (Alemán-Vázquez et al., 2012; Liu and Fan, 2002). It has been reported that at high reaction temperature the asphaltene side chains start cracking leading to the formation of poly-aromatic core radicals and lower molecular weight hydrocarbons, this forms an asphaltene core radical and causes the precipitation of the asphaltene core, a known coke precursor. In light of this, phase separation occurs as the asphaltene aggregate forms a new phase (coke precursor) which is poorer phase for hydrogen transfer. In the absence of a hydrogen supply, an addition reaction between the precipitated asphaltene core radicals occur and the aggregate becomes more dominant, which results in the formation of a carbonaceous solid product termed coke (Rahmani et al., 2002; Wiehe, 1993). The presence of an aromatic solvent such as tetralin would fulfil two functions: (1) to enhance the dissolution of the coke precursor in the oil mixture, and (2) donate hydrogen to the asphaltene core (Rahmani et al., 2003; Watanabe et al., 2010). As result, phase separation can be avoided as the asphaltene core remains in solution, as asphaltene is known to be soluble in aromatic solvents such as tetralin and benzene. This would explain the reason for the low coke yields observed with the addition of tetralin.

Table 6.3 shows the effect of different (T/O) on API and viscosity for the original feed oil. Notably, the slight changes in API gravity and viscosity of the tetralin and heavy oil mixtures as the T/O ratio increases from 0.03 to 0.11 compared to that without tetralin. Figure 6.2 shows the API gravity and viscosity for the obtained upgraded oil and tetralin mixtures at different T/O ratios at 425°C, 10 bar initial N_2 pressure and 60 min reaction time.

Table 6.3. Effect of (T/O) on API and viscosity for original oil.

T/O ratio (g/g) before reaction	API gravity at 15 °C	Viscosity cP 20 °C
0	12.8°	1482.0
0.03	13.0°	1437.6
0.06	13.2°	1393.2
0.11	13.3°	1319.2

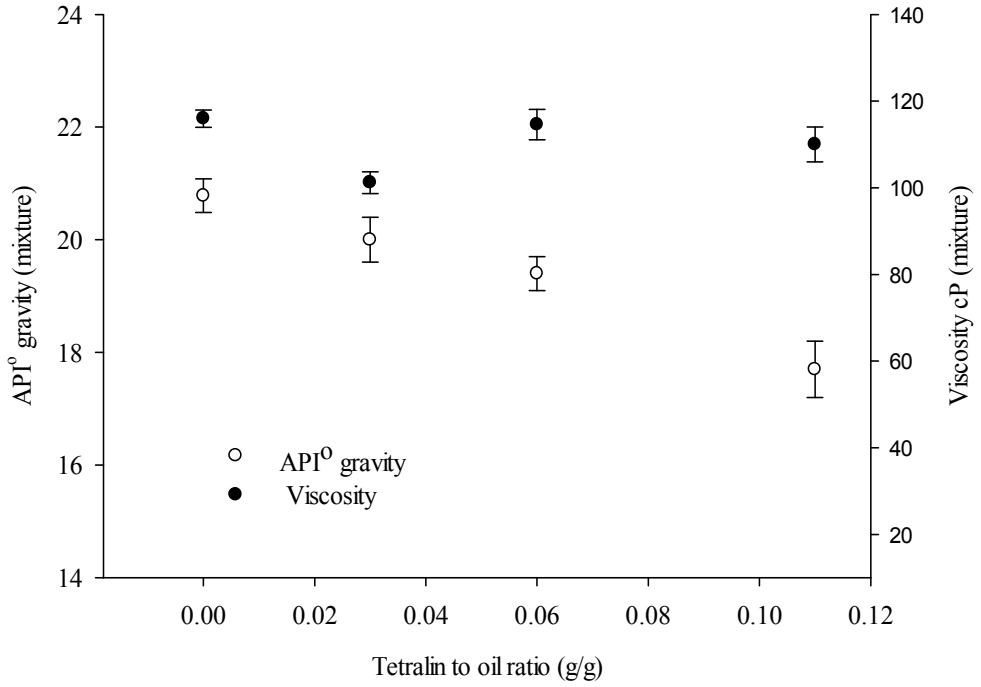

Figure 6.2. API gravity and viscosity of produced mixture at different T/O ratio at 425 C reaction temperature, 10 bar initial N_2 pressure and 60 min reaction time.

As expected, the obtained API gravity and viscosity of the mixtures remained within a narrow range at different T/O ratios and they are also close to results obtained for thermal upgrading under N_2. The API gravity increased from 12.8° for original feed oil (in the absence of tetralin) to 20.5° (N_2), 20° (0.03 T/O), 19.5° (0.06 T/O) and 18 ° (0.11 T/O) ratios. Conversely, the viscosity dropped to 115 cP (N_2), 101 cP (0.03 T/O) 114 cP (0.06 T/O) and 110 cP (0.11 T/O) relative to 1482 cp of the feed oil. These results are in agreement with the

literature where a similar trend has been observed and reported (Alemán-Vázquez et al., 2012).

The API gravity and viscosity results confirmed that tetralin did not contribute to cracking of C-C bonds. The cracking of C-C bonds are mainly controlled by reaction temperature, whose breakage leads to molecular weight reduction of large molecules resulting in reduced viscosity and increased API gravity observed in produced upgraded oils (Hart et al., 2013; Wu et al., 2010; Hongfu et al., 2002; Ovalles et al., 1995). Also, the presence of tetralin as a solvent contributed to the further reduced viscosity noticed in the upgraded of oil (Liu and Fan, 2002), and is dependent on the ratio of the tetralin to feed oil. The observed dropped in API gravity as the T/O ratio increases can be attributed to the presence of tetralin in the final upgraded oil as tetralin has high density (0.97 g/cm^3, 25 °C) when compared to the upgraded oil without added tetralin (see Table 6.3).

Figure 6.3 shows the effect of T/O ratios on product quality (sulphur and metal content) at 425 °C reaction temperature, 10 bar initial N_2 pressure and 60 min reaction time.

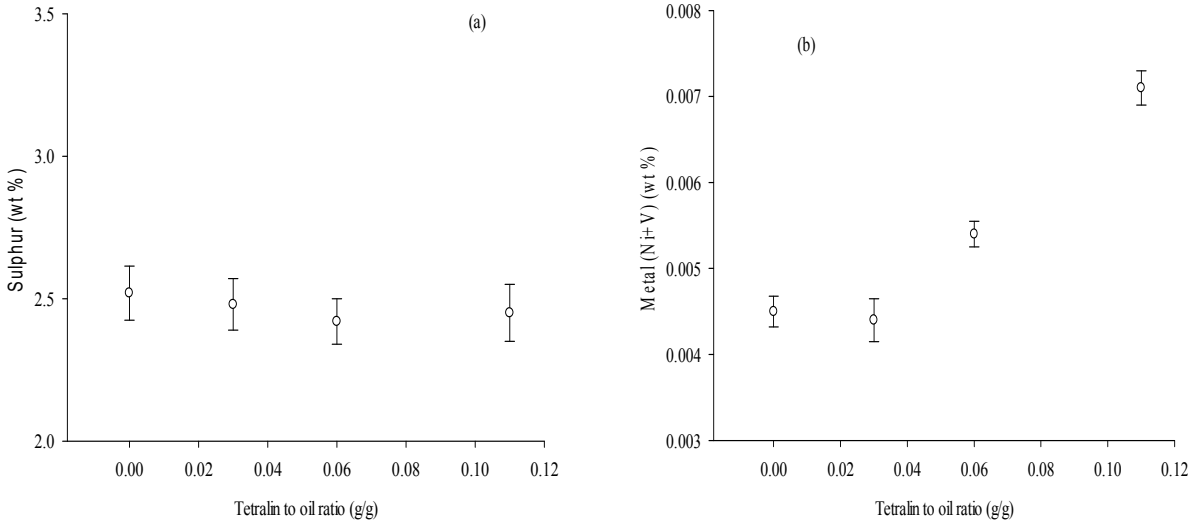

Figure 6.3. Effect of T/O ratio on product quality (a) sulphur wt % (b) metal content (Ni+V) wt % at 425 °C reaction temperature, 10 bar initial N_2 pressure and 60 min for reaction time.

It can be seen clearly from Figure 6.3 (a) and (b) that the presence of tetralin did not achieve significant reduction in sulphur content of the upgraded oil. However, the metal content is slightly increased compared with thermal upgrading under N_2 (in the absence of tetralin). The sulphur content was 2.52 wt% for N_2, 2.48 wt% for 0.03 T/O (g/g), 2.42 wt% for 0.06 T/O (g/g) and 2.48 wt% for 0.11 T/O (g/g). Conversely, the metal (Ni+V) increased from 0.0041 wt% for N_2 to 0.0071 wt% for 0.11 T/O ratios. Tetralin does not promote cracking of C-C and C-heteroatom bonds hence, further cracking was not experienced with the addition of the tetralin as the main mechanism of upgrading is by free radical driven temperature (Vernon, 1980; Neavel, 1976). The tetralin performed as diluents for coke precursors which helped to stabilize asphaltene in the reaction medium (Gawel et al., 2005; Dealy, 1979) and would explain the increase in metal (Ni+V) content of the produced liquid as metals are mainly associated with asphaltene (see Figure 6.3 (b)).

6.2.3 Effect of unsupported dispersed iron oxide with tetralin on heavy oil upgrading

The unsupported dispersed catalyst activation experiment was conducted following the same procedure discussed in section 4.2. As stated earlier, the heavy oil upgrading reaction was performed at 10 bar N_2 initial pressure to maintain the presence of tetralin in the liquid phase at the high reaction temperature which would increase the tetralin and oil interaction (Johannes et al., 2012; Hooper et al., 1979). Figure 6.4 shows the effect of tetralin (0.11 (g/g)T/O) on coke formation and asphaltene content in the absence and presence of unsupported dispersed iron oxide catalyst ($Fe_2O_3 \leq 50$ nm, 0.1 wt %).

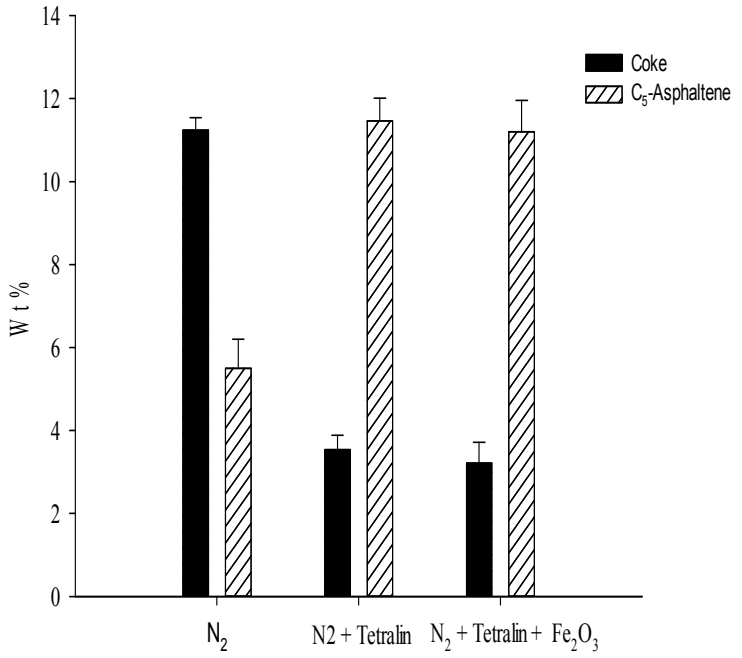

Figure 6.4. Effect of tetralin (0.11 (g/g) T/O) on coke formation and asphaltene content in the absence and presence of unsupported dispersed iron oxide catalyst ($Fe_2O_3 \leq 50$ nm, 0.1 wt %) at 425 °C for reaction temperature, 10 bar initial N_2 pressure 60min, mixing speed 900 rpm.

It can be seen that the coke formation significantly reduced from the introduction of tetralin, however the presence of Fe_2O_3 with tetralin did not show further reduction in the amount of coke produced. The coke yield significantly dropped from 11 wt % for thermal upgrading under N_2 to 3.54 wt % for tetralin and 3.22 wt % for tetralin + Fe_2O_3. The further decrease of 0.32 wt% can be noticed upon the addition NPs. The asphaltene content of the produced upgraded oil drastically increased in the presence of tetralin. However, the addition of Fe_2O_3 to tetralin did not indicate any further changes on asphaltene content, where the asphaltene content was in the range of 12 wt% for tetralin and tetralin + Fe_2O_3, relative to 5.5 wt% for N_2.

Table 6.4 shows the liquid and gas yields as well as the distilled fractions of produced upgraded oil under N_2, tetralin, and tetralin with dispersed catalyst (Fe_2O_3), respectively.

Table 6.4. Liquid, gas yield and distilled fractions distribution of produced liquid under N_2, tetralin and tetralin with dispersed catalyst [a]. (Feedstock: API 12.8°, Viscosity 1482 cP, C_5-aphaltene 14 wt%, 0.68 wt% (IBP-177 °C), 28.18 wt% (177-343 °C), 71.6 wt% 343 °C+, 3.09 wt% sulphur , 0.0132 wt% (Ni+V)).

Reactions media	SIMDIST D2887 ASTM (wt %)			Yield (wt %)	
	(IBP-177 °C)	(177-343 °C)	(343°C+)	Liquid	Gas
N_2	26	45	29	76.00 ±0.4	13.00 ±0.6
Tetralin + N_2	16	52	32	82.91 ±1	13.46 ±0.9
Tetralin + N_2+ Fe_2O_3	19	50	31	83.47 ±1.1	13.36 ±1

[a] Reaction conditions 425 °C for reaction temperature, 10 bar initial N_2 pressure 60min, mixing speed 900 rpm and dispersed iron oxide catalyst ($Fe_2O_3 \leq 50$ nm, 0.1 wt %). Errors were expressed in terms of standard deviation for triplicate experiments

In the presence of tetralin the liquid yield increased compared to thermal upgrading under N_2, while the gas yield remained within a narrow range. Upon the addition of Fe_2O_3 NPs little or no change was observed in the liquid and gas yields. The liquid and gas yield was almost 83 wt% and 13 wt% for tetralin and tetralin + Fe_2O_3 NPs, respectively in comparison to 76 wt% and 13 wt% for thermal upgrading under N_2. The middle distillate fraction (177-343°C) was higher for tetralin and tetralin + Fe_2O_3 compare to thermal upgrading under N_2. The middle distillate fraction (177-343°C) was 52 wt% for tetralin, 50 wt% for tetralin with Fe_2O_3 NPs relative to 43 wt% for thermal upgrading under N_2. The increased middle distillate fraction can be attributed to the presence of tetralin in the final mixture as its boiling point overlaps with the middle distillate boiling point range (177-343°C) (Alemán-Vázquez et al., 2012). The reduction in coke formation as well as the increase liquid yield and asphaltene content follows the same explanation discussed in Section 6.3.1.

Table 6.5 shows the effect of thermal upgrading under N_2, tetralin and tetralin with dispersed catalyst on the physical properties and product quality.

Table 6.5. Effect of thermal upgrading under N_2, tetralin and tetralin with dispersed catalyst on physical properties and product quality [a]. (Feedstock: API 12.8°, Viscosity 1482 cP, C_5-aphaltene 14 wt%, 0.68 wt% (IBP-177 °C), 28.18 wt% (177-343 °C), 71.6 wt% 343 °C+, 3.09 wt% sulphur , 0.0132 wt% (Ni+V)).

Reactions media	Product Quality			Physical properties	
	N %	S wt %	(Ni+V) wt %	API	Viscosity (cP)
N_2	0.13	2.30	0.0031	22.4	74.0
Tetralin + N_2	0.34	2.27	0.0060	18.4	161.0
Tetralin + N2+ Fe_2O_3	0.08	2.16	0.0052	20.1	83.3

[a] Reaction conditions 425 °C for reaction temperature, 10 bar initial N_2 pressure 60min, mixing speed 900 rpm and dispersed iron oxide catalyst ($Fe_2O_3 \leq 50$ nm, 0.1 wt %). Errors were expressed in terms of standard deviation for triplicate experiments as follows: API° ±0.4, viscosity ±4, S% ±0.04, and metal (Ni + V) % ±0.0005

The data in Table 6.5 show that there is no further improvement of upgrading under tetralin and tetralin + Fe_2O_3 NPs in terms of API gravity and viscosity compared to thermal upgrading under N_2. The API gravity was 18° (tetralin) and 20.1° for (tetralin + Fe_2O_3) relative to 22.4° for thermal upgrading under N_2. The viscosity was 161 cP for tetralin and 83.30 cP for tetralin+Fe_2O_3. Furthermore, it was found that the sulphur content of the produced upgraded oil was maintained within the narrow range 2.30-2.16 wt% after upgrading under N_2, tetralin and tetralin + Fe_2O_3 NPs. The metal content increased from 0.003 wt% to 0.006 wt% for tetralin, and 0.0052 wt% for tetralin + Fe_2O_3. This is because the breaking of the C-heteroatom bonds is mainly controlled by temperature although the presence of NPs promotes hydrogen transfer reactions (Sahu et al., 2015; Shuyi et al., 2008). Additionally, the lack of cracking functionality of the unsupported Fe_2O_3 particles as well as the high amount of asphaltene in the produced oil contributed to this suggestion (Wu et al., 2010; Argillier et al., 2002; Altgelt and Harle, 1975).

It is clear that upgrading of heavy oil under tetralin in the presence and absence of Fe_2O_3 NPs in terms of coke formation was superior compared to the other hydrogen sources (H_2, CH_4 and H_2O). The activity in terms of coke reduction for tetralin and the hydrogen sources in the presence of Fe_2O_3 were established as follows: tetralin > $CH_4 \geq H_2 > H_2O > N_2$ where the coke yield was 3.22 wt% (tetralin + Fe_2O_3), 6.19 wt% (CH_4 + Fe_2O_3), 6.79 wt% (H_2 + Fe_2O_3) and 7.48 wt% (H_2O + Fe_2O_3) relative to 11 wt% (N_2) during heavy oil upgrading

6.3 Effect of different hydrogen sources and tetralin on formed coke

The main objective of catalytic and thermal upgrading of heavy oil and bitumen is to increase conversion of heavy molecules to produce more valuable products (middle distillate) as well as minimizing coke formation. The type and quality of produced coke during heavy oil upgrading mainly depend on heavy feed properties as well as the upgrading conditions. There are several reports of research directed to increase the desired coke quality in order to use for applications such as industrial fuel or making anodes for aluminium manufacturing (Termeer, 2013; Ellis et al., 1998). A morphological investigation was conducted on coke samples obtained from thermal upgrading under N_2, upgrading under different hydrogen sources and solvent (tetralin) with and without Fe_2O_3 NPs in order to identify the coke quality and type.

Figure 6.5 and Figure 6.6 (a) show the SEM micrographs of coke recovered after thermal upgrading under N_2 and H_2 alone (for reaction conditions see Table 6.1).

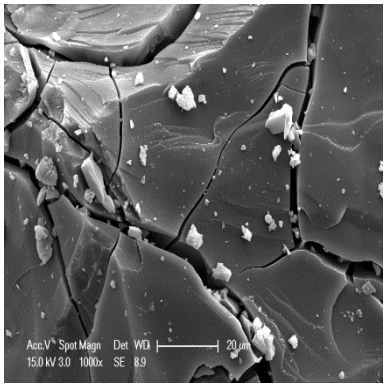

Figure 6.5. SEM photomicrograph of recovered coke from thermal upgrading under N_2.

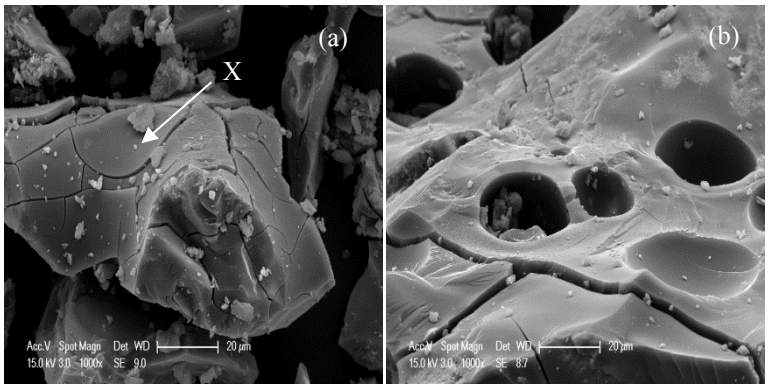

Figure 6.6. SEM photomicrograph of recovered coke from catalytic upgrading under H_2 (a) without Fe_2O_3 (b) with Fe_2O_3.

It can be observed that the coke texture is characterised by a smooth and concave surface (see position x in Figure 6.6 (a)) with no evidence of pores. From a morphological standpoint, the coke produced by thermal upgrading under N_2 and H_2 alone could be classified as shot-coke type, where similar observations have been reported in the literature (Kelemen et al., 2007; Siskin et al., 2006; Elliott, 2000). The type of coke formed is mainly dependent on feed properties; particularly, it has been reported that a feed with high asphaltene and metal content leads to shot-type coke (Picón-Hernández et al., 2008; Kelemen et al., 2007; Marsh et al., 1985). This result also, reaffirmed the high level of metal removal and low asphaltene content of the produced oil observed with thermal cracking under N_2 and H_2 alone (see Table 6.1). Picon-Hernandez et al. (2008) observed during coking processes that the feed oil which has an asphaltene amount of 14 wt%, and 600 ppm of metal (Ni+V)

content leads to the formation of shot-type coke. Under thermal upgrading of heavy feed the asphaltene stability in the oil mixture could be disturbed (Gawel et al., 2005), and that could lead to precipitation and aggregation of asphaltene and eventually, promote shot-type coke formation (Siskin et al., 2006). The feed oil used in this study has asphaltene and metal content of the 14 wt% and 0.0132 wt% (132 ppm), respectively (previously shown in Table 1), which may have the tendency to produce shot–type coke. Shot-type coke consists of individual particles that are spherical to slightly ellipsoidal, with average diameters of about 1-4 mm (Siskin et al., 2006). It is low in economic value and could be used as source of fuel. Nevertheless, understanding feed properties as well as controlling upgrading reaction conditions can help to produce more economically valuable coke types with better quality (Elliott, 2000).

Figure 6.6, 6.7, 6.8 and 6.9 show the SEM micrographs of the coke recovered after upgrading under H_2, H_2O, CH_4 and tetralin with and without Fe_2O_3 NPs respectively; for reaction conditions see Table 6.1(for hydrogen source) and Figure 6.4 (for tetralin).

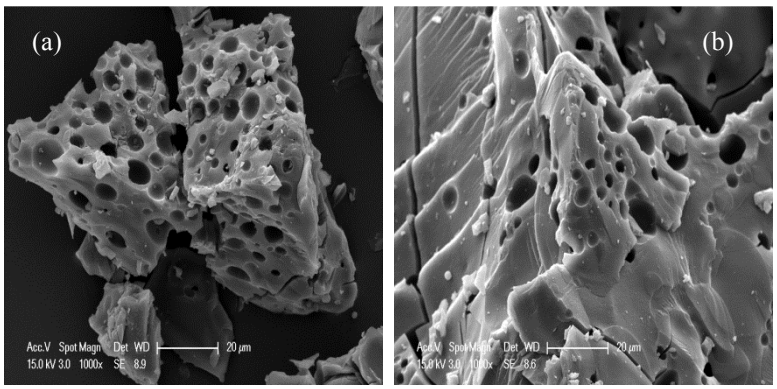

Figure 6.7. SEM photomicrograph of recovered coke from catalytic upgrading under H_2O (a) without Fe_2O_3 (b) with Fe_2O_3.

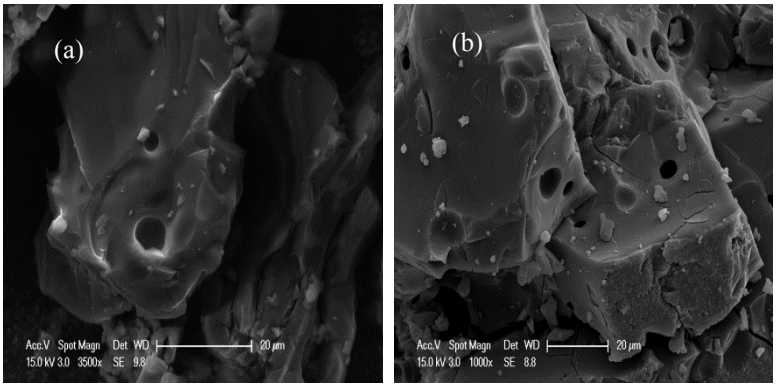

Figure 6.8. SEM photomicrograph of recovered coke from catalytic upgrading under CH_4 (a) without Fe_2O_3 (b) with Fe_2O_3.

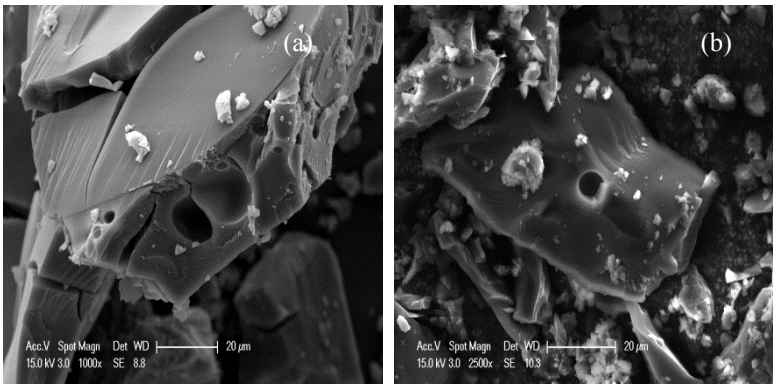

Figure 6.9. SEM photomicrograph of recovered coke from catalytic upgrading under tetralin (a) without Fe_2O_3 (b) with Fe_2O_3.

It can be seen from Figure 6.6 (b), 6.7 (a-b), 6.8 (a-b) and 6.9 (a-b) that the coke texture is characterised by a porous microstructure with a wide variety of pore sizes. From a morphological standpoint, the coke produced after upgrading reactions under H_2, H_2O, CH_4 and tetralin with and without Fe_2O_3 NPs could be classified as sponge-type coke. This finding is in agreement with other researchers' observations (Picón-Hernández et al., 2008; Marsh et al., 1985; Watanabe et al., 2010). As the name suggests, sponge-type coke has a sponge-like appearance with various bubble and pore sizes. In comparison to shot-type coke observed for coke produced after thermal cracking under N_2 and H_2 alone (Figure 6.5), sponge-type coke has a higher economic value with a high potential to be used as fuel (Ellis et al., 1998). It has been reported that the asphaltene content in the feed oil is the main factor

responsible for promoting shot-type coke over sponge-type coke in delayed cokers (Siskin et al., 2006; Ellis et al., 1998; Marsh et al., 1985). Furthermore, Picon-Hernandez et al. (2008) observed the formation of sponge-type coke from coking processes of feed oil, with a moderate metal (Ni+V) and asphaltene content.

It can be reaffirmed that the free-radical reaction mechanism can lead to the incorporation of CH_4 and H_2O (in the absence of catalysts) into hydrocarbon molecules via methyl (CH_3) and hydroxyl (OH). Additionally, the presence of Fe_2O_3 NPs actually could further promote the formation of free radicals by activation of H_2 or other hydrogen sources (CH_4) (Peureux et al., 1995; Weitkamp, 2012; Ovalles et al., 2003; Dutta et al., 2000). This stabilizes the asphaltene in the oil mixture, and is attributed to the production of sponge-type coke during catalytic upgrading under different hydrogen sources with and without Fe_2O_3. Additionally, SEM micrographs for the coke recovered after upgrading of heavy oil in the presence of tetralin with and without Fe_2O_3 follows the similar trend as the previous results. Sponge-type cokes are porous clusters surrounded by comparatively thin walls with no interconnection between pores (Reis, 1975; Jakob, 1971). In the reservoir the flow of upgraded oil could crack and convey sponge-type coke to the production well and to the surface because of its physical appearance. Coke lay down ahead of the combustion front during the THAI process acts as fuel for the process.

Chapter 7
Conclusions and Recommendations

7.1 Conclusions

The main target during this study to perform high level of upgrading of heavy feed (Whitesands heavy feed) in term of product distribution (i.e., liquid, gas and coke) and (naphtha, middle distillate and gas oil fractions), physical properties (i.e., API gravity and viscosity) and product quality (i.e., sulphur, metals and nitrogen contents). The in situ upgrading reactions were simulated in laboratory scale using 100 ml stirred reactor. The optimisation of upgrading reaction factors, effect of different type of dispersed unsupported catalysts and different hydrogen source and tetralin on upgrading of heavy feed was studied.

Effect of reaction factors and optimisation of upgrading reaction factors

The Taguchi method was applied to study the effect of reaction factors and select the optimum values that maximise level of heavy oil upgrading while suppressing coke yield. A comprehensive optimization study has been made of process variable effects of dispersed nanoparticles of iron oxide during THAI-CAPRI in situ catalytic upgrading of heavy oil, in a stirred batch reactor. The following process variables were investigated over the following range, reaction temperature 355 – 425 ^{o}C, reaction time 20 – 80 min, initial hydrogen pressure 10 – 50, agitation 200-900 rpm and iron-metal loading 0.03 – 0.4 wt%. The results confirmed that the reaction time, initial hydrogen pressure agitation and dispersed catalyst loading do not exhibit as much effect upon upgrading as reaction temperature because the cleavage of C-C and C-heteroatom bonds is mainly dependent on temperature. However, the chemistry of hydroconversion reactions can be enhanced by these factors. Additionally it was noticed that the hydrogenation reaction became more active at moderate pressure while at high pressure the hydrocracking dominates. Also it was observed that a long reaction time

promotes cracking, secondary cracking of intermediates and more yield of coke, light naphtha, middle distillate and gas. Furthermore, it was concluded that the nano-dispersed iron oxide catalysts boosts hydrogen uptake during hydro-cracking reactions which helped to control the rate of free radical propagation via β-scission reactions. The optimum conditions were 425 °C for reaction temperature, 60 min for reaction time, 400 rpm for agitation, 0.1 wt% metals loading, and 50 bar for initial hydrogen pressure obtained by the Taguchi method. Under these optimal conditions, the viscosity reduction was 92.9%, API gravity increase 8.3^{o}, sulfur reduction 37.54%, and metals (Ni + V) reduction 68.9%, relative to the feed oil values, while coke formation was 6.7 wt%. It was also found that the naphtha (IBP – 177 ^{o}C) and middle distillate fractions (177 – 343 ^{o}C) at the optimum condition increased from 0.68 and 28.18 wt% in feed oil, to 21 and 47 wt%, respectively in the upgraded oil.

Effectiveness of different transition metal dispersed unsupported catalysts

Hydroconversion of heavy oil was carried out in a stirred batch reactor at 425˚C, 50 bar (initial H_2 pressure), 900 rpm and 60 min reaction time using a range of unsupported transition metals (Mo, Ni and Fe) catalysts. The effect of active metal was evaluated in terms of product distribution, physical properties and product quality. It was found that the dispersed catalysts (Ni, Mo, and Fe) in sulphide form could enhance hydrogen uptake and help in controlling the rate of free radical propagation via β-scission reactions during heavy oil upgrading. Despite the improved API gravity and viscosity of the produced oil by thermal cracking (24˚ and 54 cP) over that achieved with unsupported metal catalyst (approximately 21˚ and 108 cP), thermal cracking gave a lower amount of upgraded oil (76 wt%) compared to an average of 83.5 wt% for dispersed catalysts. Thermal cracking also yielded 12 wt% coke, while the coke yields for dispersed unsupported catalysts are remarkably lower at 4.35 wt% (Mo catalyst), 5.76 wt% (Ni catalyst) and 6.79 wt% (Fe catalyst). The high coke yield with thermal cracking contributed significantly to sulphur and metal (Ni + V) removal as they

mostly associate with macromolecules such as resins and asphaltenes, which are the major coke precursors. This is confirmed from the lower asphaltene content of the upgraded oil after thermal cracking compared to catalytic upgrading with dispersed unsupported Fe, Mo and Ni metals. However, unsupported Mo catalysts showed higher activity in suppressing coke formation and improving middle distillate compared to Ni and Fe catalysts. Also, a morphological investigation was conducted on coke samples obtained from thermal and unsupported catalytic upgrading in order to identify the coke quality and type. It was found that the presence of dispersed catalysts helped in producing sponge-type coke compared to shot-type coke from thermal cracking. Shot-type coke is low in economic value and consists of individual particles that are spherical to slightly ellipsoidal, with average diameters of about 1-4 mm. However, sponge-type coke is named for its sponge-like appearance with different sized pores and bubbles in the coke matrix. Compared to shot-type coke, observed for coke produced after thermal cracking, sponge-type coke has a higher economic value with a high potential to be used as fuel.

Effect of different hydrogen sources and tetralin

The upgrading reactions were carried out using Fe_2O_3 NPs at 425 ˚C, 50 bar, 0.1 wt% (NPs loading) and 60 min reaction time. The effect of hydrogen sources and tetralin with and without Fe_2O_3 NPs was investigated in terms of product distribution; physical properties and product quality, also, the produced coke after upgrading were studied. It was found that the in the presence and absence of Fe_2O_3 NPs the coke formation was significantly reduced under tetralin compared to H_2, CH_4 and H_2O where the activity in term of coke formation reduction settled as follows: tetralin > CH4 > H_2O> $H_2 \geq N_2$ without Fe_2O_3 NPs and Tetralin > $CH_4 \geq H_2 > H_2O > N_2$ with Fe_2O_3 NPs. The coke yield further reduced with addition of Fe_2O_3 NPs as follows: 3.22 wt % (tetralin), 6.19 wt % (CH_4+ Fe_2O_3), 6.79 wt % (H_2+ Fe_2O_3), and 7.48 wt % (H_2O+ Fe_2O_3) relative to 3.54 wt (tetralin), 7.19 wt % (CH_4), 12 wt % (H_2) and 7.32 wt

% (H_2O) without Fe_2O_3 addition, where presence of catalysts in sulphide form could enhance controlling the rate of free polymerization reactions during heavy oil upgrading. Despite the improved API gravity and viscosity of the produced oil by thermal cracking (24˚ and 54 cP) over that achieved with Fe_2O_3 catalyst under different hydrogen sources (an average of 21˚ and 105 cP), thermal cracking (under N_2) gave a lower amount of upgraded oil (76 wt%) compared to an average of 80 wt% for Fe_2O_3 with different hydrogen sources and tetralin. The high coke yield with thermal cracking contributed significantly to sulphur and metal (Ni + V) removal as they mostly associate with macromolecules such as resins and asphaltenes, which are the major coke precursors. Also, the presence of Fe_2O_3NPs with tetralin, CH_4, H_2, and H_2O helped in producing coke with desired quality (sponge-type coke) compared to shot-type coke from thermal cracking under N_2 and H_2 alone. Additionally, the upgrading reactions under tetralin, CH_4 and H_2O without addition of Fe_2O_3 NPs helped to producing sponge-type coke.

7.2 Recommendations

The use of dispersed unsupported catalysts instead of pelleted commercial catalysts which are surrounding horizontal production well during the THAI process could reduce the susceptibility of catalysts to deactivation and avoid the subsequent process shutdown. However, the produced liquid after catalytic upgrading using dispersed catalysts did not show further improvement in term of product quality and physical properties relative to thermal upgrading. Hence, further investigation of dispersed catalysts composition and properties are recommended to modify dispersed catalysts functionality to enhance heavy molecule conversion and improve product quality as well as physical properties. The NPs catalysts could be impregnated on the surface of zeolite or Al_2O_3 which have the acidic character to promote cracking of C-C and heteroatms-C bonds. Additionally, NP catalysts derived as waste or by-products of other industrial process could be investigated as promising low cost

once through catalysts for in situ upgrading of heavy oil. The following are examples of low cost once through dispersed catalysts which could be examined (1) the NPs iron-based catalysts sourcing from waste and made by biofabrication, (2) the reservoir rock metals such as Fe, (3) red mud which is a by-product of aluminium industries. The upgrading of heavy feedstock under batch mode was performed during this project to the study activity and selectivity of unsupported dispersed catalysts as well as to optimise the upgrading reaction factors. Therefore, further studies of heavy oil upgrading reaction should be performed in continuous mode to understand the kinetics of upgrading reaction using NPs catalysts. Furthermore, the movement and penetration of dispersed catalyst in porous medium should be studied to understand the efficiency of injection of dispersed catalysts into oil reservoir. Also, as alternatives, liquid and gas hydrogen donors could be investigated in order to overcome the further cost of utilizing expensive hydrogen gas. Naphthalene and decalin are examples of liquid hydrogen donors which could be a feasible choice to test during the THAI process.

Appendix A

Table A.1. Experimental data for 16 experiments run. For reaction conditions see Table 3.6

Experiment No.	Measured response (average of 3 runs)							
	Coke wt %	Gas wt %	Light naphtha fraction (IBP-177 °C) wt%	Middle distillate fraction (177-343 °C) wt %	API °gravity @ 15 °C	Viscosity @ 20 °C	HDS %	Metal (Ni+V) wt
1	0	1.30	7.51	51.06	13.5	1415.14	5.65	0.0148
2	0	1.64	8.85	51.61	13.8	1294.34	3.22	0.0146
3	0	1.41	7.60	49.14	13.9	1256.71	2.00	0.015
4	0	1.34	7.57	52.91	13.6	1373.50	5.79	0.0147
5	0	2.96	9.31	48.42	14.5	1055.50	4.88	0.0145
6	0	2.72	8.68	48.24	14.1	1185.14	6.41	0.0146
7	0	2.06	10.46	48.67	15.1	890.26	13.48	0.0144
8	0	2.66	9.81	48.40	15.0	915.62	10.65	0.0149
9	0.90	4.49	13.06	47.32	16.3	575.69	17.11	0.0147
10	0.66	3.24	12.92	46.75	16.4	550.96	15.35	0.017
11	0.42	2.53	10.19	45.96	15.7	757.37	10.05	0.0147
12	0.50	2.54	11.38	46.44	16.3	575.69	11.05	0.0146
13	8.16	12.40	30.53	37.91	18.2	269.11	26.18	0.0025
14	7.42	10.79	33.86	44.40	19.0	203.24	28.64	0.0034
15	6.74	7.59	34.83	40.54	21.0	108.83	25.69	0.0043
16	3.61	7.48	26.14	23.36	19.8	156.40	24.7	0.0062

Appendix B
Effect of dispersed catalysts on type of formed coke

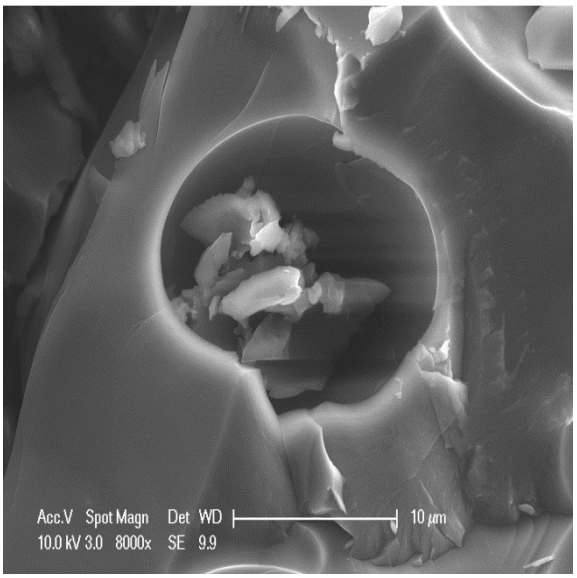

Figure B.1. SEM photomicrograph of recovered coke from catalytic upgrading FeS.

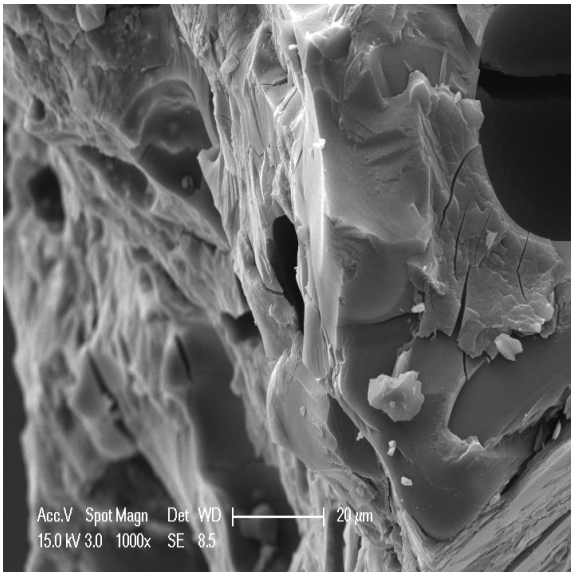

Figure B.2. SEM photomicrograph of recovered coke from catalytic upgrading NiO.

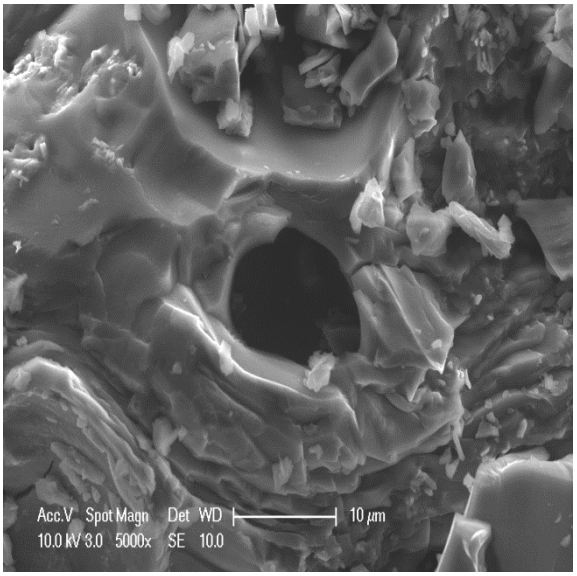

Figure B.3. SEM photomicrograph of recovered coke from catalytic upgrading MoO_3.

Appendix C
Publications

C.1. Publications (available upon request)

C.1.1 Journal paper

1. Abdullah Al-Marshed, Abarasi Hart, Gary Leeke, Malcolm Greaves and Joseph Wood, (2015) Optimization of Heavy Oil Upgrading using Dispersed Nanoparticulate Iron Oxide as a Catalyst, Energy & Fuels, 29, 6306-6316.

2. Abdullah Al-Marshed, Abarasi Hart, Gary Leeke, Malcolm Greaves and Joseph Wood, (2015) Effectiveness of Different Transition Metal Dispersed Catalysts for In-Situ Heavy Oil Upgrading, Industrial & Engineering Chemistry Research, 54, 10645-10655.

References

ALEMÁN-VÁZQUEZ, L. O., DOMÍNGUEZ, J. L. C. & GARCÍA-GUTIÉRREZ, J. L. 2012. Effect of Tetralin, Decalin and Naphthalene as Hydrogen Donors in the Upgrading of Heavy Oils. *Procedia Engineering,* 42**,** 532-539.

ALI, S. 1974. Current status of steam injection as a heavy oil recovery method. *Journal of Canadian Petroleum Technology,* 13.

ALI, S. & MELDAU, R. 1979. Current steamflood technology. *Journal of Petroleum Technology,* 31**,** 1,332-1,342.

ALIKHLALOV, K. & DINDORUK, B. Conversion of cyclic steam injection to continous steam injection. SPE Annual Technical Conference and Exhibition, 2011. Society of Petroleum Engineers.

ALPAK, F. O., VINK, J. C., GAO, G. & MO, W. 2013. Techniques for effective simulation, optimization, and uncertainty quantification of the in-situ upgrading process. *Journal of Unconventional Oil and Gas Resources,* 3–4**,** 1-14.

ALTGELT, K. H. & HARLE, O. L. 1975. The Effect of Asphaltenes on Asphalt Viscosity. *Product R&D,* 14**,** 240-246.

ALVAREZ, J. & HAN, S. 2013. Current overview of cyclic steam injection process. *Journal of Petroleum Science Research*.

ANCHEYTA, J. 2013. *Modeling of procesesses and reactors for upgrading of heavy petroleum*.

ANCHEYTA, J., SÁNCHEZ, S. & RODRÍGUEZ, M. A. 2005. Kinetic modeling of hydrocracking of heavy oil fractions: A review. *Catalysis Today,* 109**,** 76-92.

ANDERSEN, S. I. 1994. DIBSOLUTION OF SOLID BOBCAN ASPHALTENES IN MIXED SOLVENTS. *Fuel science & technology international,* 12**,** 1551-1577.

ANGELES, M. J., LEYVA, C., ANCHEYTA, J. & RAMÍREZ, S. 2014. A review of experimental procedures for heavy oil hydrocracking with dispersed catalyst. *Catalysis Today,* 220–222**,** 274-294.

ARGILLIER, J., COUSTET, C. & HENAUT, I. Heavy oil rheology as a function of asphaltene and resin content and temperature. SPE International thermal operations and heavy oil symposium and international horizontal well technology conference, 2002. Society of Petroleum Engineers.

ASAOKA, S., NAKATA, S., SHIROTO, Y. & TAKEUCHI, C. 1987. Characteristics of Vanadium Complexes in Petroleum Before and After Hydrotreating. *Metal Complexes in Fossil Fuels.* American Chemical Society.

ATHREYA, S. & VENKATESH, Y. 2012. Application Of Taguchi Method For Optimization Of Process Parameters In Improving The Surface Roughness Of Lathe Facing Operation. *International Refereed Journal of Engineering and Science (IRJES) ISSN (Online)***,** 2319-1821.

AUREL, C. 1992. *Applied enhanced oil recovery*, Prentice Hall

BAGCI, S. & KOK, M. V. 2001. In-situ combustion laboratory studies of Turkish heavy oil reservoirs. *Fuel Processing Technology,* 74**,** 65-79.

BARTHOLDY, J. & ANDERSEN, S. I. 2000. Changes in asphaltene stability during hydrotreating. *Energy & Fuels,* 14**,** 52-55.

BARTHOLDY, J., LAURIDSEN, R., MEJLHOLM, M. & ANDERSEN, S. I. 2001. Effect of hydrotreatment on product sludge stability. *Energy & Fuels,* 15**,** 1059-1062.

BEARDEN JR, R. & ALDRIDGE, C. L. 1979. Hydroconversion of heavy hydrocarbons. Google Patents.

BEARDEN JR, R. & ALDRIDGE, C. L. 1980. Catalyst for the hydroconversion of heavy hydrocarbons. Google Patents.

BEARDEN, R. 1997. MICROCAT-RC: Technology for Hydroconversion Upgrading of Petroleum Residues. *Division of Petroleum Chemistry, American Chemical Society, San Francisco, California*.

BELLUSSI, G., RISPOLI, G., LANDONI, A., MILLINI, R., MOLINARI, D., MONTANARI, E., MOSCOTTI, D. & POLLESEL, P. 2013. Hydroconversion of heavy residues in slurry reactors: Developments and perspectives. *Journal of Catalysis,* 308**,** 189-200.

BENSON, S. W. 1976. *Thermochemical kinetics*, Wiley.

BERA, A. & BABADAGLI, T. 2015. Status of electromagnetic heating for enhanced heavy oil/bitumen recovery and future prospects: A review. *Applied Energy,* 151**,** 206-226.

BHATTACHARYYA, A. & MEZZA, B. J. 2012. Process for using catalyst with rapid formation of iron sulfide in slurry hydrocracking. Google Patents.

BLACKWELL 2006. Bitumen and heavy crudes: the energy security problem solved? *Oil and Energy Trends,* 31**,** 3-6.

BOCKRATH, B., LACOUNT, R., KERN, D., PARFITT, D., FROMMELL, E. & KELLER, M. 1998. 'Characterization of unsupported MoS2 catalysts by controlledatmosphere programmed-temperature oxidation. *Am. Chem. Soc. Div. Fuel Chem. Prepr,* 43**,** 717-721.

BODUSZYNSKI, M. M. 1988. Composition of heavy petroleums. 2. Molecular characterization. *Energy & Fuels,* 2**,** 597-613.

BREYSSE, M., FURIMSKY, E., KASZTELAN, S., LACROIX, M. & PEROT, G. 2002. Hydrogen activation by transition metal sulfides. *Catalysis Reviews-Science and Engineering,* 44**,** 651-735.

BREYSSE, M. & KASZTELAN, S. 2002. Catalytic hydrodesulfurization of automotive fuels. *Actualite Chimique***,** 12-15.

BUCKLEY, S. E. & LEVERETT, M. 1942. Mechanism of fluid displacement in sands. *Transactions of the AIME,* 146**,** 107-116.

BUTLER, R. M. & MOKRYS, I. J. 1993. Recovery of heavy oils using vapourized hydrocarbon solvents: further development of the VAPEX process. *Journal of Canadian Petroleum Technology,* 32.

CARRILLO, J. A. & CORREDOR, L. M. 2013. Upgrading of heavy crude oils: Castilla. *Fuel Processing Technology,* 109**,** 156-162.

CASTAÑEDA, L. C., MUÑOZ, J. A. D. & ANCHEYTA, J. 2012. Combined process schemes for upgrading of heavy petroleum. *Fuel,* 100**,** 110-127.

CASTANIER, L. M. & BRIGHAM, W. E. 2003. Upgrading of crude oil via in situ combustion. *Journal of Petroleum Science and Engineering,* 39**,** 125-136.

CHAO, K., CHEN, Y. L., LI, J., ZHANG, X. M. & DONG, B. Y. 2012. Upgrading and visbreaking of super-heavy oil by catalytic aquathermolysis with aromatic sulfonic copper. *Fuel Processing Technology,* 104**,** 174-180.

CHEN, X. & YAN, Y. 2008. Study on the technology of thermal cracking of paraffin to alpha olefins. *Journal of Analytical and Applied Pyrolysis,* 81**,** 106-112.

CLARKE, A. & TRINNAMAN, J. A. 2004. *2004 Survey of Energy Resources*, Elsevier.

CLARKE, B. 2007. NPC Global Oil and Gas Study: Topic Paper 22—Heavy Oil. *Washington, DC: National Petroleum Council*.

COOK, M. & GRAHAM, M. 2008. *Hydrocarbon Exploration and Production. Developments in Petroleum Science*, Elsevier Science & Technology.

DABKOWSKI, M. J., SHIH, S. S. & ALBINSON, K. R. 1991. *UPGRADING OF PETROLEUM RESIDUE WITH DISPERSED ADDITIVES,* New York, Amer Inst Chemical Engineers.

DANESH, A. 1998. *PVT and phase behaviour of petroleum reservoir fluids*, Elsevier.

DEALY, J. M. 1979. Rheological properties of oil sand bitumens. *The Canadian Journal of Chemical Engineering,* 57**,** 677-683.

DEL BIANCO, A., PANARITI, N., DI CARLO, S., BELTRAME, P. L. & CARNITI, P. 1994. New Developments in Deep Hydroconversion of Heavy Oil Residues with Dispersed Catalysts. 2. Kinetic Aspects of Reaction. *Energy & Fuels,* 8**,** 593-597.

DEL BIANCO, A., PANARITI, N., DI CARLO, S., ELMOUCHNINO, J., FIXARI, B. & LE PERCHEC, P. 1993. Thermocatalytic hydroconversion of heavy petroleum cuts with dispersed catalyst. *Applied Catalysis A: General,* 94**,** 1-16.

DEMIRBAS, A. 2002. Physical and chemical characterizations of asphaltenes from different sources. *Petroleum Science and Technology,* 20**,** 485-495.

DERBYSHIRE, F. & HAGER, G. T. 1992. DISPERSED CATALYSTS FOR COAL DISSOLUTION. *Abstracts of Papers of the American Chemical Society,* 203**,** 51-CATL.

DOEHLER, W., KRETSCHMAR, D., MERZ, L. & NIEMANN, K. 1987. Veba-Combi-Cracking-A technology for upgrading of heavy oils and bitumen. *American Chemical Society, Division of Petroleum Chemistry, Preprints;(USA),* 32.

DONALDSON, GEORGE V. CHILINGARIAN & YEN, T. F. 1985. *Enhanced Oil Recovery Fundamentals and Analyses (Developments in Petroleum Science)* Netherlands, ELSEVIER.

DONG, M., MA, S. & LIU, Q. 2009. Enhanced heavy oil recovery through interfacial instability: A study of chemical flooding for Brintnell heavy oil. *Fuel,* 88**,** 1049-1056.

DONG, X., LIU, H., HOU, J., ZHANG, Z. & CHEN, Z. 2015. Multi-thermal fluid assisted gravity drainage process: A new improved-oil-recovery technique for thick heavy oil reservoir. *Journal of Petroleum Science and Engineering,* 133**,** 1-11.

DU, Z. W., ZENG, F. H. & CHAN, C. 2015. An Experimental Study of the Post-CHOPS Cyclic Solvent Injection Process. *Journal of Energy Resources Technology-Transactions of the Asme,* 137**,** 15.

DUSSEAULT, M. Reservoir Enhancements and Production Technology Sequencing. World Heavy Oil Congress, 2008. 10-12.

DUSSEAULT, M. B. 2002. *CHOPS: Cold heavy oil production with sand in the Canadian heavy oil industry*, Alberta Department of Energy.

DUTTA, R. P., MCCAFFREY, W. C., GRAY, M. R. & MUEHLENBACHS, K. 2000. Thermal Cracking of Athabasca Bitumen: Influence of Steam on Reaction Chemistry. *Energy & Fuels,* 14**,** 671-676.

DWYER, J. & RAWLENCE, D. J. 1993. Fluid catalytic cracking: chemistry. *Catalysis Today,* 18**,** 487-507.

EDWARDS, J. H., SCHLUTER, K. & TYLER, R. J. 1986. Upgrading of flash pyrolysis tars to synthetic crude oil: 3. Overall performance of the two-stage hydrotreating process and characterization of the synthetic crude oil. *Fuel,* 65**,** 208-211.

EGIEBOR, N. O. & GRAY, M. R. 1990. Evidence for methane reactivity during coal pyrolysis and liquefaction. *Fuel,* 69**,** 1276-1282.

ELIZALDE, I., RODRÍGUEZ, M. A. & ANCHEYTA, J. 2009. Application of continuous kinetic lumping modeling to moderate hydrocracking of heavy oil. *Applied Catalysis A: General,* 365**,** 237-242.

ELIZALDE, I., RODRÍGUEZ, M. A. & ANCHEYTA, J. 2010. Modeling the effect of pressure and temperature on the hydrocracking of heavy crude oil by the continuous kinetic lumping approach. *Applied Catalysis A: General,* 382**,** 205-212.

ELLIOTT, J. D. 2000. Shot coke: Design & operations. *Todays' Refinery,* 15**,** 1-9.

ELLIS, P. J., PAUL, C. A. & SESSION, T. 1998. *Tutorial: Delayed coking fundamentals*, American Institute of Chemical Engineers.

FABUSS, B., SMITH, J. & SATTERFIELD, C. 1964. Thermal cracking of pure saturated hydrocarbons. *Advances in petroleum chemistry and refining,* 9**,** 157-201.
FAROUQ ALI, S. 1982. Steam injection theories: a unified approach.
FELDMAN, Y., WASSERMAN, E., SROLOVITZ, D. J. & TENNE, R. 1995. HIGH-RATE, GAS-PHASE GROWTH OF MOS2 NESTED INORGANIC FULLERENES AND NANOTUBES. *Science,* 267**,** 222-225.
FIXARI, B., PEUREUX, S., ELMOUCHNINO, J., LE PERCHEC, P., VRINAT, M. & MOREL, F. 1994. New Developments in Deep Hydroconversion of Heavy Oil Residues with Dispersed Catalysts. 1. Effect of Metals and Experimental Conditions. *Energy & Fuels,* 8**,** 588-592.
FORD, T. J. 1986. Liquid-phase thermal decomposition of hexadecane: reaction mechanisms. *Industrial & engineering chemistry fundamentals,* 25**,** 240-243.
FRATILA, D. & CAIZAR, C. 2011. Application of Taguchi method to selection of optimal lubrication and cutting conditions in face milling of AlMg3. *Journal of Cleaner Production,* 19**,** 640-645.
FUJIMOTO, K., CHANG, J. & TSUBAKI, N. 2000. Hydrothermal cracking of residual oil. *Sekiyu Gakkaishi-Journal of the Japan Petroleum Institute,* 43**,** 25-36.
GALARRAGA, C. E. & PEREIRA-ALMAO, P. 2010. Hydrocracking of Athabasca bitumen using submicronic multimetallic catalysts at near in-reservoir conditions. *Energy & Fuels,* 24**,** 2383-2389.
GATES, I. D. 2007. Oil phase viscosity behaviour in Expanding-Solvent Steam-Assisted Gravity Drainage. *Journal of Petroleum Science and Engineering,* 59**,** 123-134.
GAWEL, I., BOCIARSKA, D. & BISKUPSKI, P. 2005. Effect of asphaltenes on hydroprocessing of heavy oils and residua. *Applied Catalysis A: General,* 295**,** 89-94.
GHANI, J. A., CHOUDHURY, I. A. & HASSAN, H. H. 2004. Application of Taguchi method in the optimization of end milling parameters. *Journal of Materials Processing Technology,* 145**,** 84-92.
GHOODJANI, E., KHARRAT, R., VOSSOUGHI, M. & BOLOURI, S. H. A review on thermal enhanced heavy oil recovery from fractured carbonate reservoirs. SPE Heavy Oil Conference Canada, 2012. Society of Petroleum Engineers.
GIAVARINI, C. & VECCHI, C. 1987. Characterization of visbreaker bitumens by n.m.r. spectroscopy. *Fuel,* 66**,** 868-869.
GRAY, M., CHOI, J., EGIEBOR, N., KIRCHEN, R. & SANFORD, E. 1989. Structural group analysis of residues from Athabasca bitumen. *Fuel science & technology international,* 7**,** 599-610.
GRAY, M. R. 2015. *Upgrading Oilsands Bitumen and Heavy Oil*, University of Alberta.
GRAY, R. M. 1994. *Upgrading petroleum residues and heavy oils*, CRC press.
GREAVES, M. 2004. Air injection-improved oil recovery strategy for the UK continental shelf. *Bus Br: Explor Prod: Oil Gas Rev***,** 118-121.
GREAVES, M., DONG, L. L. & RIGBY, S. P. 2012. Simulation Study of the Toe-to-Heel Air Injection Three-Dimensional Combustion Cell Experiment and Effects in the Mobile Oil Zone. *Energy & Fuels,* 26**,** 1656-1669.
GREAVES, M., EL-SAGHR, A. & XIA, T. X. 2000a. CAPRI horizontal well reactor for catalytic upgrading of heavy oil: Advances in oil field chemistry: Downhole upgrading. *Preprints-American Chemical Society. Division of Petroleum Chemistry,* 45**,** 595-598.
GREAVES, M. & XIA, T. Simulation studies of THAI process. Canadian International Petroleum Conference, 2000. Petroleum Society of Canada.

GREAVES, M. & XIA, T. CAPRI-Downhole Catalytic Process for Upgrading Heavy Oil: Produced Oil Properties and Composition. Canadian International Petroleum Conference, 2001. Petroleum Society of Canada.

GREAVES, M., XIA, T. & TURTA, A. 2008. Stability of THAI™ process-Theoretical and experimental observations. *Journal of Canadian Petroleum Technology,* 47.

GREAVES, M., XIA, T., TURTA, A. & AYASSE, C. Recent laboratory results of THAI and its comparison with other IOR processes. SPE/DOE Improved Oil Recovery Symposium, 2000b. Society of Petroleum Engineers.

GUAN, W., XI, C., CHEN, Y., ZHANG, X., LIANG, J., HUANG, J. & WU, J. 2011. Fire-flooding technologies in post-steam-injected heavy oil reservoirs. *Petroleum Exploration and Development,* 38**,** 452-463.

GUERRA ARISTIZÁBAL, J.-J. & GROSSO VARGAS, J.-L. 2005. Modeling segregated insitu combustion processes through a vertical displacement model applied to a colombian field. *CT&F-Ciencia, Tecnología y Futuro,* 3**,** 111-126.

HART, A., GREAVES, M. & WOOD, J. 2015. A comparative study of fixed-bed and dispersed catalytic upgrading of heavy crude oil using-CAPRI. *Chemical Engineering Journal*.

HART, A., LEEKE, G., GREAVES, M. & WOOD, J. 2014. Down-hole heavy crude oil upgrading by CAPRI: Effect of hydrogen and methane gases upon upgrading and coke formation. *Fuel,* 119**,** 226-235.

HART, A., SHAH, A., LEEKE, G., GREAVES, M. & WOOD, J. 2013. Optimization of the CAPRI Process for Heavy Oil Upgrading: Effect of Hydrogen and Guard Bed. *Industrial & Engineering Chemistry Research,* 52**,** 15394-15406.

HASHEMI, R., NASSAR, N. N. & ALMAO, P. P. 2013. Enhanced Heavy Oil Recovery by in Situ Prepared Ultradispersed Multimetallic Nanoparticles: A Study of Hot Fluid Flooding for Athabasca Bitumen Recovery. *Energy & Fuels,* 27**,** 2194-2201.

HASHEMI, R., NASSAR, N. N. & PEREIRA ALMAO, P. 2014. Nanoparticle technology for heavy oil in-situ upgrading and recovery enhancement: Opportunities and challenges. *Applied Energy,* 133**,** 374-387.

HAWKINS, B. C. M. 1991. *Applied petroleum reservoir engineering*, Prentice Hall Inc New Jersey.

HEIN, F. 2006. Heavy Oil and Oil (Tar) Sands in North America: An Overview & Summary of Contributions. *Natural Resources Research,* 15**,** 67-84.

HIRSCH, R. L., BEZDEK, R. & WENDLING, R. 2006. Peaking of world oil production and its mitigation. *Aiche Journal,* 52**,** 2-8.

HO, D. & MORGAN, B. Effects of Steam Quality on Cyclic Steam Stimulation at Cold Lake, Alberta. SPE Annual Technical Conference and Exhibition, 1990. Society of Petroleum Engineers.

HO, T. C. 1988. Hydrodenitrogenation catalysis. *Catalysis Reviews Science and Engineering,* 30**,** 117-160.

HOLDITCH, S. A. 2013. Unconventional oil and gas resource development – Let's do it right. *Journal of Unconventional Oil and Gas Resources,* 1–2**,** 2-8.

HONGFU, F., YONGJIAN, L., LIYING, Z. & XIAOFEI, Z. 2002. The study on composition changes of heavy oils during steam stimulation processes. *Fuel,* 81**,** 1733-1738.

HOOPER, R. J., BATTAERD, H. A. J. & EVANS, D. G. 1979. Thermal dissociation of tetralin between 300 and 450 °C. *Fuel,* 58**,** 132-138.

HOSHYARGAR, V. & ASHRAFIZADEH, S. N. 2013. Optimization of Flow Parameters of Heavy Crude Oil-in-Water Emulsions through Pipelines. *Industrial & Engineering Chemistry Research,* 52**,** 1600-1611.

HSU, C. S. & ROBINSON, P. 2007. *Practical advances in petroleum processing*, Springer Science & Business Media.

HUANG, W., MARCUM, B., CHASE, M. & YU, C. Cold production of heavy oil from horizontal wells in the Frog Lake Field. International Thermal Operations and Heavy Oil Symposium, 1997. Society of Petroleum Engineers.

IL YOON, Y., WOOK KIM, M., SEUNG YOON, Y. & KIM, S. H. 2003. A kinetic study on medium temperature desulfurization using a natural manganese ore. *Chemical Engineering Science,* 58**,** 2079-2087.

ISTCHENKO, C. M. & GATES, I. D. 2014. Well/Wormhole Model of Cold Heavy-Oil Production With Sand. *Spe Journal,* 19**,** 260-269.

JAFARI, R., CHAOUKI, J. & TANGUY, P. A. 2012. A Comprehensive Review of Just Suspended Speed in Liquid-Solid and Gas-Liquid-Solid Stirred Tank Reactors. *International Journal of Chemical Reactor Engineering,* 10.

JAKOB, R. R. 1971. Coke quality and how to make it. *Hydrocarbon Processing,* 50**,** 132-&.

JIMENEZ, J. The field performance of SAGD projects in Canada. International petroleum technology conference, 2008. International Petroleum Technology Conference.

JOHANNES, I., TIIKMA, L., LUIK, H., TAMVELIUS, H. & KRASULINA, J. 2012. Catalytic Thermal Liquefaction of Oil Shale in Tetralin. *ISRN Chemical Engineering,* 2012**,** 11.

KANEKO, T., TAZAWA, K., KOYAMA, T., SATOU, K., SHIMASAKI, K. & KAGEYAMA, Y. 1998. Transformation of iron catalyst to the active phase in coal liquefaction. *Energy & Fuels,* 12**,** 897-904.

KANEKO, T., TAZAWA, K., OKUYAMA, N., TAMURA, M. & SHIMASAKI, K. 2000. Effect of highly dispersed iron catalyst on direct liquefaction of coal. *Fuel,* 79**,** 263-271.

KASZTELAN, S. & MCGARVEY, G. B. 1994. HYDROGEN CONTENT AND HYDROGENATION ACTIVITY OF MOS2/GAMMA-AL2O3 AND GAMMA-AL2O3 MECHANICAL MIXTURES. *Journal of Catalysis,* 147**,** 476-483.

KELEMEN, S. R., SISKIN, M., GORBATY, M. L., FERRUGHELLI, D. T., KWIATEK, P. J., BROWN, L. D., EPPIG, C. P. & KENNEDY, R. J. 2007. Delayed Coker Coke Morphology Fundamentals: Mechanistic Implications Based on XPS Analysis of the Composition of Vanadium- and Nickel-Containing Additives during Coke Formation. *Energy & Fuels,* 21**,** 927-940.

KENNEPOHL, D. & SANFORD, E. 1996. Conversion of Athabasca bitumen with dispersed and supported Mo-based catalysts as a function of dispersed catalyst concentration. *Energy & Fuels,* 10**,** 229-234.

KHALIL, M., LEE, R. L. & LIU, N. 2015. Hematite nanoparticles in aquathermolysis: A desulfurization study of thiophene. *Fuel,* 145**,** 214-220.

KHULBE, C. P., RANGANATHAN, R. & PRUDEN, B. B. 1981. Hydrocracking of heavy oils/fly ash slurries. Google Patents.

KISSIN, Y. V. 1987. Free-radical reactions of high molecular weight isoalkanes. *Industrial & engineering chemistry research,* 26**,** 1633-1638.

KOLAHAN, F., MANOOCHEHRI, M. & HOSSEINI, A. Application of Taguchi Method and ANOVA Analysis for Simultaneous Optimization of Machining Parameters and Tool Geometry in Turning. 2011.

KOMERY, D. P., LUHNING, R. W. & O'ROURKE, J. C. 1999. Towards commercialization of the UTF project using surface drilled horizontal SAGD wells. *Journal of Canadian Petroleum Technology,* 38**,** 36-43.

KOWALCZYK, M. 2014. Application of Taguchi and ANOVA methods in selection of process parameters for surface roughness in precision turning of titanium. *Advances in Manufacturing Science and Technology,* 38**,** 21-35.

KRISHNAMOORTI, R. 2006. Extracting the benefits of nanotechnology for the oil industry. *Journal of petroleum technology,* 58.

LEE, D. K., YOON, W. L. & WOO, S. I. 1996. Hydrotreatment of an atmospheric residual oil over the dispersed cobalt and molybdenum catalysts in a carbon expanded-bed reactor. *Fuel,* 75**,** 1186-1192.

LEE, J., HWANG, S., SEO, J. G., HONG, U. G., JUNG, J. C. & SONG, I. K. 2011. Pd catalyst supported on SiO2–Al2O3 xerogel for hydrocracking of paraffin wax to middle distillate. *Journal of Industrial and Engineering Chemistry,* 17**,** 310-315.

LI, Q., NEWBERG, J. T., WALTER, E. C., HEMMINGER, J. C. & PENNER, R. M. 2004. Polycrystalline Molybdenum Disulfide (2H−MoS2) Nano- and Microribbons by Electrochemical/Chemical Synthesis. *Nano Letters,* 4**,** 277-281.

LIANG, J., GUAN, W. & JIANG, Y. 2012. Propagation and control of fire front in the combustion assisted gravity drainage process using horizontal wells. *Petroleum Exploration and Development,* 39**,** 720-727.

LIU, D., KONG, X., LI, M. Y. & QUE, G. H. 2009. Study on a Water-Soluble Catalyst for Slurry-Phase Hydrocracking of an Atmospheric Residue. *Energy & Fuels,* 23**,** 958-961.

LIU, D., LI, M. Y., DENG, W. A. & QUE, G. H. 2010. Reactivity and Composition of Dispersed Ni Catalyst for Slurry-Phase Residue Hydrocracking. *Energy & Fuels,* 24**,** 1958-1962.

LIU, Q., DONG, M., MA, S. & TU, Y. 2007. Surfactant enhanced alkaline flooding for Western Canadian heavy oil recovery. *Colloids and Surfaces A: Physicochemical and Engineering Aspects,* 293**,** 63-71.

LIU, Y. & FAN, H. 2002. The Effect of Hydrogen Donor Additive on the Viscosity of Heavy Oil during Steam Stimulation. *Energy & Fuels,* 16**,** 842-846.

LIU, Z. S., JESSEN, K. & TSOTSIS, T. T. 2011. Optimization of in-situ combustion processes: A parameter space study towards reducing the CO2 emissions. *Chemical Engineering Science,* 66**,** 2723-2733.

LOSER, U., SCHERZER, K. & WEBER, K. 1989. KINETIC-DATA ESTIMATION FOR HYDROGEN-TRANSFER REACTIONS, USING THE BOND-STRENGTH-BOND-LENGTH (BSBL) METHOD. *Zeitschrift Fur Physikalische Chemie-Leipzig,* 270**,** 237-245.

LUO, H., DENG, W. N., GAO, J. J., FAN, W. Y. & QUE, G. H. 2011. Dispersion of Water-Soluble Catalyst and Its Influence on the Slurry-Phase Hydrocracking of Residue. *Energy & Fuels,* 25**,** 1161-1167.

LUO, P. & GU, Y. 2007. Effects of asphaltene content on the heavy oil viscosity at different temperatures. *Fuel,* 86**,** 1069-1078.

MAGARIL, R. 1967. Mechanism of thermal cracking of normal paraffins. *Chemistry and Technology of Fuels and Oils,* 3**,** 8-9.

MARCHIONNA, M., DELBIANCO, A., PANARITI, N., MONTANARI, R., ROSI, S. & CORRERA, S. 2002. The combined use of three process units: hydroconversion with catalysts in slurry phase, distillation or flash, deasphalting is characterized in that the three units operate on mixed streams; catalyst reuse; receptivity; stability; quality. Google Patents.

MARSH, H., CALVERT, C. & BACHA, J. 1985. Structure and formation of shot coke—a microscopy study. *Journal of materials science,* 20**,** 289-302.

MARTÍNEZ-PALOU, R., MOSQUEIRA, M. D. L., ZAPATA-RENDÓN, B., MAR-JUÁREZ, E., BERNAL-HUICOCHEA, C., DE LA CRUZ CLAVEL-LÓPEZ, J. & ABURTO, J. 2011. Transportation of heavy and extra-heavy crude oil by pipeline: A review. *Journal of Petroleum Science and Engineering,* 75**,** 274-282.

MCGARVEY, G. B. & KASZTELAN, S. 1994. AN INVESTIGATION OF THE REDUCTION BEHAVIOR OF MOS2/AL2O3 AND THE SUBSEQUENT DETECTION OF HYDROGEN ON THE SURFACE. *Journal of Catalysis,* 148**,** 149-156.

MERDRIGNAC, I. & ESPINAT, D. 2007. Physicochemical characterization of petroleum fractions: the state of the art. *Oil & Gas Science and Technology-Revue de l'IFP,* 62**,** 7-32.

MEYER, R. F., ATTANASI, E. D. & FREEMAN, P. A. 2007. Heavy oil and natural bitumen resources in geological basins of the world.

MIKI, Y., YAMADAYA, S., OBA, M. & SUGIMOTO, Y. 1983. Role of catalyst in hydrocracking of heavy oil. *Journal of Catalysis,* 83**,** 371-383.

MILLER, B. J. & HAMILTON-SMITH, T. Field case: Cyclic gas recovery for light oil-using carbon dioxide/nitrogen/natural gas. SPE Annual Technical Conference and Exhibition, 1998. Society of Petroleum Engineers.

MITCHELL, P. C. H. 1990. Hydrodemetallisation of crude petroleum: fundamental studies. *Catalysis Today,* 7**,** 439-445.

MITCHELL, P. C. H. & SCOTT, C. E. 1990. Interaction of vanadium and nickel porphyrins with catalysts, relevance to catalytic demetallisation. *Catalysis Today,* 7**,** 467-477.

MOCHIDA, I., SAKANISHI, K., SUZUKI, N., SAKURAI, M., TSUKUI, Y. & KANEKO, T. 1998. Progresses of coal liquefaction catalysts in Japan. *Catalysis Surveys from Japan,* 2**,** 17-30.

MONGER, T. & COMA, J. 1988. A Laboratory and Field Evaluation of the CO2 Huff'n'Puff Process for Light-Oil Recovery. *SPE reservoir engineering,* 3**,** 1,168-1,176.

MONTANARI, R., ROSI, S., PANARITI, N., MARCHIONNA, M. & DELBIANCO, A. 2003. Convert heaviest crude & bitumen extra-clean fuels via EST-Eni Slurry Technology in NPRA Annual meeting. *San Antonio, USA March*.

MOORE, R. G., LAURESHEN, C. J., BELGRAVE, J. D. M., URSENBACH, M. G. & MEHTA, S. A. 1995. In situ combustion in Canadian heavy oil reservoirs. *Fuel,* 74**,** 1169-1175.

MOORE, R. G., MEHTA, S. A., URSENBACH, M. G. & GUTIERREZ, D. Potential for In Situ Combustion in Depleted Conventional Oil Reservoirs. SPE Improved Oil Recovery Symposium, 2012. Society of Petroleum Engineers.

MUKHERJEE, I. & RAY, P. K. 2006. A review of optimization techniques in metal cutting processes. *Computers & Industrial Engineering,* 50**,** 15-34.

MUSHRUSH, G. W. & HAZLETT, R. N. 1984. Pyrolysis of organic compounds containing long unbranched alkyl groups. *Industrial & engineering chemistry fundamentals,* 23**,** 288-294.

MYERS, K. J., FASANO, J. B. & CORPSTEIN, R. R. 1994. THE INFLUENCE OF SOLID PROPERTIES ON THE JUST-SUSPENDED AGITATION REQUIREMENTS OF PITCHED-BLADE AND HIGH-EFFICIENCY IMPELLERS. *Canadian Journal of Chemical Engineering,* 72**,** 745-748.

NAKAO, Y., YOKOYAMA, S., MAEKAWA, Y. & KAERIYAMA, K. 1984. Coal liquefaction by colloidal iron sulphide catalyst. *Fuel,* 63**,** 721-722.

NATH, M., GOVINDARAJ, A. & RAO, C. N. R. 2001. Simple synthesis of MoS2 and WS2 nanotubes. *Advanced Materials,* 13**,** 283-+.

NEAVEL, R. C. 1976. Liquefaction of coal in hydrogen-donor and non-donor vehicles. *Fuel,* 55**,** 237-242.

OMOLE, O., OLIEH, M. N. & OSINOWO, T. 1999. Thermal visbreaking of heavy oil from the Nigerian tar sand. *Fuel,* 78**,** 1489-1496.

ORTIZ-MORENO, H., RAMÍREZ, J., CUEVAS, R., MARROQUÍN, G. & ANCHEYTA, J. 2012. Heavy oil upgrading at moderate pressure using dispersed catalysts: Effects of temperature, pressure and catalytic precursor. *Fuel,* 100**,** 186-192.

OTTERSTEDT, J. E., GEVERT, S. B., JÄÅS, S. G. & MENON, P. G. 1986. Fluid catalytic cracking of heavy (residual) oil fractions: a review. *Applied Catalysis,* 22**,** 159-179.

OVALLES, C., FILGUEIRAS, E., MORALES, A., ROJAS, I., DE JESUS, J. C. & BERRIOS, I. 1998. Use of a Dispersed Molybdenum Catalyst and Mechanistic Studies for Upgrading Extra-Heavy Crude Oil Using Methane as Source of Hydrogen. *Energy & Fuels,* 12**,** 379-385.

OVALLES, C., FILGUEIRAS, E., MORALES, A., SCOTT, C. E., GONZALEZ-GIMENEZ, F. & PIERRE EMBAID, B. 2003. Use of a dispersed iron catalyst for upgrading extra-heavy crude oil using methane as source of hydrogen☆. *Fuel,* 82**,** 887-892.

OVALLES, C., HAMANA, A., ROJAS, I. & BOLÍVAR, R. A. 1995. Upgrading of extra-heavy crude oil by direct use of methane in the presence of water: Deuterium-labelled experiments and mechanistic considerations. *Fuel,* 74**,** 1162-1168.

PANARITI, N., DEL BIANCO, A., DEL PIERO, G. & MARCHIONNA, M. 2000a. Petroleum residue upgrading with dispersed catalysts: Part 1. Catalysts activity and selectivity. *Applied Catalysis A: General,* 204**,** 203-213.

PANARITI, N., DEL BIANCO, A., DEL PIERO, G., MARCHIONNA, M. & CARNITI, P. 2000b. Petroleum residue upgrading with dispersed catalysts: Part 2. Effect of operating conditions. *Applied Catalysis A: General,* 204**,** 215-222.

PETRAKIS, L. & GRANDY, D. W. 1981. Free radicals in coal and coal conversions. 6. Effects of liquefaction process variables on the in-situ observation of free radicals. *Fuel,* 60**,** 1017-1021.

PEUREUX, S., BONNAMY, S., FIXARI, B., LAMBERT, F., LE PERCHEC, P., PEPIN-DONAT, B. & VRINAT, M. 1995. Deep Hydroconversion of Heavy Oil Residues with Dispersed Catalysts: Analysis of the Transformation. *Bulletin des Sociétés Chimiques Belges,* 104**,** 359-366.

PHADKE, M. S., KACKAR, R. N., SPEENEY, D. V. & GRIECO, M. J. 1983. Off-Line Quality Control in Integrated Circuit Fabrication Using Experimental Design. *Bell System Technical Journal,* 62**,** 1273-1309.

PICÓN-HERNÁNDEZ, H.-J., CENTENO-HURTADO, A. & PANTOJA-AGREDA, E.-F. 2008. Morphological classification of coke formed from the castilla and jazmín crude oils. *CT&F-Ciencia, Tecnología y Futuro,* 3**,** 169-183.

PIGNATIELLO JR, J. J. 1993. Strategies for robust multiresponse quality engineering. *IIE transactions,* 25**,** 5-15.

PITAULT, I., FONGARLAND, P., MITROVIC, M., RONZE, D. & FORISSIER, M. 2004. Choice of laboratory scale reactors for HDT kinetic studies or catalyst tests. *Catalysis Today,* 98**,** 31-42.

POUTSMA, M. L. 1990. Free-radical thermolysis and hydrogenolysis of model hydrocarbons relevant to processing of coal. *Energy & Fuels,* 4**,** 113-131.

PRINS, R., DEBEER, V. H. J. & SOMORJAI, G. A. 1989. STRUCTURE AND FUNCTION OF THE CATALYST AND THE PROMOTER IN CO-MO HYDRODESULFURIZATION CATALYSTS. *Catalysis Reviews-Science and Engineering,* 31**,** 1-41.

RAD, M. R., RASHIDI, A., VAFAJOO, L. & RASHTCHI, M. 2014. Preparation of Co–Mo supported multi-wall carbon nanotube for hydrocracking of extra heavy oil. *Journal of Industrial and Engineering Chemistry,* 20**,** 4298-4303.

RAGHAVA RAO, K., REWATKAR, V. & JOSHI, J. 1988. Critical impeller speed for solid suspension in mechanically agitated contactors. *AIChE journal,* 34**,** 1332-1340.

RAHMANI, S., MCCAFFREY, W., ELLIOTT, J. A. W. & GRAY, M. R. 2003. Liquid-Phase Behavior during the Cracking of Asphaltenes. *Industrial & Engineering Chemistry Research,* 42**,** 4101-4108.

RAHMANI, S., MCCAFFREY, W. & GRAY, M. R. 2002. Kinetics of Solvent Interactions with Asphaltenes during Coke Formation. *Energy & Fuels,* 16**,** 148-154.

RANA, M. S., SÁMANO, V., ANCHEYTA, J. & DIAZ, J. A. I. 2007. A review of recent advances on process technologies for upgrading of heavy oils and residua. *Fuel,* 86**,** 1216-1231.

RANKEL, L. A. 1994. Hydrocracking vacuum resid with Ni・W bifunctional slurry catalysts. *Fuel Processing Technology,* 37**,** 185-202.

REIS, T. 1975. To coke, desulfurize and calcine. Part 2: coke quality and its control.[Coke formed when feed heated to 900-950/sup 0/F; coke formation reactions are endothermic]. *Hydrocarbon Process.;(United States),* 54.

REN, R., WANG, Z., GUAN, C. & SHI, B. 2004. Study on the sulfurization of molybdate catalysts for slurry-bed hydroprocessing of residuum. *Fuel Processing Technology,* 86**,** 169-178.

REYNIERS, G. C., FROMENT, G. F., KOPINKE, F.-D. & ZIMMERMANN, G. 1994. Coke Formation in the Thermal Cracking of Hydrocarbons. 4. Modeling of Coke Formation in Naphtha Cracking. *Industrial & Engineering Chemistry Research,* 33**,** 2584-2590.

REYNOLDS, J. G. 1991. MODELING HYDRODESULFURIZATION, HYDRODENITRIFICATION AND HYDRODEMETALATION. *Chemistry & Industry***,** 570-574.

REZAEI, H., ARDAKANI, S. J. & SMITH, K. J. 2012. Comparison of MoS2 Catalysts Prepared from Mo-Micelle and Mo-Octoate Precursors for Hydroconversion of Cold Lake Vacuum Residue: Catalyst Activity, Coke Properties and Catalyst Recycle. *Energy & Fuels,* 26**,** 2768-2778.

REZAEI, M., SCHAFFIE, M. & RANJBAR, M. 2013. Thermocatalytic in situ combustion: Influence of nanoparticles on crude oil pyrolysis and oxidation. *Fuel,* 113**,** 516-521.

RHOE, A. & DEBLIGNIERES, C. 1979. VISBREAKING - FLEXIBLE PROCESS. *Hydrocarbon Processing,* 58**,** 131-136.

RIAZI, M. 2005. *Characterization and properties of petroleum fractions*, ASTM international.

RIVERO, J. A., COSKUNER, G., ASGHARI, K., LAW, D. H.-S., PEARCE, A., NEWMAN, R., BIRCHWOOD, R. A., ZHAO, J. & INGHAM, J. P. Modeling CHOPS Using a Coupled Flow-Geomechanics Simulator With Nonequilibrium Foamy-Oil Reactions: A Multiwell History Matching Study. SPE Annual Technical Conference and Exhibition, 2010. Society of Petroleum Engineers.

ROMERO-ZERÓN, L. 2012. *Advances in Enhanced Oil Recovery Processes*, INTECH Open Access Publisher.

SAHU, R., SONG, B. J., IM, J. S., JEON, Y.-P. & LEE, C. W. 2015. A review of recent advances in catalytic hydrocracking of heavy residues. *Journal of Industrial and Engineering Chemistry*.

SAMBI, I. S., KHULBE, K. C. & MANN, R. S. 1982. CATALYTIC HYDROTREATMENT OF HEAVY GAS OIL. *Industrial & Engineering Chemistry Product Research and Development,* 21**,** 575-580.

SANFILIPPO, D. 2009. Bottom of the Barrel Technology within Refining Extracting Additiona l Value from Oil Feedstocks using EST Technology. *WTG Webinar Connected from San Donato Milanese, Italy*.

SANFORD, E. C. 1995. Conradson Carbon Residue Conversion during Hydrocracking of Athabasca Bitumen: Catalyst Mechanism and Deactivation. *Energy & Fuels,* 9**,** 549-559.

SANTOS, R., LOH, W., BANNWART, A. & TREVISAN, O. 2014. An overview of heavy oil properties and its recovery and transportation methods. *Brazilian Journal of Chemical Engineering,* 31**,** 571-590.

SAVAGE, P. E. & KLEIN, M. T. 1987. Asphaltene reaction pathways. 2. Pyrolysis of n-pentadecylbenzene. *Industrial & Engineering Chemistry Research,* 26**,** 488-494.

SAVAGE, P. E. & KLEIN, M. T. 1988. Asphaltene reaction pathways. 4. Pyrolysis of tridecylcyclohexane and 2-ethyltetralin. *Industrial & engineering chemistry research,* 27**,** 1348-1356.

SAVAGE, P. E., KLEIN, M. T. & KUKES, S. G. 1988. Asphaltene reaction pathways. 3. Effect of reaction environment. *Energy & Fuels,* 2**,** 619-628.

SCHACHT, P., DÍAZ-GARCÍA, L., AGUILAR, J. & RAMÍREZ, S. 2014. Upgrading of Heavy Crude Oil with W-Zr Catalyst. *Advances in Chemical Engineering and Science,* 2014.

SCHUETZE, B. & HOFMANN, H. 1984. How to upgrade heavy feeds. *Hydrocarbon Processing,* 63**,** 75-82.

SHAH, A., FISHWICK, R., WOOD, J., LEEKE, G., RIGBY, S. & GREAVES, M. 2010. A review of novel techniques for heavy oil and bitumen extraction and upgrading. *Energy & Environmental Science,* 3**,** 700-714.

SHAH, A. A., FISHWICK, R. P., LEEKE, G. A., WOOD, J., RIGBY, S. P. & GREAVES, M. 2011. Experimental optimization of catalytic process in situ for heavy-oil and bitumen upgrading. *Journal of Canadian Petroleum Technology,* 50**,** 33-47.

SHAH, J., JAN, M. R. & ADNAN 2014. Catalytic activity of metal impregnated catalysts for degradation of waste polystyrene. *Journal of Industrial and Engineering Chemistry,* 20**,** 3604-3611.

SHAH, N., ZHAO, J. M., HUGGINS, F. E. & HUFFMAN, G. P. 1996. In situ XAFS spectroscopic studies of direct coal liquefaction catalysts. *Energy & Fuels,* 10**,** 417-420.

SHARMA, B., SHARMA, C., BHAGAT, S. & ERHAN, S. 2007. Maltenes and asphaltenes of petroleum vacuum residues: physico-chemical characterization. *Petroleum science and technology,* 25**,** 93-104.

SHENG, J. J. 2015. Enhanced oil recovery in shale reservoirs by gas injection. *Journal of Natural Gas Science and Engineering,* 22**,** 252-259.

SHENG, J. J. & CHEN, K. 2014. Evaluation of the EOR potential of gas and water injection in shale oil reservoirs. *Journal of Unconventional Oil and Gas Resources,* 5**,** 1-9.

SHUYI, Z., WENAN, D., HUI, L., DONG, L. & GUOHE, Q. 2008. Slurry-phase residue hydrocracking with dispersed nickel catalyst. *Energy & Fuels,* 22**,** 3583-3586.

SIMPSON, J. R. 1998. Robust Design and Analysis for Quality Engineering. *Journal of Quality Technology,* 30**,** 182.

SISKIN, M., KELEMEN, S. R., GORBATY, M. L., FERRUGHELLI, D. T., BROWN, L. D., EPPIG, C. P. & KENNEDY, R. J. 2006. Chemical Approach to Control Morphology of Coke Produced in Delayed Coking. *Energy & Fuels,* 20**,** 2117-2124.

SPEIGHT, J. 2011. *Chapter 5: Thermal Cracking The Refinery of the Future, and Hydrotreating (HDT)*.

SPEIGHT, J. G. 1997. *Petroleum chemistry and refining*, CRC Press.

SPEIGHT, J. G. 2004. New approaches to hydroprocessing. *Catalysis Today,* 98**,** 55-60.
SPEIGHT, J. G. 2005. Natural Bitumen (Tar Sands) and Heavy Oil. *G. Jinsheng, Coal, Oil Shale, Natural Bitumen, Heavy Oil and Peat, from Encyclopedia of Life Support Systems (EOLSS). Oxford: UNESCO, EOLSS.*
SPEIGHT, J. G. 2013. Chapter 2 - Thermal Cracking. *In:* SPEIGHT, J. G. (ed.) *Heavy and Extra-heavy Oil Upgrading Technologies.* Boston: Gulf Professional Publishing.
SPEIGHT, J. G. 2014. *The chemistry and technology of petroleum*, CRC press.
SPIECKER, P. M., GAWRYS, K. L., TRAIL, C. B. & KILPATRICK, P. K. 2003. Effects of petroleum resins on asphaltene aggregation and water-in-oil emulsion formation. *Colloids and surfaces A: Physicochemical and engineering aspects,* 220**,** 9-27.
STEER, J. G., MUEHLENBACHS, K. & GRAY, M. R. 1992. Stable isotope analysis of hydrogen transfer during catalytic hydrocracking of residues. *Energy & Fuels,* 6**,** 540-544.
SUN, M., ADJAYE, J. & NELSON, A. E. 2004. Theoretical investigations of the structures and properties of molybdenum-based sulfide catalysts. *Applied Catalysis A: General,* 263**,** 131-143.
SUNDARAM, K. M., KATZER, J. R. & BISCHOFF, K. B. 1988. MODELING OF HYDROPROCESSING REACTIONS. *Chemical Engineering Communications,* 71**,** 53-71.
TABER, J. J., MARTIN, F. & SERIGHT, R. 1997. EOR screening criteria revisited-Part 1: Introduction to screening criteria and enhanced recovery field projects. *SPE Reservoir Engineering,* 12**,** 189-198.
TANG, W., FANG, M., WANG, H., YU, P., WANG, Q. & LUO, Z. 2014. Mild hydrotreatment of low temperature coal tar distillate: Product composition. *Chemical Engineering Journal,* 236**,** 529-537.
TANSEL, I. N., GÜLMEZ, S., DEMETGUL, M. & AYKUT, Ş. 2011. Taguchi Method–GONNS integration: Complete procedure covering from experimental design to complex optimization. *Expert Systems with Applications,* 38**,** 4780-4789.
TERMEER, C. 2013. *Fundamentals of Investing in Oil and Gas*, Chris Termeer.
THOMAS, S. 2008. Enhanced oil recovery-an overview. *Oil & Gas Science and Technology-Revue de l'IFP,* 63**,** 9-19.
TIMKO, M. T., GHONIEM, A. F. & GREEN, W. H. 2015. Upgrading and desulfurization of heavy oils by supercritical water. *Journal of Supercritical Fluids,* 96**,** 114-123.
TONN, R. 2010. Depth Conversion and Seismic Lithology Inversion of a McMurray Oil Sands Reservoir. *CSEG Recorder, November***,** 26-35.
TORABI, F., QAZVINI FIROUZ, A., KAVOUSI, A. & ASGHARI, K. 2012. Comparative evaluation of immiscible, near miscible and miscible CO2 huff-n-puff to enhance oil recovery from a single matrix–fracture system (experimental and simulation studies). *Fuel,* 93**,** 443-453.
TOWFIGHI, J., SADRAMELI, M. & NIAEI, A. 2002. Coke Formation Mechanisms and Coke Inhibiting Methods in Pyrolysis Furnaces. *JOURNAL OF CHEMICAL ENGINEERING OF JAPAN,* 35**,** 923-937.
TÜZÜNOĞLU, E. & BAĞCI, S. 2000. Scaled 3-D model studies of immiscible CO2 flooding using horizontal wells. *Journal of Petroleum Science and Engineering,* 26**,** 67-81.
VASIREDDY, S., MORREALE, B., CUGINI, A., SONG, C. & SPIVEY, J. J. 2011. Clean liquid fuels from direct coal liquefaction: chemistry, catalysis, technological status and challenges. *Energy & Environmental Science,* 4**,** 311-345.
VERNON, L. W. 1980. Free radical chemistry of coal liquefaction: role of molecular hydrogen. *Fuel,* 59**,** 102-106.

VILLARROEL, T. & HERNÁNDEZ, A. R. 2013. Technological Developments for Enhancing Extra Heavy Oil Productivity in Fields of the Faja Petrolifera del Orinoco (FPO), Venezuela. *Search and Discovery Article*

WAILES, P. C., BELL, A. P., TRIFFETT, A. C. K., WEIGOLD, H. & GALBRAITH, M. N. 1980. Continuous hydrogenation of Yallourn brown-coal tar. *Fuel,* 59**,** 128-132.

WANG, J. & DONG, M. 2009. Optimum effective viscosity of polymer solution for improving heavy oil recovery. *Journal of Petroleum Science and Engineering,* 67**,** 155-158.

WATANABE, M., KATO, S.-N., ISHIZEKI, S., INOMATA, H. & SMITH JR, R. L. 2010. Heavy oil upgrading in the presence of high density water: Basic study. *The Journal of Supercritical Fluids,* 53**,** 48-52.

WEISSMAN, J. G. 1997. Review of processes for downhole catalytic upgrading of heavy crude oil. *Fuel Processing Technology,* 50**,** 199-213.

WEISSMAN, J. G., KESSLER, R. V., SAWICKI, R. A., BELGRAVE, J. D. M., LAURESHEN, C. J., MEHTA, S. A., MOORE, R. G. & URSENBACH, M. G. 1996. Down-Hole Catalytic Upgrading of Heavy Crude Oil. *Energy & Fuels,* 10**,** 883-889.

WEITKAMP, J. 2012. Catalytic Hydrocracking—Mechanisms and Versatility of the Process. *ChemCatChem,* 4**,** 292-306.

WIEHE, I. A. 1993. A PHASE-SEPARATION KINETIC-MODEL FOR COKE FORMATION. *Industrial & Engineering Chemistry Research,* 32**,** 2447-2454.

WILCOXON, J. P., NEWCOMER, P. P. & SAMARA, G. A. 1997. Synthesis and optical properties of MoS2 and isomorphous nanoclusters in the quantum confinement regime. *Journal of Applied Physics,* 81**,** 7934-7944.

WU, C., LEI, G.-L., YAO, C.-J., SUN, K.-J., GAI, P.-Y. & CAO, Y.-B. 2010. Mechanism for reducing the viscosity of extra-heavy oil by aquathermolysis with an amphiphilic catalyst. *Journal of Fuel Chemistry and Technology,* 38**,** 684-690.

XIA, T., GREAVES, B., WERFILLI, M. & RATHBONE, R. THAI Process-Effect of Oil Layer Thickness on Heavy Oil Recovery. Canadian International Petroleum Conference, 2002. Petroleum Society of Canada.

XIA, T. X. & GREAVES, M. 2002. Upgrading Athabasca tar sand using toe-to-heel air injection. *Journal of Canadian Petroleum Technology,* 41**,** 51-57.

XIA, T. X. & GREAVES, M. 2006. In situ upgrading of Athabasca Tar Sand bitumen using THAI. *Chemical Engineering Research & Design,* 84**,** 856-864.

XIA, T. X., GREAVES, M., TURTA, A. T. & AYASSE, C. 2003. THAI—A 'Short-Distance Displacement' In Situ Combustion Process for the Recovery and Upgrading of Heavy Oil. *Chemical Engineering Research and Design,* 81**,** 295-304.

YANG, L., ZHOU, D.-S. & SUN, Y.-H. SAGD as follow-up to cyclic steam stimulation in a medium deep and extra heavy oil reservoir. International Oil & Gas Conference and Exhibition in China, 2006. Society of Petroleum Engineers.

YEE, C. T. & STROICH, A. 2004. Flue gas injection into a mature SAGD steam chamber at the Dover Project (formerly UTF). *Journal of Canadian Petroleum Technology,* 43**,** 54-61.

YUI, S. M. & SANFORD, E. C. 1989. Mild hydrocracking of bitumen-derived coker and hydrocracker heavy gas oils: kinetics, product yields, and product properties. *Industrial & Engineering Chemistry Research,* 28**,** 1278-1284.

ZHANG, H. Q., SARICA, C. & PEREYRA, E. 2012. Review of High-Viscosity Oil Multiphase Pipe Flow. *Energy & Fuels,* 26**,** 3979-3985.

ZHANG, S., LIU, D., DENG, W. & QUE, G. 2007. A Review of Slurry-Phase Hydrocracking Heavy Oil Technology. *Energy & Fuels,* 21**,** 3057-3062.

ZHAO, D. W., WANG, J. & GATES, I. D. 2014. Thermal recovery strategies for thin heavy oil reservoirs. *Fuel,* 117, Part A**,** 431-441.

ZHOU, P. & CRYNES, B. L. 1986. Thermolytic reactions of dodecane. *Industrial & Engineering Chemistry Process Design and Development,* 25**,** 508-514.

ZHOU, P., HOLLIS, O. & CRYNES, B. L. 1987. Thermolysis of higher molecular weight straight-chain alkanes (C9-C22). *Industrial & engineering chemistry research,* 26**,** 846-852.

ZUO, Y.-X., CHU, J.-Z., KE, S.-L. & GUO, T.-M. 1993. A study on the minimum miscibility pressure for miscible flooding systems. *Journal of Petroleum Science and Engineering,* 8**,** 315-328.